Modelling the LA River: Threats and opportunities for the Los Angeles River, USA

Master's thesis

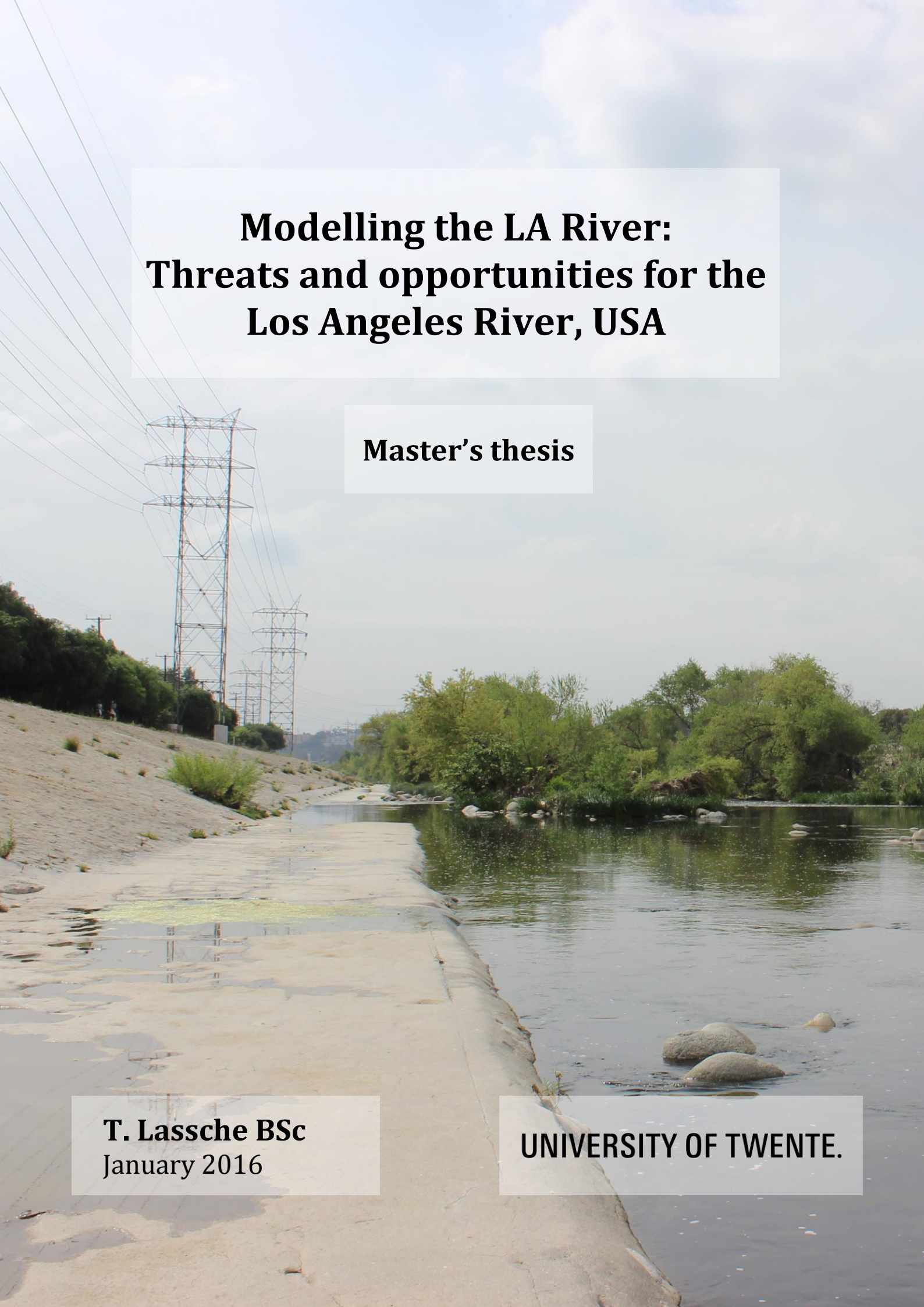

T. Lassche BSc
January 2016

UNIVERSITY OF TWENTE.

Modelling the LA River: Threats and opportunities for the Los Angeles River, USA

Master's thesis

in Civil Engineering & Management
Faculty of Engineering Technology
University of Twente

Author	T. Lassche BSc	
Contact	t.lassche@solcon.nl	

Location and date	Enschede, January 22, 2016	
Thesis defense date	January 29, 2016	

Graduation committee		
Graduation supervisor	Dr. ir. D.C.M. Augustijn	University of Twente
Daily supervisor	Dr. R.M.J. Schielen	Rijkswaterstaat, University of Twente

ABSTRACT

In the early 1900's the Los Angeles River in the Los Angeles County, California, USA was an uncontrolled, meandering river, which provided valuable resources (fresh water, irrigation) for the inhabitants. After some devastating floods in the period 1914 – 1938 the Congress and the U.S. Army Corps of Engineers (USACE) decided to change the river into a concrete channel. This channel, which was completed by 1960, has increased the safety of the city by prevented for big floods, but nowadays it causes other problems. Due to the huge urbanization of the city the river became literally and figuratively isolated from people and communities and this is increasingly considered as unwanted and a missed opportunity to make the inhabitants of Los Angeles familiar with its river. Another problem is that due to the high flow velocities as a result of the low friction of the concrete and the steep character of the river (an average slope of 0.29 percent), the concrete washes away at some places, which decreases the safety of the city. Finally, due to the unsystematic channelization of the river (because it happened over a period of many decades), the flood protection levels along its reaches vary considerably. At some places along the river the flood probability seems to be approximately once in 10 years, which is a very low protection level. In 1991 the first plans to revitalize the LA River arose, which finally resulted in a Master Plan published in 2007 by the City of Los Angeles. An Integrated Feasibility Study was published by the USACE in 2013, in which different alternatives (sets of measures) were reviewed, using 1D-model HEC-RAS, in which setting up a 2D-model was recommended.

In this study a 2D-model of the LA River is set up which is used to investigate flood probabilities in the current situation. After investigating the flood probabilities in the current or reference situation some scenarios with different measures to reduce flood risks along the river are implemented in the model and their consequences are assessed. Using the model and the measures an analysis of changes in flood safety is carried out.

The data series of the precipitation in the catchment area of the LA River and of the discharge in the river are analyzed as input for the model and as a check for the model results. Also the relation between the precipitation and the discharge is investigated to be used in the calculations of the scenario with the climate change. The precipitation series and the discharge series are related to each other according to the cross-correlation analysis. However, it is hard to determine a quantitative and accurate relation between the precipitation and the discharge. With the data series of the discharge three extreme value distributions are determined, namely the Gumbel distribution, the Generalized Extreme Value distribution and the Log-Pearson Type III distribution, to estimate the return times at the different stream gauging stations along the river in the current situation and in the different scenarios. It turned out that the extreme value distributions have a high level of uncertainty, due to the limited availability of data, which is reflected in large differences between the distribution. The Generalized Extreme Value distribution is chosen to determine the return times for the current situation and the scenarios based on the R^2 and RMSE values of the distributions.

To set up the 2D-model the module Delft3D-FLOW of the suite Delft3D, developed by Deltares, is used. This module is a hydrodynamic simulation program which is used to calculate non-steady flow phenomena on a curvilinear, boundary fitted grid. The grid includes the river itself from the Sepulveda Dam to the ocean, as well as the floodplains and some areas in which measures are planned. The bathymetry is obtained from a Digital Elevation Map, obtained by use of LIDAR, and is corrected at some locations with the cross sections used in the 1D-model HEC-RAS of the USACE. The friction coefficients (roughness) are estimated with help of personal experience, Google Earth and information of the USACE. The boundary conditions are the downstream boundary, set by harmonic constituents, the upper boundary condition at the Sepulveda Dam, set

as a variable input, and the lateral inflows. For these lateral inflows relations are determined between the available data of the tributaries and of the upper boundary condition and these relations are used to estimate the boundary conditions for the lateral inflow. For the calibration and the validation of the model the available hourly data series of the discharge for the hydrological years 2009 – 2012 was split up in two parts, one for the calibration and the other part for the validation. The results of the calibration and validation are tested and assessed as sufficient to use the model for the different scenarios.

With the model described above the reference situation (i.e. current geometry and representative discharge wave) is investigated. For the representative discharge wave it has been decided to choose the most extreme hydrograph instead of a typical hydrograph, because the peak of the most extreme event was overestimated too much by the typical hydrograph. This is due to the use of daily averaged peak discharges for the extreme value distributions instead of maximum or hourly peak discharges. This caused also a difference between the return times determined in this study for the reference situation, namely for the most critical point in the river a return time of about once in 160 years, and the return times used in the Feasibility Study of the USACE, namely a return time of once in 10 years for the most critical point in the river. Also the uncertainties in the model set up of for example the grid, the bathymetry and the estimation of the boundary conditions for the lateral inflows may explain these differences. However, the design discharges used in the HEC-RAS model of the USACE are quite the same as the hourly peak discharges found in this study. Therefore, the uncertainty lies mainly in the determination of the return times.

Four other scenarios are defined to investigate the change in flood probabilities. For the first scenario a reduction of the lateral inflows is defined, simulating the storage of precipitation water in the catchment before it flows into the LA River. It turned out that this scenario has the biggest positive effects on the flood safety in the city. A reduction of 5% of the total discharge in the LA River will increase the safety in the city by 20% in terms of return times due to a decrease in water level of about 15 centimeters. The safety in the city will be increased by about 60% by reducing the total discharge in the LA River by 15%, which will decrease the water level by 40 centimeters. Both the second and the third scenario form the implementations of some measures along the river, as are recommended in the Feasibility Study of the USACE. In scenario 2 two side channels are implemented near the 90-degree corner at Griffith Park and in scenario 3 a retention basin is set up at the location of the Piggyback Yard where a revitalization of the river is planned. For both scenarios the effects on the return times at the stream gauging stations are negligible. These measures appear to have only local effects on the water levels and the safety for the city. By extrapolating the return times of station C to the location of the river next to the Piggyback Yard it can be concluded that only the implementation of a retention basin without a levee has positive effects on the safety, namely an increase of 12 to 16% locally. However, it is not recommended to implement a retention basin at this location because this part of the river is not experiencing any problems related to flood safety. By extrapolating the return times of stations B and C to the part of the river next to the side channels it can be concluded that the safety will be increased locally by 40 to 50% for the first side channel and by 30 to 40% for the second side channel. Due to the steep slope and small friction of the river bottom both measures have negligible effects upstream and downstream. The measures could be very effective in solving other problems in the river, but for this study this is out of scope. For the last scenario the change in peak precipitation due to climate change is discussed. This scenario is not simulated, because a quantified relation between precipitation and discharge could not be found and scientists do not agree about the expected change in precipitation. By a change in precipitation intensity the daily averaged discharge would probably not change and therefore the return times determined by the method used in this study will remain the same. In reality the river will flood earlier, and therefore, unfortunately, this method of determining return times is not suitable to study the effects of change in precipitation due to climate change.

PREFACE

With this thesis I complete my Master's program Civil Engineering and Management at the University of Twente. This study started about one year ago by executing a preparation study to get more insight in the Los Angeles River and their problems. As part of this, in March 2015 I spent a few days in Los Angeles to talk about the river with an expert of the U.S. Army Corps of Engineers and to see the river with my own eyes. This has given me a better feeling about the sizes of the river, although the river was almost empty during my visit. In June 2015 I started with the execution of this study, which I finish with this report and the related defense during the colloquium.

I want to express some words of thank to several people. First of all, I would like to thank my supervisors during this project: Denie Augustijn and Ralph Schielen. Denie, thank you for your detailed feedback and advice during this project, which I appreciated very much. You were not my daily supervisor officially, however, I have discussed the project with you mostly, which were enriching conversations to keep me on track. Ralph, we have discussed not very much with each other, because of your limited presence at the University of Twente due to your main job at Rijkswaterstaat. However, the discussion sessions with you, required me to reflect on much earlier executed work, which helped me to keep the research scope in mind. You have initiated the subject and I would like to thank you for your confidence to let me conduct the research. Also many thanks for your feedback and advice during the project. Both of you also many thanks for your confidence to write a conference paper together about my study to be presented on the conference River Flow 2016 in St. Louis, USA.

I also would like to thank some other people who helped me during the execution of the project. I am very grateful to Koen Berends for his help with the modelling suite Delft3D. Koen, in the first part of the project you helped me in understanding the different modules of Delft3D and in putting the first steps of setting up the model. Also during the period in which I encountered quite some problems in the model I was not able to solve, you offered me to help to find and understand the problems and to solve these problems together. Thank you very much for your support. I would like to thank the U.S. Army Corps of Engineers located in Los Angeles too for the information and data provided to help me with my research. Especially Kerry Casey I would like to thank for welcoming me at his office in Los Angeles, for answering my questions and for pointing me some interesting spots along the river to visit.

Finally, I would like to thank my roommates during this graduation period and my housemates during the whole study in Enschede. Also I am very thankful to my parents who supported me during my study not only mentally and with love, but also financially. Last, but certainly not least, I would like to thank Gera for her love and support. I've always said: 'I don't want to marry before I finish my study'. Well, I am finished now…

Teun Lassche
Enschede, January 2016

CONTENTS

1 INTRODUCTION

This chapter provides an introduction to the study. The first section contains some background information of the Los Angeles River. Section 1.2 gives the problem statement. The research objective and the research questions are described in sections 1.3. The last section gives an outline of the report.

1.1 BACKGROUND

The Los Angeles River (LA River) is a river in the Los Angeles County, which is located in California, United States of America. In the early decades of the 20th century, the river was an uncontrolled, meandering river, which provided a valuable source of water for the inhabitants. Nevertheless, often the river flooded, with disastrous consequences. After some big devastating floods in the early 1900's the channelization of the whole river reach of about 82 kilometers was started. The channelization of the river with concrete was finished by 1960, when the river was changed into a big concrete structure and a major flood protection waterway.

FIGURE 1: MAP OF THE LOS ANGELES RIVER AND ITS CATCHMENT (Wikipedia, 2015)

After the channelization of the LA River it turned out that the goal of the channelization, which was discharging the water as soon as possible to prevent flooding, has been reached. In the 50 years after the channelization the City of Los Angeles experienced some floods, but mostly not with such big damage as before (Los Angeles County - Department of Public Works (LACDPW), 1996). In general, the system of channels performed well. It has even been said that Los Angeles would not have become the city it is without this flood protection (Williams-Villano, 2014). However, not many years after the completion of this flood protection, the side effects, which were not taken into account specifically during designing the channelization, became slowly visible.

In 1991 the Los Angeles County Board of Supervisors directed some departments of the County to coordinate several public and private parties to create a Master Plan to revitalize the LA River. This document was published in 2007 and contains an analysis of the problems in the river accompanied with a lot of recommendations to revitalize the river (City of Los Angeles - Department of Public Works et al., 2007).

1.2 PROBLEM STATEMENT

During the years after the completion of the concrete structure, the river had become literally and figuratively isolated from people and communities. The establishment of railroads, highways, warehouses and other industrial uses, which lined the river's edge, had caused this (City of Los Angeles - Department of Public Works et al., 2007). Although the river had been of great importance in the origin and the development of the city, the river was considered as an eyesore and not particularly as a welcome to humans and nature. There was also a need to create more open space in the city. This is because the City of Los Angeles has very little public open space, namely only about 4 percent, which is the least percentage of any major urban centers in the nation (LACDPW, 1996). The LA River may offer some of the best opportunities for developing multi-use public open space. At the aforementioned meeting in 1991, the Los Angeles County Board of Supervisors noted a growing public sentiment for transforming the LA River into a community amenity and an urban treasure. Therefore, the Board of Supervisors directed the Department of Public Works, Parks and Recreation and Regional Planning to coordinate several public and private parties to create a Master Plan to revitalize the LA River. In this Master Plan the need for public open space was recognized. New public open spaces should significantly improve the quality of life in the urban environment of Los Angeles, for example by recreational and health benefits (LACDPW, 1996).

Another problem that was encountered in the years after the channelization was the degradation of the ecological processes, such as the exchange and flow of nutrients and sediment within the system (U.S. Army Corps of Engineers (USACE), 2013a). Almost all the wetlands and other habitats dried up and the river's ecological functions were lost. Due to the urbanization of the City of Los Angeles and the channelization of the river almost 100 percent of the original wetlands and up to 95 percent of the in-stream riparian habitat in the LA River watershed were lost, according to the California Coastal Conservancy (City of Los Angeles - Department of Public Works et al., 2007). Only two areas with some riparian habitat exists within the river, namely the Sepulveda Basin and the Glendale Narrows. Nevertheless, these areas are increasingly stressed also, partly due to the degraded water quality. Due to the urbanization the water quality and the aquatic habitat has been degraded significantly, mostly due to the untreated storm water runoff that is discharged directly into the river (USACE, 2013a). The LA River has become the "floor drain" of the city, containing lots of pesticides, fertilizers and household chemicals. Due to a lack of functional riparian habitats and wetlands in and around the river, which could have improved the water quality by removing or sequestering many contaminants, the water quality has become very bad. Due to the concrete bottom it is also not possible anymore for the surface flows to infiltrate and recharge groundwater aquifers, which is necessary to restore native flow regimes and support native habitat communities (USACE, 2013a). In the Los Angeles River Revitalization Master Plan increasing the water quality and restoring a functional ecosystem are two of the most important goals of the revitalizing of the river (City of Los Angeles - Department of Public Works et al., 2007).

Finally, there is also a hydrodynamic problem. The LA River has been channelized to prevent the city from flooding and therefore to increase the safety of the citizens and their belongings. Although there have not been very big floods of the river in the years after the channelization anymore, still the risk for flooding exists. It is needed to know these risks and to quantify them. Citizens need to be aware of the extent of the risks of the river they are living nearby and for example also insurance companies need to know these risks. By making the citizens aware of these risks, they will be more cautious which can save lives during devastating floods. There are several aspects that are influencing or that will influence these flood risks.
Firstly, at this moment the LA River has several flood protection levels alternating along its reaches, not in a logical sequence, which is due to the unsystematic channelization of the river. At some reaches the flood protection level is no more than once in 10 years, which is quite a big problem (Casey, 2015; USACE, 2013b). The flood protection levels are also influenced by the

sedimentation of the river at some places, which provides an environment for the growing of bushes and trees in the river, which decreases the designed flood protection levels.
Secondly, a problem that results from the concrete lining of the river bed is that the water flows very quickly. During high water this fast flowing water creates tremendous forces, which not only destroy the small vegetation on bottoms that are soft (USACE, 2013a), but it also washes out portions of the concrete or other armoring systems. This is very bad for the structural integrity of the channel and therefore it affects the safety of the citizens and their belongings. At the moment a big part of the concrete-lined river experiences flow velocities that can be more than 10 meter per second. To assure the safety of the citizens and to reestablish a riparian habitat in the river it is required to slow down the flow velocities in the river. However, removing the concrete lining of the river at the whole river length would require a river of about 5 times its current width, which is impossible in a densely built city as Los Angeles (Casey, 2015).
Lastly, the measures planned to be taken due to the the hydrodynamic problems and also due to the esthetic and ecologic problems as mentioned earlier, will have an effect on the flow characteristics of the LA River and hence on the flood risks. However, these revitalization measures are not allowed to change the safety of the citizens negatively, because the citizens' safety should be the first priority. Also a changing climate can affect the flood risks of the river, for example due to a changing precipitation frequency, amount and intensity.
To sum up, the safety of the citizens is at stake due to the flood risks of the LA River. At some points along the river the risks are already high at the moment, but these risks will possibly increase in the future due to the human interventions and the changes of the climate. However, the impact of the interventions or the climate changes on the flood safety in the river is not known. In their Feasibility Study, the U.S. Army Corps of Engineers have used a one dimensional model, HEC-RAS, to do hydraulic analyses. In the Feasibility Study it is recommended to set up a two-dimensional flow model to simulate more accurately the proposed alterations in and adjacent to the channel (USACE, 2013b).

1.3 RESEARCH QUESTIONS

In this research project a two dimensional model will be set up to investigate the relation between the discharges and the return times of the Los Angeles River. With this model a reference situation will be constructed of the current state of the river. By implementing some of the measures that are planned or that are possible to take, new return times in the river will be investigated and will be compared with the reference situation. Further the effects of change in climate for California on the precipitation in the city of Los Angeles in the future will be estimated and along with this the return times in the future will be investigated and will be compared with the reference situation. The main research question for this project is:

In what way will the flood risks of the Los Angeles River change after the revitalization of the river?

The main research question is split up into several sub questions. In this research project the following research sub questions will be answered.

1. What is the current relation between precipitation in the Los Angeles River catchment and the discharge in the Los Angeles River and what is the current frequency distribution of these discharges?
2. How well can the current system of the Los Angeles River be described by the two dimensional model Delft3D?

3. How will the return times of the Los Angeles River change due to human and natural environmental changes?

1.4 THESIS OUTLINE

The report is structured into different chapters. Chapter 2 gives a description of the study area by describing the history and the geography of the river. In chapter 3 the first research question is answered by doing data analysis on the available precipitation and discharge data series. In this chapter also a frequency distribution is determined to be used for determining the return times in the reference situation and the different scenarios. The description of the model set up is given in chapter 4, to answer the second research question. It also gives the process of the calibration and validation and its results. Chapter 5 gives the descriptions of the reference situation and the scenarios and the results of modelling them. In chapter 6 the results of the study are discussed and the report is being closed in chapter 7 by answering the research questions as being the conclusion of the report and by giving some recommendations for further research.

2 STUDY AREA

This chapter provides the information about the study area, the whole Los Angeles River. First a brief history of this river is given, divided in the period before the channelization, the period of the channelization and the period after it. Besides this, a description is given of the geography of the river, described at 3 levels, namely on catchment level, on main river level, and on the level of the reaches.

2.1 HISTORY

2.1.1 Before channelization

The Los Angeles River is the original source of life for the city of Los Angeles. Along its banks the Pueblo de Los Angeles was founded by a group of about 45 Mexican and Spanish settlers in 1781. In the beginning the community grew very slowly, but with the Gold Rush of 1849 large numbers of people came to California. This resulted in the formation of the City of Los Angeles in 1850 (City of Los Angeles - Department of Public Works et al., 2007). From these years on the river was used for its water and as a transportation route to allow the city to grow. Railroads and industrial lands were established along the river. In the beginning of the 20th century the LA River was an uncontrolled, meandering river, which provided a valuable source of water for the early inhabitants (LACDPW, 2014).

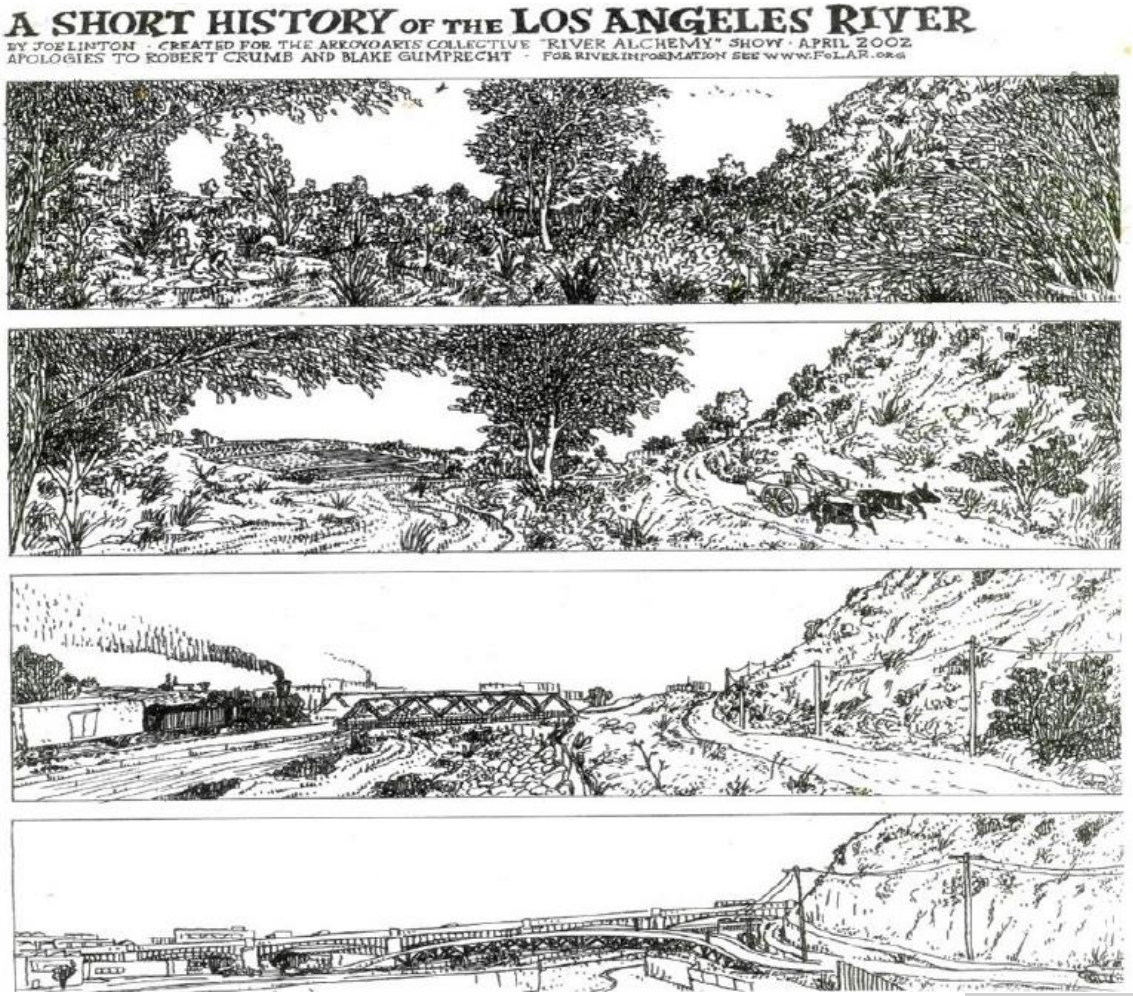

FIGURE 2: ARTIST'S IMPRESSIONS OF CHANGES TO THE LOS ANGELES RIVER THROUGH URBANIZATION (USACE, 2013a)

2.1.2 Channelization

After a big flood in 1914, which caused $470 million (in 1990 dollars) in damages throughout the developing basin (LACDPW, 1996), a public outcry for action to address the current flooding problems was done. Therefore, the Los Angeles County Flood Control District was formed, which implemented flood control measures by channelization and construction of dams and check dams. Taxpayers approved bond issues to build the initial major dams. However, they were not willing to provide enough funds for substantial infrastructure downstream of the dams (Gumprecht, 2001). On New Year's Eve 1934 another big flood occurred, which caused a damage of $100 million (in 1990 dollars) and the loss of 41 lives (LACDPW et al., 1996; Starr, 1996). After this devastating flood the Congress stepped in and the U.S. Army Corps of Engineers took a lead role in the development and implementation of a structural solution to manage the flood risks of the river. Due to the highly modified floodplains, which included agricultural, residential, commercial, and industrial uses, as well as paved surfaces and railroads alongside the channel, the options for a structural solution were very limited (USACE, 2013a). Immediately after another big devastating flood in 1938, which caused damages for $795 million (in 1990 dollars) and the loss of 49 lives (LACDPW, 1996), the channelization of the 82 kilometer long river and its tributaries by mainly concrete started. Also some dams and debris basins were constructed.

2.1.3 After channelization

By 1960 the whole LA River was channelized by a concrete structure and was thereby changed in a major flood protection waterway. In the years after the construction of the concrete channel and the dams the city was flooded again sometimes, but in general the system of channels performed well. Most of these floods were caused by excess precipitation in a big part of the state and the county. These floods were less destructive in terms of damages than before, but sometimes it killed many people. For example, in 1969 flooding in the Los Angeles County caused damages of only $4.5 million (in 1990 dollars) but it killed 73 people. Still some floods were destructive in terms of damages, for example floods in 1978 and 1980 with damages of $350 million and $375 million, respectively (both in 1990 dollars). During the floods in 1980 the measured peak discharge of the river at Long Beach was 3,600 m^3 per second, which was a record. This very high peak discharge gave concern to the protection of the river. Levees in Long Beach were designed to provide better than one-hundred-year protection, but the maximum stream flows of the 1980 storm were later calculated to be equal to the level that could be expected in the type of storms that occurs once every forty years (Gumprecht, 2001). During this storm the most significant problem observed was localized water disturbances caused by large storm drain side inflows. Standing waves, sometimes almost one meter high, required throttling back reservoir releases in order to prevent possible damage to the channel itself (Evelyn, 1980).
In total the floods between 1960 and 1994 caused damages of about $850 million (in 1990 dollars) and killed about 120 people. Nevertheless, in 1994 it was concluded that the existing flood control system, in the Los Angeles County Drainage Area, had prevented a total of nearly $3.6 billion in flood damages (LACDPW, 1996).

2.2 GEOGRAPHY

2.2.1 Watershed

The Los Angeles County is one of the 58 counties of California, one of the United States of America. With a population of 9,818,610 in 2010 (U.S. Census Bureau, 2015), the Los Angeles County is the most populous county and even more populous than 43 of the states of the United States of America. The metropolitan Los Angeles, defined as Los Angeles–Long Beach–Anaheim has a population of 12,828,837 in 2010 (U.S. Census Bureau, 2015). Also the U.S. Census Bureau defines a wider region based on commuting patterns, which is the Los Angeles-Long Beach, CA Combined

Statistical Area, more commonly known as the Greater Los Angeles Area. This area had a population of 17,877,006 in 2010 (U.S. Census Bureau, 2015), which is almost half the population of the state California. In this high populous area there are six major watersheds of which the Los Angeles River Watershed is the one with the highest population, with about 5 million people in an area of 2,160 square kilometers (U.S. Environmental Protection Agency, 2014).

FIGURE 3: WATERSHEDS IN LOS ANGELES COUNTY, WITH LOS ANGELES RIVER WATERSHED IN THE CENTER (City of Los Angeles, 2014a)

2.2.2 Main river

The main river in the Los Angeles River Watershed is the Los Angeles River, which has a length of about 82 kilometers. The confluence point of the Arroyo Calabasas and the Bell Creek in Canoga Park forms the start of the river (USACE, 2013a). The river flows from its headwaters in the mountains of the San Fernando Valley, the Simi Hills and the Santa Susana Mountains eastwards to the northern corner of Griffith Park. At this point the channel turns southward through the Glendale Narrows before it flows across the coastal plain and into San Pedro Bay near Long Beach (LACDPW, 2014). Along the way, several tributaries, e.g., Tujunga Wash (which receives flows from the USACE's Hansen Dam), Verdugo Wash, Arroyo Seco and Rio Hondo Diversion Channel (which receives flow from Whittier Narrows Dam), join the river. The river flows for approximately 51 kilometers through the City of Los Angeles, as is highlighted by the red polygon in Figure 3. The last 30 kilometers of the river flows through other cities that are part of the metropolitan Los Angeles.

The elevation at the origin of the LA River (in Canoga Park) is 235 meter and the elevation at the outlet to the Pacific Ocean is 0 meter. This means that with a length of 82 kilometers the average slope of the river is 0.29 percent, meaning that the river is short but steep (City of Los Angeles, 2014b).

2.2.3 Reaches

The LA River has different dimensions and characteristics along the river. To describe these characteristics, the river has been divided into 8 reaches, which is shown in Figure 4. For each of these reaches a short description is given of for example the channel geometry, the flow velocities, etcetera. Most of the information is taken from the Los Angeles Revitalization Master Plan and from the Los Angeles River Ecosystem Restoration Integrated Feasibility Report (City of Los Angeles - Department of Public Works et al., 2007; USACE, 2013a).

FIGURE 4: SATELLITE MAP OF THE LOS ANGELES RIVER (BLUE) AND LOCATIONS OF THE DIFFERENT REACHES (RED BOXES), ADAPTED FROM (Google Earth, 2015)

Reach 1: Arroyo Calabasas-Bell Creek Confluence to White Oak Ave Bridge near Sepulveda Basin
This reach flows mainly through residential environment. In this segment, the river is a concrete-lined trapezoidal channel. It is approximately 6 meters deep and it has a bottom width of 13.5 to 41 meter wide. In this reach three small tributaries, namely the Browns Canyon Wash, Aliso Creek and Caballero Creek, are entering the LA River. These tributaries are concrete-lined channels. Unfortunately, all these tributaries, including Arroyo Calabasas and Bell Creek, do not have stream gauging stations. Only a few manually collected flow and water depth measurements are available (Los Angeles Regional Water Quality Control Board, 2013).

Reach 2: Sepulveda Basin
The Sepulveda Basin is one of two segments where the river has a soft bottom and displays a more natural character. This results in lower flow velocities than in most other parts of the river.

This river segment is approximately 18 meters wide and is surrounded by park area and open space. The Sepulveda Basin can be closed by the Sepulveda Dam, finished in 1941, which is one of the dams constructed in response to the floods in the early 1900's, as is described in section 2.1.2. When the dam is closed, the park area and open space of the Sepulveda Basin is being used as a retention basin. Unfortunately, a scheme when to close the dam and when the dam was closed, which would have been important for this study, is not available. When the dam is open, the gate in the outlet channel is open, through which the water can flow out. Pictures of the dam and the river are shown in Figure 5.

FIGURE 5: LOS ANGELES RIVER AT SEPULVEDA BASIN (LEFT, LOOKING UPSTREAM) AND THE SEPULVEDA DAM (RIGHT, LOOKING DOWNSTREAM) (PHOTOS: T. LASSCHE, 03/18/2015)

FIGURE 6: LOS ANGELES RIVER AT REACH 3 (PHOTOS: T. LASSCHE, 03/18/2015)

Reach 3: Sepulveda Dam to confluence with Tujunga Wash

Downstream of the Sepulveda Dam, the river is constrained within a rectangular, concrete-lined channel ranging in width from 13 to 18 meter. Land uses surrounding this segment are primarily residential. This reach is the narrowest part of the LA River and also the curviest part of the river, as can be seen in Figure 6. This reach ends at the confluence point with the Tujunga Wash, which is a tributary with also a concrete-lined channel. The Tujunga Wash comes from the Hansen Dam, also one of the dams built after the floods in the 1900's. On its way from the Hansen Dam the Pacoima Wash joins the Tujunga Wash, a tributary that has a stream gauging station.

Reach 4: Confluence with Tujunga Wash to confluence with Burbank Western Channel
This reach is also a concrete-lined rectangular channel. The last part of this channel reach, from just downstream the Warner Bros Studios, has a rougher type of concrete than the other part of the reach. The river is approximately 5 meters deep and has a bottom width that ranges from 18 to 49 meter. During storm events peak flow velocities in this channel reach can be more than 10 meter per second. Because of these speeds, this is one of the most challenging sections from the standpoint of restoration. At the end of the reach the Burbank Western Channel is entering the LA River, which is also a concrete-lined channel.

Reach 5: Confluence with Burbank Western Channel to I-5 Freeway Bridge
At the upstream part of this reach the bed changes from rectangular concrete-lined to a trapezoidal cobblestone bed with grouted stone banks for a short part, and then back to rectangular concrete bed just before the 90-degree curve to the south at Griffith Park. The width of this part is about 70 meter. Just after the corner the Verdugo Wash is joining the LA River, which leads to a much wider channel at the confluence, namely a width of 130 meter for a length of about 200 meters. About 1.5 kilometer downstream of the corner, the river bed changes to a trapezoidal channel with cobblestone bed and grouted stone banks. These banks, as well the banks at the upstream part of this reach, are toed-down with sheet pile and quarry run stone. Under each of the large bridges across the river the bed is a concrete-lined rectangular channel with pier noses to protect the bridges and then it changes back to a trapezoidal channel with a cobblestone bed and grouted stone banks between the bridges. The width of the channel is approximately 100 meters from top to top and the depth is about 5.5 meters from the top of the bank for the largest part of the reach. At the last part of the reach the channel slowly deepens to about 9 meters. The channel narrows to about 50 meter and changes again to a rectangular concrete configuration just upstream of the I-5 and SR-110 interchange.
In the parts of the reach with a cobblestone bed, sediment is deposited on the bed, which has formed sand bars/islands. Those island have stabilized as the root systems of the many trees and other vegetation in the channel have trapped sediment over time. Due to this vegetation the flow velocities during storm events are much lower, about 4.5 meter per second, which is comparable to flow velocities in the Sepulveda Basin. A picture of this part of the reach is shown in Figure 7.

FIGURE 7: LOS ANGELES RIVER AT REACH 5 (PHOTO: T. LASSCHE, 03/18/2015)

Reach 6: I-5 Freeway Bridge to First Street Bridge

The channel in this reach is a rectangular concrete channel at the Arroyo Seco confluence, which enters the LA River just downstream of the I-5 Freeway Bridge. After this confluence it becomes a trapezoidal concrete channel. The channel depth from top of the banks is about 9 meter and the width from top of the bank to top of the bank ranges from approximately 60 to 75 meter. The channel has adjacent rail tracks on both banks and several bridges cross the river in this reach. On the bank of this reach lies the Piggyback Yard, which is a big intermodal facility. The flow velocities in this reach can become more than 10 meter per second during storm events.

Reach 7: First Street Bridge to confluence with Rio Hondo

Also in this reach, the river is constrained by rail tracks and freeways. Several roads and rail roads are crossing the river by bridges. The river channel in this part ranges from 80 to 130 meter. Also in this reach the channel is formed as a concrete-lined trapezoid and it has flow velocities greater than 10 meter per second during storm events. From the last part of this reach the LA River is outside the City of Los Angeles and on the territory of the other cities of the Los Angeles metropolitan. At the end of this reach is the confluence with the Rio Hondo. This river flows from the Whittier Narrows Dam, which is also one of the dams constructed after the floods in the early 1900's.

Reach 8: Confluence with Rio Hondo to Pacific Ocean

The last part of the river, the part from the confluence with the Rio Hondo is the widest part of the LA River. The width of the river in this reach is up to 180 meter from the top of the banks. This is also a concrete-lined trapezoidal channel, but at the end some sediment has been deposited, due to the lower flow velocities. These lower flow velocities are due to the influence of the tides of the Pacific Ocean. On some parts of the reach plants are growing on the sediment, but they wash away with a big flow event. This last segment of the river, including the Rio Hondo, is already revitalized between 1992 and the early 2000's (Casey, 2015). A picture of a part of this reach is shown in Figure 8.

FIGURE 8: LOS ANGELES RIVER AT REACH 8 (PHOTO: T. LASSCHE, 03/18/2015)

3 DATA ANALYSIS

To set up a model and to interpret the results of the model, first a thorough data analysis is needed. In this chapter the data series of the precipitation and of the discharge are analyzed and it is tried to establish relations between these series. Also an extreme value distribution of the discharge series is determined.

3.1 PRECIPITATION

Precipitation in the Los Angeles County is observed by several weather stations across the county. Historical data sets of 6 stations are taken from the National Climatic Data Center of the National Oceanic and Atmospheric Administration (NOAA) (2015a). The data sets are taken for a period of 55 hydrological years, from October 1, 1959 to September 30, 2014. The start of this period is chosen because of the completion of the channelization of the LA River with concrete before 1960. Unfortunately, not all weather stations have the same periods of record. Also, for some of the stations not for each day in the periods of record a precipitation value has been recorded, so the coverage of each station differs. Table 1 shows the station names, the elevation of the stations, the periods of record and the coverage of the data in these periods. The numbers of the stations correspond with the numbers on the map in Figure 11, which shows the locations of the stations.

TABLE 1: INFORMATION OF THE WEATHER STATIONS

			Period of record		
Number	**Station Name**	**Elevation**	**Start**	**End**	**Coverage**
1	Burbank Glendale Pasadena Airport	225.9 m	6/1/1998	9/30/2014	93%
2	Downey Fire Station FC107C	33.5 m	10/1/1959	8/31/2000	99%
3	Long Beach Daugherty Field	9.4 m	10/1/1959	9/30/2014	100%
4	Los Angeles Downtown USC	54.6 m	10/1/1959	9/30/2014	100%
5	Los Angeles International Airport	29.6 m	10/1/1959	9/30/2014	100%
6	Torrance Airport	27.4 m	10/1/1959	9/30/2014	99%

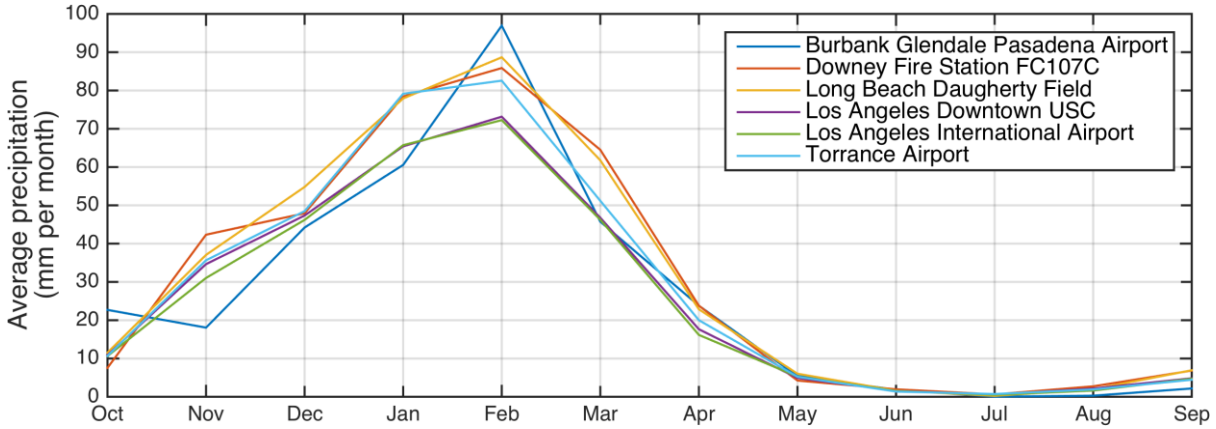

FIGURE 9: AVERAGE PRECIPITATION PER MONTH FOR DIFFERENT WEATHER STATIONS IN THE LOS ANGELES COUNTY

For each of these weather stations the average monthly precipitation is calculated, which is shown in Figure 9. The number of months over which the precipitation is averaged differs per station, which can be seen in Table 1. This means that the stations at the Burbank Glendale Pasadena Airport and at the Downey Fire Station have less months to calculate the average than

the other stations. Especially the station at Burbank Airport gives a bit different graph of the monthly averaged precipitation, which might be due to the shorter period of record. Each graph shows clearly a peak of precipitation in the winter period, with a maximum peak in February, and a deep valley in summer, with almost no precipitation in July. The average precipitation in a whole year, averaged for all weather stations, is 241.9 mm, which implies a dry climate.
The peak precipitation during a hydrological year is shown in Figure 10 for each weather station. This figure shows that, despite of the low average precipitation per month, the peaks can be high, namely up to 140 mm per day. Due to the incompleteness of some data sets, it is possible that for some years the real peak precipitation on a day could have been higher on a day for which no record is available. This could be the case for the weather stations with a coverage of less than 100%.

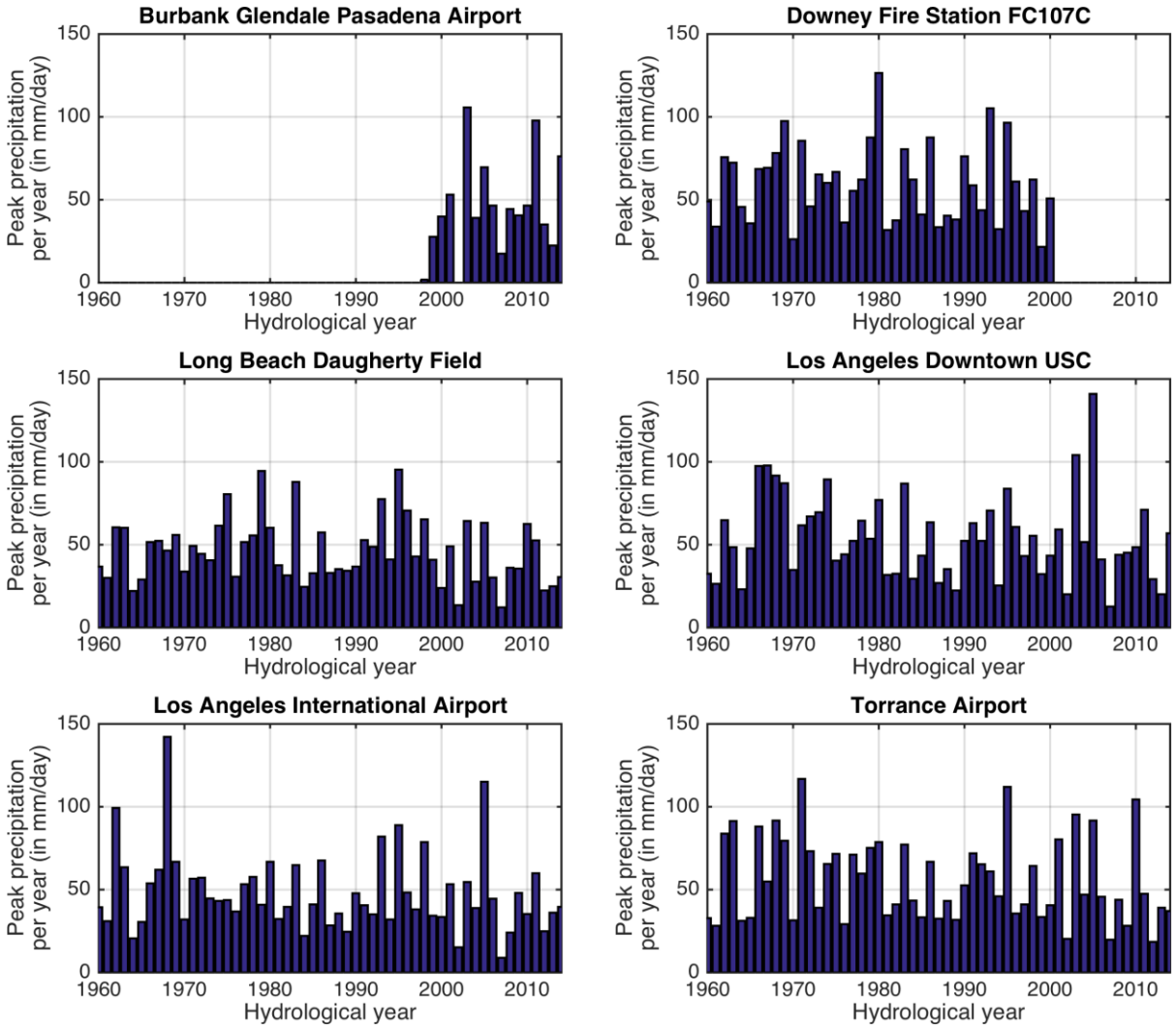

FIGURE 10: HISTOGRAMS OF PEAK PRECIPITATION PER DAY PER HYDROLOGICAL YEAR FOR DIFFERENT WEATHER STATIONS IN THE LOS ANGELES COUNTY

3.2 DISCHARGE

Along the LA River several stream gauging stations are located. These stations collect, among others, the mean daily flow per day. These discharges are recorded in cubic feet per second and for this study converted into cubic meter per second. The historical data sets are taken for the same period as the precipitation data records, namely for a period of 55 hydrological years, from October 1, 1959 to September 30, 2014. Unfortunately, none of the stations have a data coverage of 100% over this period, because for some days no discharge values are recorded. Table 2 shows

the station names, the period of record and the coverage of the data in this period for each of the stream gauging stations. The locations of the stations are given in the map of Figure 11, in which the characters correspond with the characters given for each station in the table. The discharge series collected at the stream gauging stations at the Sepulveda Dam are taken from the National Water Information System of the United States Geological Survey (USGS) (2015). The other four discharge series are provided by the Department of Public Works of the Los Angeles County (2015b).

TABLE 2: INFORMATION OF THE STREAM GAUGING STATIONS ALONG THE LOS ANGELES RIVER

		Period of record		
Character	**Station Name**	**Start**	**End**	**Coverage**
A	Sepulveda Dam	10/1/1959	9/30/2014	58%
B	Los Angeles River at Tujunga Wash (F300-R)	10/1/1959	9/30/2014	92%
C	Los Angeles River above Arroyo Seco (F57C-R)	10/1/1959	9/30/2014	87%
D	Los Angeles River below Firestone Blvd. (F34D-R)	10/1/1959	9/30/2001	90%
E	Los Angeles River below Wardlow River Road (F319-R)	10/1/1959	9/30/2014	95%

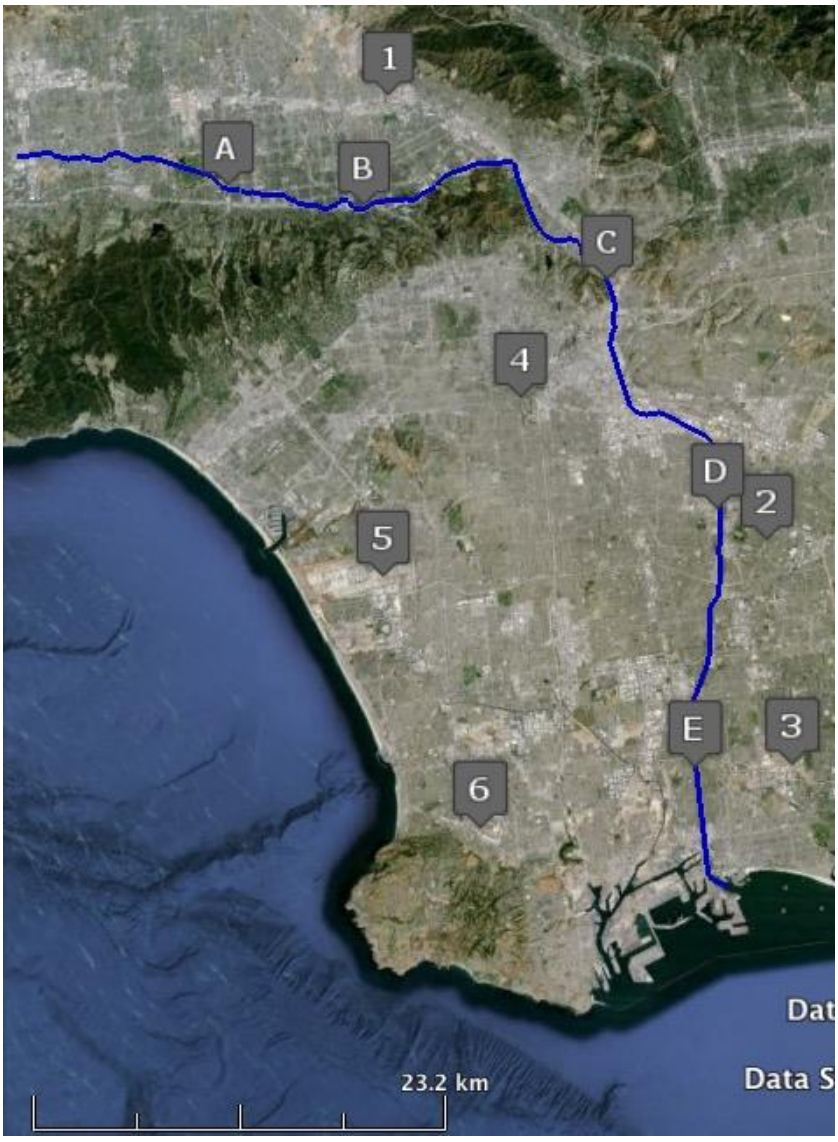

FIGURE 11: SATELLITE MAP OF LOS ANGELES COUNTY WITH THE LOS ANGELES RIVER (BLUE) AND THE LOCATIONS OF THE WEATHER STATIONS AND THE STREAM GAUGING STATIONS, ADAPTED FROM (Google Earth, 2015)

The monthly averaged discharge is calculated for each of the stream gauging stations along the LA River, of which the graphs are shown in Figure 12. The stations are sorted from upstream to downstream. This figure shows a similar pattern as in Figure 9, with the monthly averaged precipitation: high discharges in winter with a peak in February and low discharges in summer. It shows clearly the increase in discharge for subsequent stations. A remarkable thing is the base flow of the river in the months May to September. In these months the river has a more or less constant discharge, where the average precipitation in those months is not constant and nearly zero. This baseflow comes from some wastewater treatment plants. There are plans to reduce the outflow of the wastewater treatment plants into the LA River, however, it is not clear if these plans will be carried out (Casey, 2015). By comparing the graphs in Figure 12, it can be concluded that each graph has the same shape and there is almost a constant increase in discharge along the river. However, this is not exactly the case for the stream gauging station F34D-R, located below Firestone Blvd, which is mainly visible for the month January. It is unclear what causes this discrepancy.

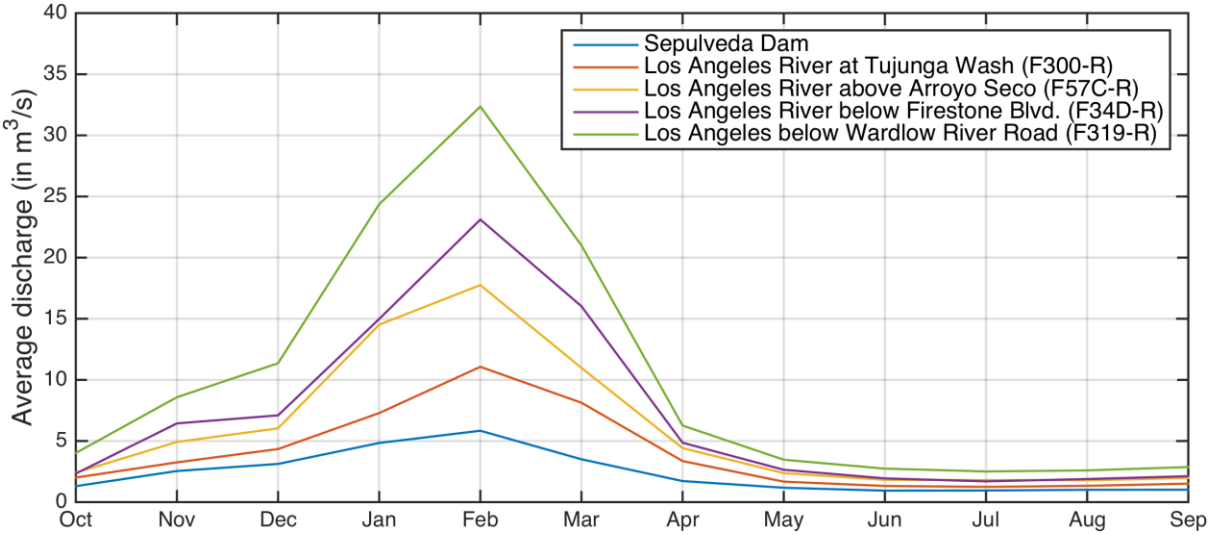

FIGURE 12: AVERAGE DISCHARGE PER DAY, MONTHLY AVERAGED FOR DIFFERENT STREAM GAUGING STATIONS ALONG THE LOS ANGELES RIVER

For the five stream gauging stations also the annual peak discharges in cubic meter per second are sampled. This leads to the histograms as shown in Figure 13. The coverage of the discharge data sets is less than 100%, as given in Table 2. For the station at the Sepulveda Dam there is no data observed for the hydrological years 1980 to 2002, which leads to a low coverage of 58%. By leaving aside these hydrological years, this discharge series has a coverage of 100%. This is in contrast to the other stations, where in each discharge series at several moments in time some years, months or days are missing. For these hydrological years the annual peak discharge might have been higher on another day in the same year, but than this data was not collected.
The discharges are the average daily discharges in cubic meter per second. This means that the actual peak discharge at a given moment of the day was higher than the discharge series provides, which will be confirmed in section 3.3.3. However, these daily averaged peak discharges are a good indication of the actual peak discharges.
By looking in more detail into the peak discharge series shown in Figure 13 it can be seen that the peak discharge of the hydrological year 1969 measured at the station below Wardlow River Road (F319-R) was 1556 m^3/s, which occurred on January 25, 1969. This is more than 60 times larger than the average discharge (24.4 m^3/s) in January for the same station. Another extreme is the peak discharge of the hydrological year 1983 measured on March 1, 1983 at the station at Tujunga Avenue (F300-R) of 554 m^3/s, which is more than 65 times larger than the average discharge of 8.1 m^3/s in March for the same station. These examples indicate that the peak discharges in the Los Angeles River are very high, but also that the river is almost empty for large periods.

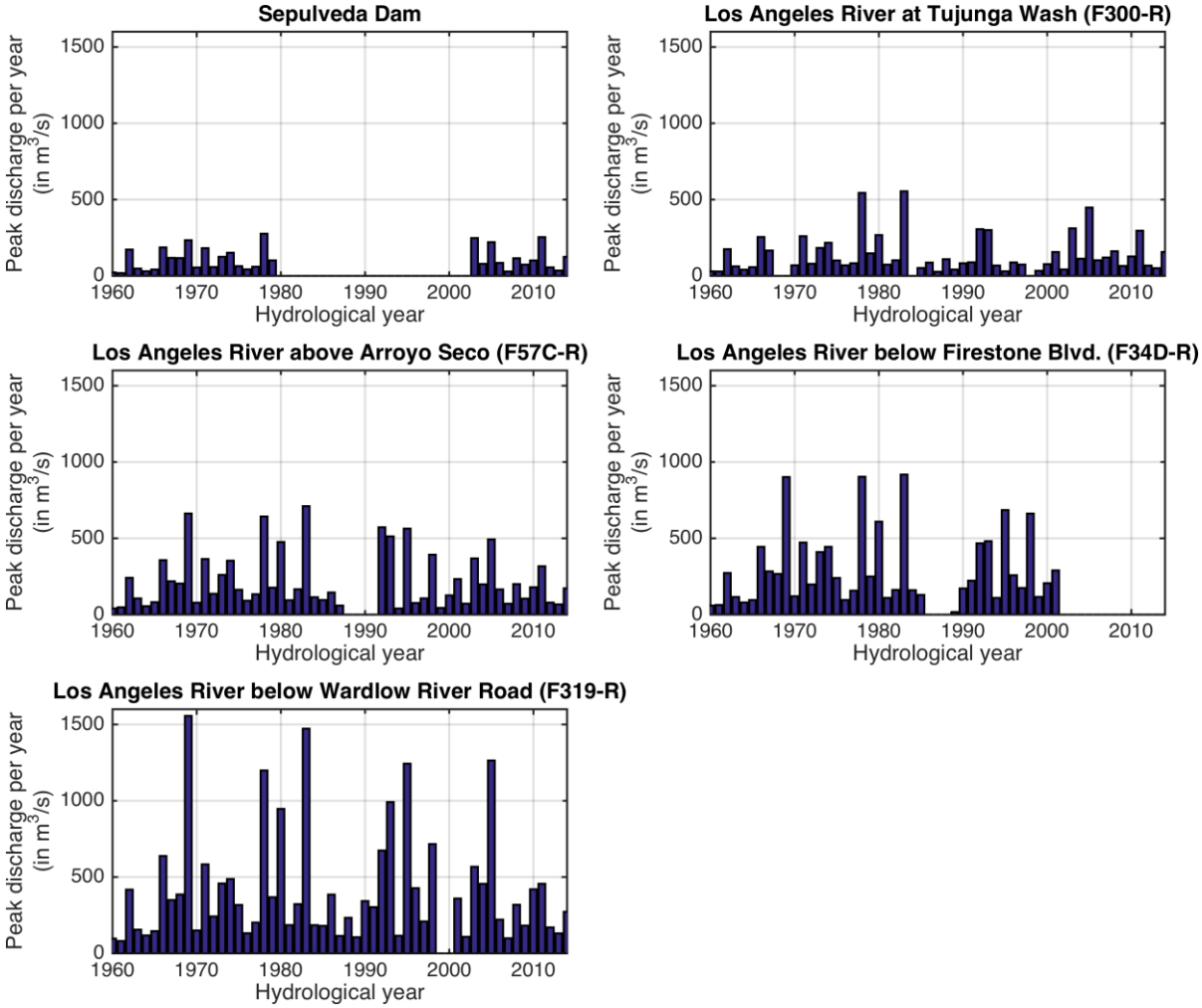

FIGURE 13: HISTOGRAMS OF PEAK DISCHARGES PER HYDROLOGICAL YEAR OF DIFFERENT STREAM GAUGING STATIONS ALONG THE LOS ANGELES RIVER

3.3 DETAILED DATA ANALYSIS

In this section a deeper analysis of the data series of discharge and precipitation is given, to obtain important information to be used in setting up the model.

3.3.1 Selection of hourly data series

To get a better insight in the relations between the different discharge series and the relations between the discharge and precipitation series, the series have to be analyzed into more detail. However, because of the high flow velocities and the high variability in the discharges, the daily data series are not detailed enough. Therefore, hourly discharge series are gathered of the stream gauging stations mentioned in Table 2, taken from the USGS (2015) and from the Department of Public Works of the Los Angeles County (2015), and the available hourly precipitation series of three weather stations, taken from the NOAA (2015a). In most of the cases these hourly data series are available from the early 2000's until today, but some series are only available from 2008 until today. To get data series of the same period and to limit the hourly data series to a manageable size to be processed for this study, a period of 4 consecutive years is chosen. With help of the histograms of the peak discharges given in Figure 13, 4 consecutive hydrological years are selected, not earlier than 2008, with peaks that are representative for the whole data set, which resulted in the selection of hourly data series for the hydrological years 2009 to 2012. Table 3 shows the station names with the character that correspond with the locations given in Figure 11, the period of record and the coverage of the data in this period. The weather station

near the Sepulveda Dam is located at almost the same location as the stream gauging station near the Sepulveda Dam. Although these are not the same stations, the character of the stations is chosen to be the same.

TABLE 3: INFORMATION OF WEATHER STATIONS (PRECIPITATION) AND STREAM GAUGING STATIONS (DISCHARGE) FOR HOURLY DATA SERIES

Weather stations

		Period of record		
Number	**Station Name**	**Start**	**End**	**Coverage**
A	Sepulveda Dam	10/1/2008	9/30/2012	81%
3	Long Beach Daugherty Field	10/1/2008	9/30/2012	87%
4	Los Angeles Downtown USC	10/1/2008	9/30/2012	67%

Stream gauging stations

		Period of record		
Character	**Station Name**	**Start**	**End**	**Coverage**
A	Sepulveda Dam	10/1/2008	9/30/2012	97%
B	Los Angeles River at Tujunga Wash (F300-R)	10/1/2008	9/30/2012	100%
C	Los Angeles River above Arroyo Seco (F57C-R)	10/1/2008	9/30/2012	100%
D	Los Angeles River below Firestone Blvd. (F34D-R)	10/1/2008	9/30/2012	100%
E	Los Angeles River below Wardlow River Road (F319-R)	10/1/2008	9/30/2012	100%

3.3.2 Inconsistencies of one of the discharge series

By comparing the hourly discharge series with each other, it is expected that the peaks and the volumes of individual events will increase when the event is flowing downstream. This is because, as far as known, there is no abstraction of water from the river at any point but at several point tributaries enter the river and at other points storm drain outfalls are entering the river. Therefore, it is expected that each stream gauging station further downstream should have recorded a higher volume of the individual event than at the upstream station. And also, due to travel time between the stations, it is expected that the peaks at each further downstream station will show up later as it did at the station upstream of it.

One of the data series, recorded by stream gauging station D, seems to be inconsistent. This can be proved by analyzing events flowing along the LA River, recorded by the different stations. Two representative events are shown in Figure 14, with the observed discharge series for each station. The graphs confirm the expectations given above, except for station D. For each event, this station shows a low total volume and a low peak discharge compared to the stations C and E. This phenomenon can not be explained logically, because as far as known there was no abstraction of water between stations C and E. And if there was any abstraction, the peaks and volumes of the event observed at station D would not have been as low as it is recorded at this stream gauging station, because this would have been an immense amount of water. Because this phenomenon can not be explained, it is suspected that the measurements of the discharge series at station D contains some errors. Due to this unexpected and unexplainable phenomenon it has been decided to leave aside the discharge series observed at station D, the stream gauging station 'Los Angeles River below Firestone Blvd.', coded by F34D-R.

We want to remark that in the Feasibility Study for the Los Angeles River Ecosystem Restoration done by the U.S. Army Corps of Engineers (USACE, 2013a) the station in the LA River below Firestone Blvd. (F34D-R), with these recorded discharge series, which seems to have encountered some measurement errors, has been used. It is not clear in what way the USACE in their study has coped with these errors.

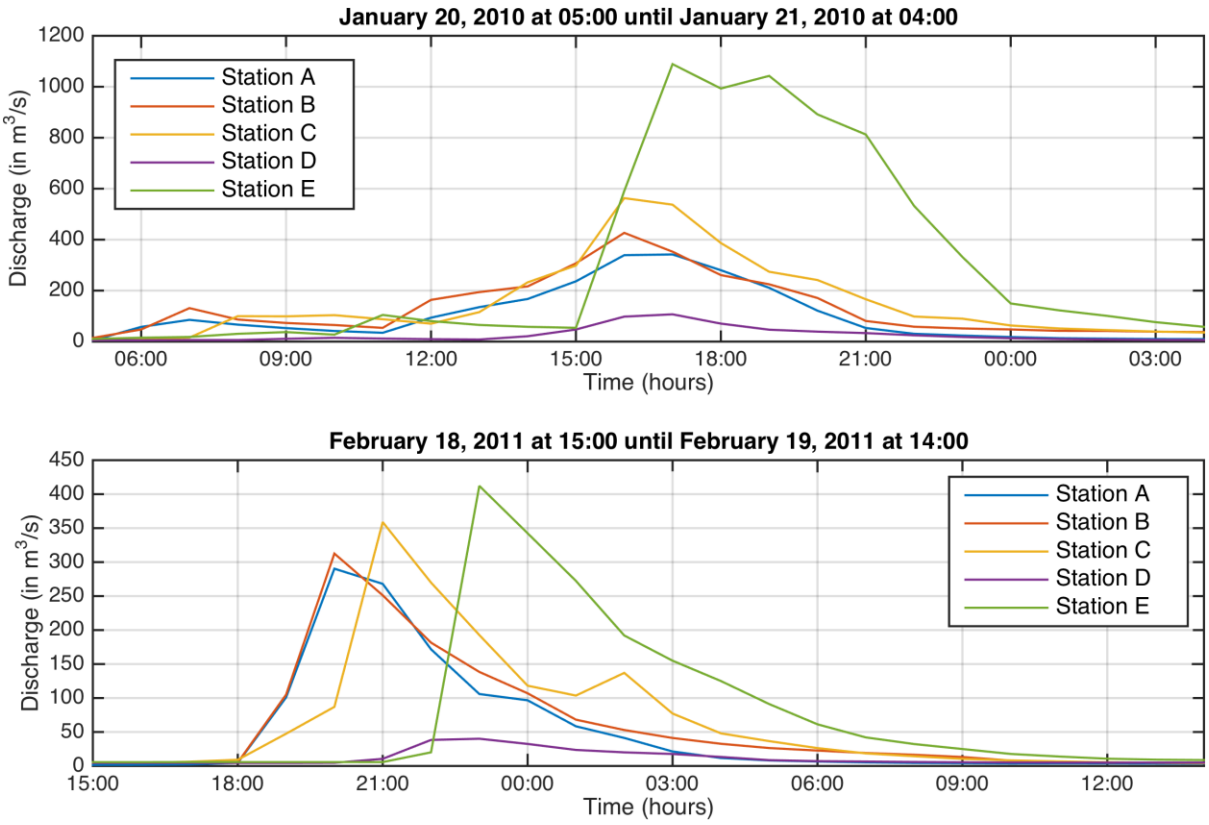

FIGURE 14: TWO EVENTS RECORDED AT THE 5 DIFFERENT STREAM GAUGING STATIONS

3.3.3 Average peak discharge vs. maximum peak discharge

In section 3.2 it is already mentioned in that the peak discharges shown in Figure 13 are the daily averaged peak discharges for each hydrological year from 1960 until 2014. These peak discharges are the average discharges on a day, which means that one discharge value per day is given being the average discharge all day at the given stations. The actual peak discharge will likely be higher. This can be proven with the hourly discharge series of which two example events are given in Figure 14. However, it should be noted that in this study the maximum peak discharge is the maximum hourly averaged discharge. This is still not the real maximum discharge, but it is probably closer than the daily averaged discharge. During the study the real maximum discharges were not available for us.

For the first event, given as an example to support the explanation, the daily averaged peak discharge for station A on January 20, 2010 was 100.81 m^3/s and for station E it was 287.27 m^3/s. The maximum hourly averaged discharge on the same day was for station A 341.93 m^3/s and 1088.89 m^3/s for station E. For this event the maximum (hourly averaged) peak discharge is 3 to 4 times bigger than the daily averaged peak discharge.

For the other event another difficulty was observed. For this event the daily averaged peak discharge for station E on February 18, 2011 was 23.29 m^3/s and on February 19, 2011 it was 70.26 m^3/s (which is a bit higher than can be seen due to another small event at the end of that day). This is because this event was spread out over 2 days, so one part of the event was part of the daily averaged discharge of day 1 and the other part of the event was part of the daily averaged discharge of day 2. This resulted into 2 low average daily discharges, although the maximum peak was much higher, namely 412.20 m^3/s.

These phenomena, as a result of using the daily averaged peak discharges, need to be taken into account further on in this study. The daily averaged peak discharges are taken to determine the frequency distributions in section 3.4, because the maximum peak discharges gathered from the hourly data series are only known for some years, which is too little to determine appropriate frequency distributions.

3.3.4 Relation between discharge series

Another aspect in setting up the model is to calculate the travel time of the event through the river to verify the model results. Therefore, the relation between the discharge series recorded at the different stream gauging stations need to be investigated. Firstly, this is done by just looking at the peaks in the different discharge series. The two representative events given in Figure 14 are used for this rough analysis of the travel times. By comparing the peaks of the first event, which was on 20-21 January, 2010, recorded by the different stations along the river, it can be concluded that this event had a travel time of only 1 hour between station A and station E. This is a distance of more than 50 kilometers, so the average velocity of the peak flowing through the river was about 15 meter per second, which is very fast. During the second event, which was on 18-19 February, 2011, the travel time of the peak between station A and station E was about 3 hours. By investigating other events in the same way it can be found that the range of travel times of events in the available discharge series is between 1 hour and up to more than 6 hours between station A and station E. With this investigation also the relation was found that an event with a high peak discharge has a travel time of 1 hour and an event with a low peak discharge has a travel time of more than 6 hours. So it can be concluded that the higher the peaks the shorter the travel time.

To get a more scientific analysis of the travel times of the events, cross-correlograms of the different discharge series are made. These cross-correlograms are the results of cross-correlation, which is a statistical measure to determine positions of pronounced correspondence between two different data series. The strength of the relationship and the lag or offset in time between the series can be investigated with this method (Davis, 2002). For this study the lag in time, which is actually the travel time, needs to be found. The two series will be placed over each other and than the cross-correlation will be calculated. Then one of the series will be placed one time step forward or backward over the other series and again the cross-correlation is calculated. This process is repeated for each time step backward and each time step forward. In this case the time step is one hour. For this study 12 time steps back and 12 time step further are enough to investigate the lag time. A positive lag time means that the staying data series is leading the moving data series. For the data series in this project positive time lags are expected, so that for example the peak of an event is recorded earlier in station A than in station E.

The cross-correlations have to be done with data series without missing values. The coverage for station A, which is near the Sepulveda Dam, is not 100%, as can be seen in Table 3. Therefore, this data series has been used to gather the largest consecutive data range, which is between February 4, 2010 and February 24, 2011. This time span is used for the discharge series of each station and is expected to be long enough to have a representative series for determining the travel time. The results can be seen in the cross-correlograms that are shown in Figure 15. In the titles for each cross-correlogram the first data series is the moving data series and the other data series is staying. The peaks of the cross-correlograms gives the investigated time lag. This means that the travel time of an event is less than 1 hour between station A and B and between 2 and 3 hours between station A and E. In the data series used for this cross-correlation, from the time span February 4, 2010 to February 24, 2011, both low peaks and high peaks are included, so these are the average travel times of the events between the different stations.

3.3.5 Relation between precipitation and discharge series

The last point in analyzing the data series in more detail is to investigate the relation between the precipitation and the discharge series to prove that the precipitation events recorded at the weather stations correlate with the discharge events recorded at the stream gauging stations. Also a possible correlation between the precipitation and the discharge can be used in the further research to examine the effects of change in precipitation due to climate change. It is expected that the peaks of the precipitation and the discharge do coincide. The investigation of the relation between those data types is done with the same cross-correlation method as described in the previous section.

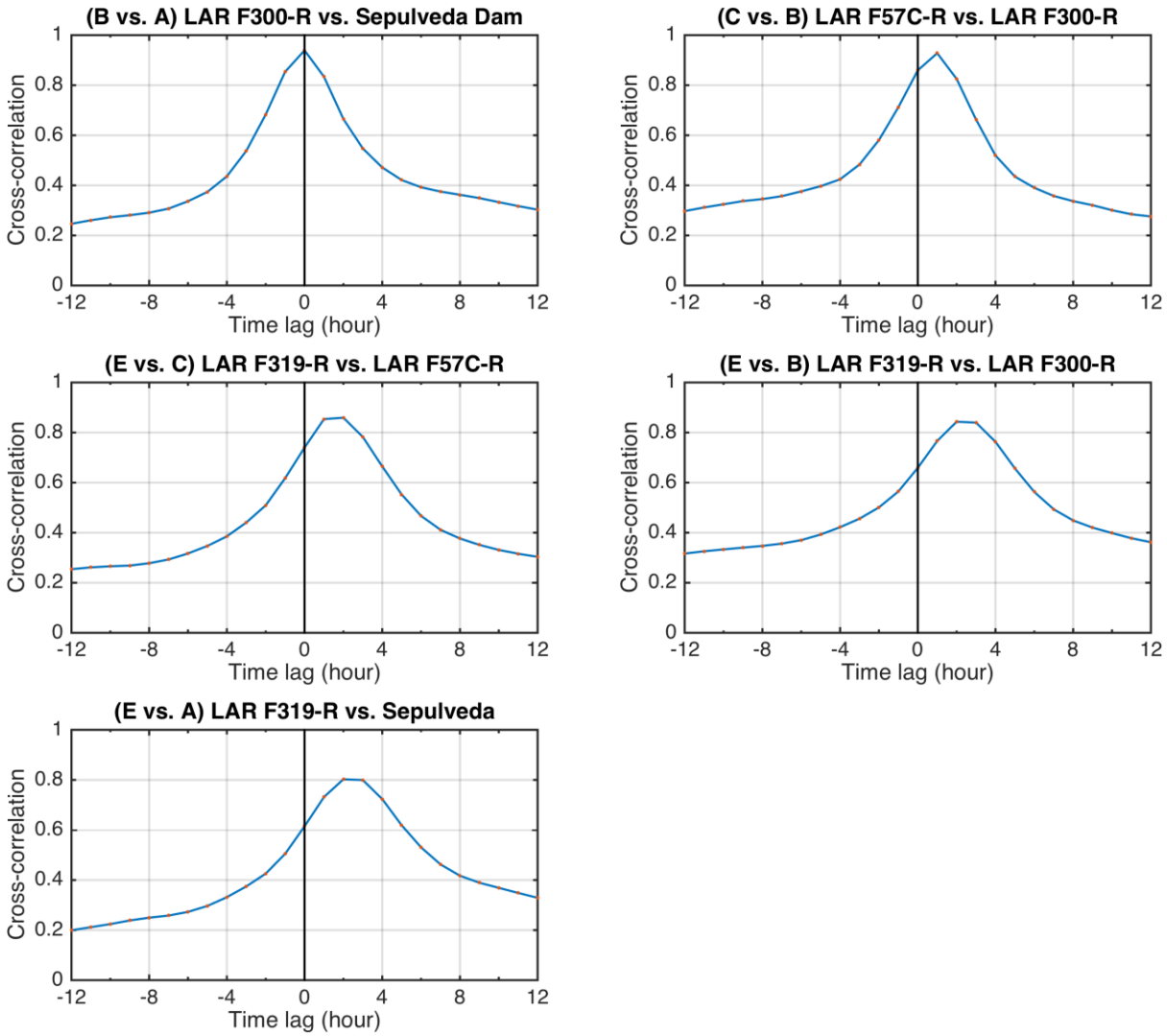

FIGURE 15: CROSS-CORRELOGRAMS FOR THE DETERMINATION OF THE TRAVEL TIMES OF THE DISCHARGE SERIES

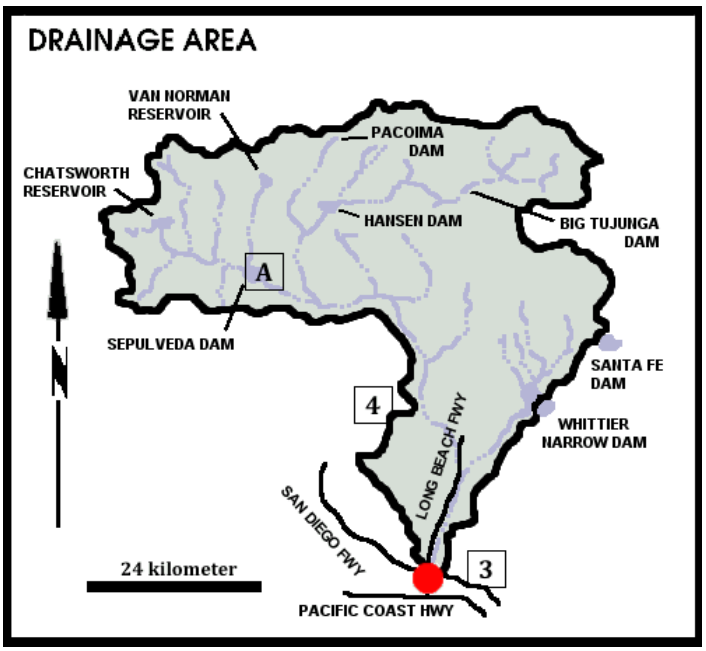

FIGURE 16: DRAINAGE AREA OF THE LOS ANGELES RIVER WITH THE LOCATIONS OF THE WEATHER STATIONS ADAPTED FROM (County of Los Angeles - Department of Public Works, 2015a)

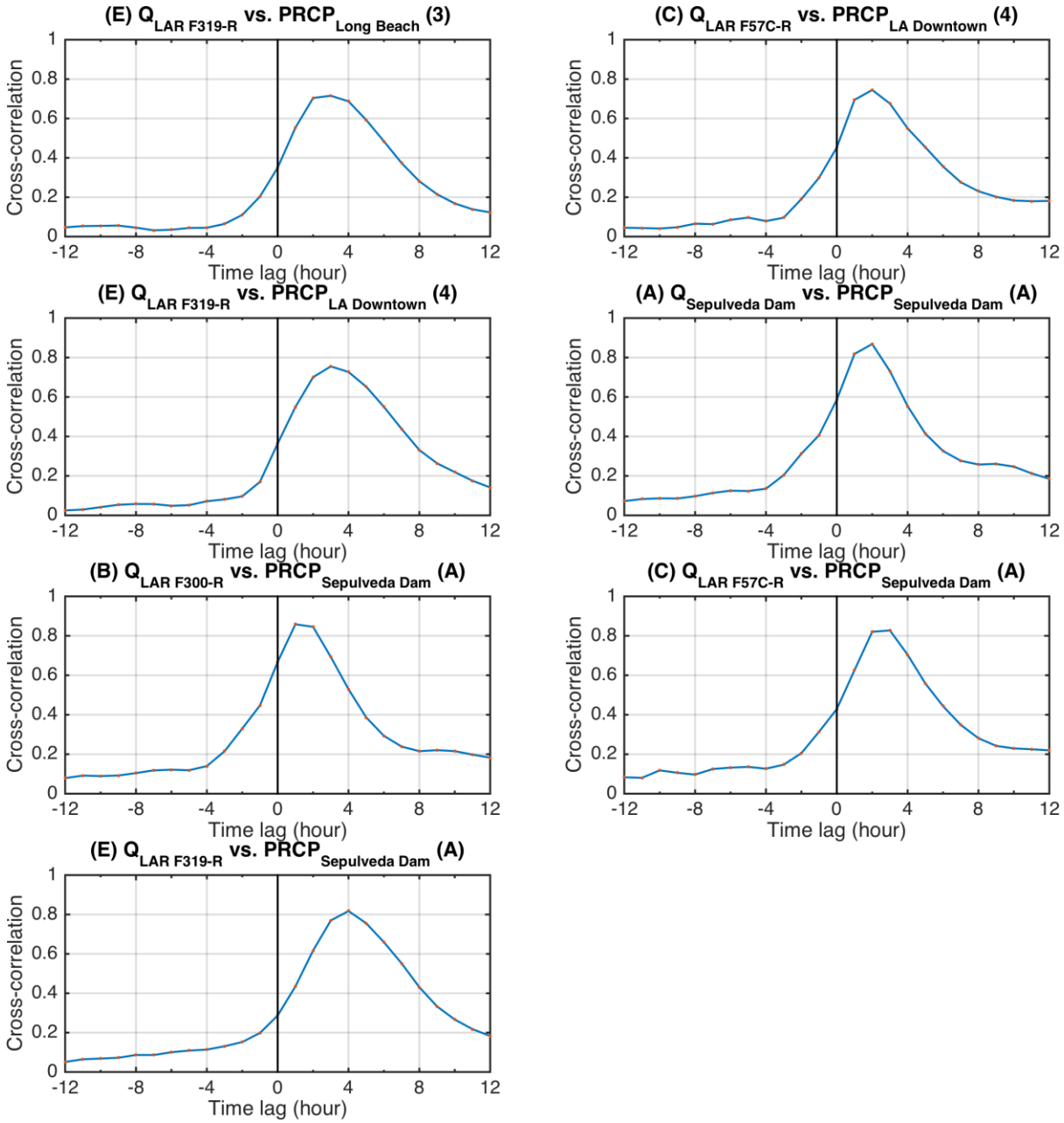

FIGURE 17: CROSS-CORRELOGRAMS OF DISCHARGE SERIES VERSUS PRECIPITATION SERIES

Only one of the weather stations is located in the drainage area of the LA River, namely the weather station near the Sepulveda Dam. The other weather stations are located outside the catchment borders of the LA River catchment. However, these stations are located quite near to the catchment borders, so these stations are used for this investigation too, because the precipitation is measured at a certain location but it is assumed to be representative for a larger area. The locations of the weather stations shown on a map with the drainage area of the LA River are shown in Figure 16. The drainage area on the map is actually the drainage area of the station at point E of the river, but this is close to the downstream boundary at the ocean and in between no other tributary is joining the river.

The cross-correlograms as a result of the cross-correlations between the discharge series and the precipitation series are given in Figure 17. This figure shows the cross-correlograms for weather station 3 with the last stream gauging station, station E, for weather station 4 with stream gauging stations C and E and the weather station at location A with all the stream gauging stations along the river. Only these relations are investigated, because for example the water recorded as precipitation at weather station 3 will not pass the stream gauging stations A, B and C because

these are located much more upstream of the river, so there is no reason to cross-correlate those series with each other. All the cross-correlograms show a high correlation between the peaks of both types of series. This means that the precipitation series correlate with the discharge series. The cross-correlograms show also a time lag between the precipitation event recorded in the weather station and the discharge event recorded in the stream gauging stations. Nevertheless, the travel time between the weather stations and the nearest stream gauging stations is very short, namely less than 3 hours. There is also a remarkable observation that the precipitation measured at weather station A is earlier at station B than at stream gauging station A. This observation could not be explained. The correlogram of discharge at the Sepulveda Dam versus precipitation near the Sepulveda Dam, both with character A, shows a travel time of 2 hours. This is because the weather station and the stream gauging station at location A are not the same stations, but located quite near to each other and therefore labeled by the same location character. The travel time of 2 hours is probably quite high due to the soil type of the Sepulveda Basin, in which the precipitation can infiltrate and travel to the river slower than at other locations, where the precipitation is discharged on a concrete surface.
The cross-correlograms show that there is a relation between the precipitation and the discharge. To use this relation in further research to study the effects of change in precipitation due to climate change on the flood safety of the river, it would be useful to quantify this relation. Therefore, it is tried to find a relation between the amount of precipitation fallen in the catchment and the amount of discharge flowing in the river. However, it turned out that this relation is hard to obtain. It went out that the amount of discharge in the river very much depends on the locations where the precipitation is fallen in the catchment and on the intensity of the precipitation at these locations. In most of the cases for the used hourly data series of 4 years the precipitation has been fallen in a part of the catchment and not in the whole catchment. This means that the area in which precipitation is fallen differs, which makes it hard to find a relation between the amount of precipitation and the amount of discharge. Therefore, we did not succeed to quantify the relation between the amount of precipitation and the amount of discharge.

3.4 Frequency distribution

To estimate the chance of flooding in the Los Angeles River at different locations, a frequency distribution is determined for the different stream gauging stations. There are two methods to select the peak discharges to be used for the frequency distribution: (1) the peak discharges per year or (2) the peak discharges above a threshold (Booij, 2010). In this study both methods are used. For the first method the peak discharges per hydrological year for each of the stream gauging stations, are selected to fit the distributions, for the hydrological years 1960 to 2014. The hydrological years in which no discharge is available are deleted from the samples, which means that in the data series for the distributions the hydrological years and their corresponding peak discharges are not completely consecutive.
For the second method the top highest peaks are chosen to fit the distributions. How many extreme discharges are used depends on the number of years for which data is available, which differs per stream gauging station. For example, for the station near the Sepulveda Dam data of 32 hydrological years is available, so the top 32 peaks are chosen. For this method a condition is required, which is independency of the peaks (Booij, 2010). This condition is achieved by taking peaks that occurred at least 10 days from each other. If there have occurred peaks within 10 days of each other, the highest peak is taken only. The events are usually of a length of less than 2 days, however, to be sure that the peaks are completely independent a much larger margin between peaks have been chosen.
These data series are used to fit three different statistical distribution types, namely the Gumbel distribution, the Generalized Extreme Value distribution and the Log-Pearson Type III distribution.

3.4.1 Gumbel distribution

The Gumbel distribution is a statistical distribution which is used often in hydrological analysis studies to model extreme events. This distribution is also known as the Extreme Value Type I distribution, which is a special case of the Generalized Extreme Value distribution (Shaw, Beven, Chappell, & Lamb, 2011). The equation of the Gumbel distribution is described by:

$$F(X) = e^{-e^{-\left(\frac{X-a}{b}\right)}} \quad (1)$$

In which $F(X)$ is the probability of an annual peak discharge X, a is the location parameter and b is the scale parameter. The parameters a and b are defined as:

$$a = \mu - \gamma b \quad (2)$$

$$b = \frac{\sigma\sqrt{6}}{\pi} \quad (3)$$

in which μ is the mean of the sample of peak discharges, σ is the variance of the sample of peak discharges and γ is the Euler's constant, which is 0.5772.

3.4.2 Generalized Extreme Value distribution

The Generalized Extreme Value (GEV) distribution is a statistical distribution type which combines the Gumbel, Fréchet and Weibull distributions. Those distributions are known also as the Extreme Value Type I, Type II and Type III distributions, respectively. This GEV distribution is a classical method for fitting extremes and is often used in hydrological analysis studies in the Netherlands (Brink, Können, & Opsteegh, 2005; Wit & Buishand, 2007).
The equation of the Generalized Extreme Value distribution is described by:

$$F(X) = e^{-\left(1+k\left(\frac{X-a}{b}\right)\right)^{-\frac{1}{k}}} \qquad for\ k \neq 0 \quad (4)$$

in which $F(X)$ is the probability of an annual peak discharge X, a is the location parameter, b is the scale parameter and k is the shape parameter. If the shape parameter k is not equal to 0, the distribution is called the type I or Gumbel distribution, as given before. When the shape parameter is positive the distribution is called the type II or Fréchet distribution and when the shape parameter is negative the distribution is called the type III or Weibull distribution (Millington, Das, & Simonovic, 2011).
The parameters a and b are defined as:

$$a = \mu - b\left(\frac{\Gamma(1-k)-1}{k}\right) \qquad if\ k \neq 0,\ k < 1 \quad (5)$$

$$b = \frac{\sigma k}{\sqrt{g_2 - {g_1}^2}} \qquad if\ k \neq 0,\ k < 0.5 \quad (6)$$

$$g_j = \Gamma(1-jk) \qquad with\ j = 1, 2 \quad (7)$$

in which μ is the mean of the sample of peak discharges, σ is the variance of the sample of peak discharges, k is the fitted shape parameter and $\Gamma(n)$ is the gamma function, defined as:

$$\Gamma(n) = (n-1)! \qquad if\ n > 0 \quad (8)$$

The shape parameter needs to be estimated to get the best fit. Because it is a time consuming work to get the best estimate for k and thus to get the best fit of the Generalized Extreme Value distribution, the software program EasyFit Professional has been used. EasyFit Professional is data analysis software to automatically fit a large number of distributions to data provided and to select the best model in seconds (Mathwave Technologies, 2015).

3.4.3 Log-Pearson Type III distribution

The Log-Pearson Type III distribution is the recommended distribution type by the U.S. Water Resource Council to be used by the Federal Agencies in the United States for hydrological analysis studies (Millington et al., 2011).
The Log-Pearson Type III distribution is a member of the family of Pearson Type III distributions. It consists of three parameters: the location parameter μ, the scale parameter σ and the shape parameter γ. The Pearson Type III distribution can be described by (Hosking & Wallis, 1997; Millington et al., 2011):

$$F(X) = G\left(\alpha, \frac{X-\xi}{\beta}\right)/\Gamma(\alpha) \qquad if\ y > 0 \tag{9}$$

$$F(X) = 1 - G\left(\alpha, \frac{\xi-X}{\beta}\right)/\Gamma(\alpha) \quad if\ y < 0 \tag{10}$$

in which $\alpha = 4/\gamma^2$, $\beta = \frac{1}{2}\sigma|\gamma|$ and $\xi = \mu - 2\sigma/\gamma$. The function $\Gamma(\alpha)$ is the gamma function as defined in formula 8 and the function $G(\alpha, X)$ is the incomplete gamma function, defined as:

$$G(\alpha, X) = \int_0^X t^{\alpha-1}e^{-t}dt \tag{11}$$

With the Log-Pearson Type III distribution, the logarithm of the discharge for any recurrence time is calculated using the following equation (Oregon State University, 2007):

$$\log X = \overline{\log X} + K\sigma_{\log X} \tag{12}$$

in which X is the flood discharge value of some specified probability, $\overline{\log X}$ is the average of the $\log X$ discharge values, K is the frequency factor and $\sigma_{\log X}$ is the standard deviation of the $\log X$ discharge values. The frequency factor $K$is a function of the skew coefficient C_s and the return period. This factor can be found using the frequency factor table provided by the IACWD (1982), given in Appendix A: Frequency factors for Log-Pearson Type III Distributions.
The standard deviation of $\log x$, $\sigma_{\log x}$, can be calculated by the following formula:

$$\sigma_{\log x} = \sqrt{\frac{\sum_i^n \left(\log x - \overline{\log x}\right)^2}{n-1}} \tag{13}$$

in which n is the number of entries, so the number of hydrological years of which the peak discharges are used to fit the distributions with.
The skew coefficient C_s, which is needed to determine the frequency factor K in the frequency factor table, can be calculated with the following formula:

$$C_s = \frac{n\sum_i^n \left(\log x - \overline{\log x}\right)^3}{(n-1)(n-2)\left(\sigma_{\log x}\right)^3} \tag{14}$$

With these formulas the recurrence times are calculated.

3.4.4 Results

All three types of distribution are applied to the peak discharges of the hydrological years 1960 to 2014, of which the results are shown in Figure 18, and to the top extreme discharges of the different stations, of which the results are shown in Figure 19. Table B 1 and Table B 2 in Appendix B: Parameters corresponding with extreme value distributions give the corresponding values of the parameters for each distribution type for the first and second method, respectively. For this study the discharges belonging to the recurrence times of once in 1.0101 years to once in 1000 years are investigated.

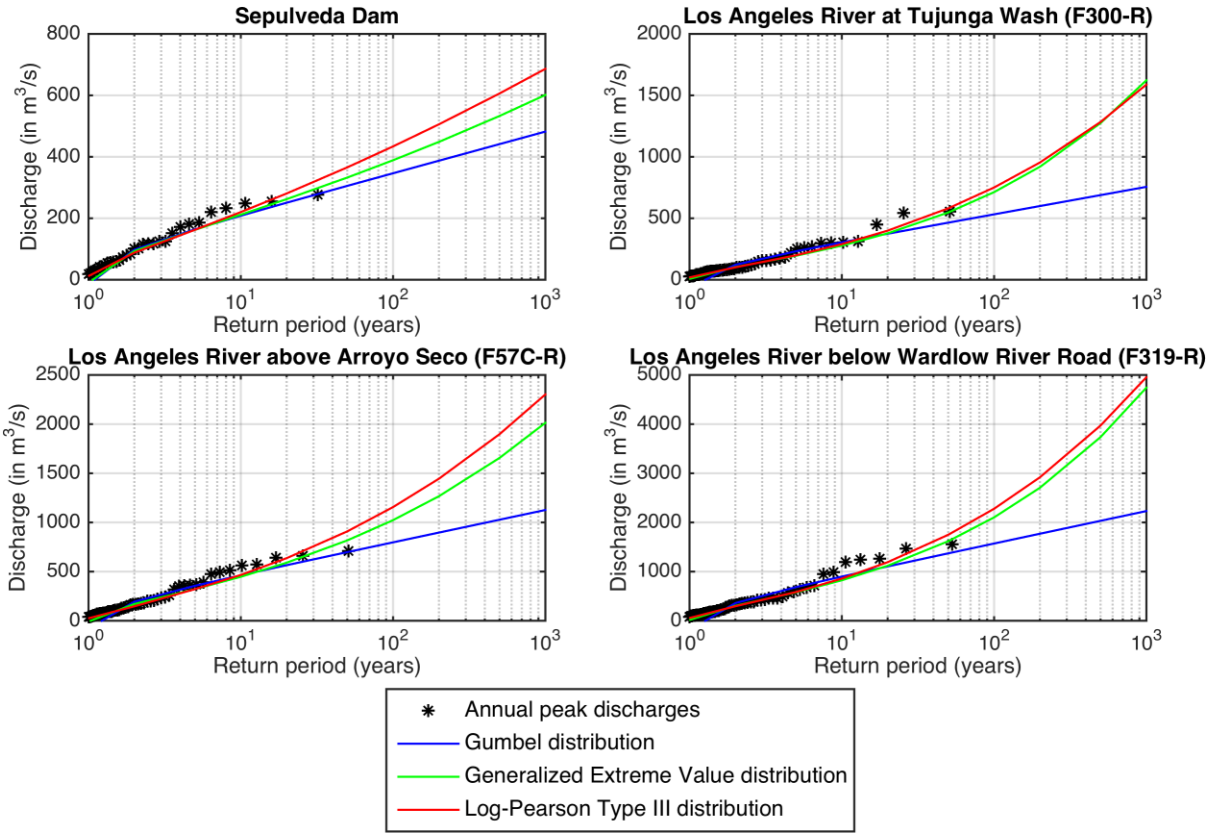

FIGURE 18: EXTREME VALUE DISTRIBUTIONS FOR DIFFERENT STREAM GAUGING STATIONS ALONG THE LOS ANGELES RIVER WITH ANNUAL PEAK DISCHARGES (FIRST METHOD), WITH LOGARITHMIC X-AXIS

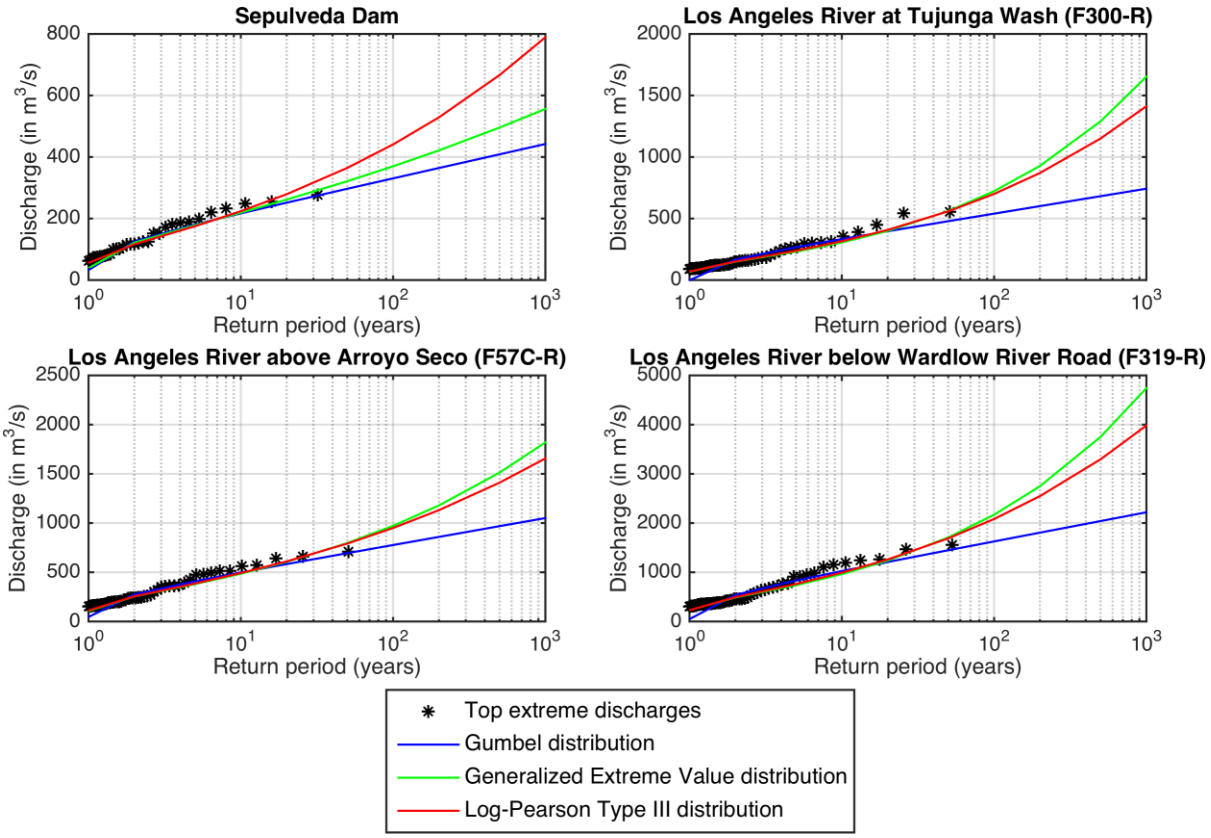

FIGURE 19: EXTREME VALUE DISTRIBUTIONS FOR DIFFERENT STREAM GAUGING STATIONS ALONG THE LOS ANGELES RIVER WITH TOP EXTREME DISCHARGES (SECOND METHOD) (TOP 32 FOR STATION AT SEPULVEDA DAM, TOP 51 FOR STATION F300-R, TOP 51 FOR STATION F57C-R AND TOP 53 FOR STATION F319-R), WITH LOGARITHMIC X-AXIS

Both figures show that none of the distribution types fit the historical extreme discharges perfectly, which also was not expected. The Gumbel distribution shows very low values of discharge, and even negative values with the first method, for a short recurrence time (less than 1.5 years), which underestimates the recorded data. This Gumbel distribution estimates also lower discharge values for high return times. The Generalized Extreme Value distribution and the Log-Pearson Type III distribution looks quite similar for both methods. However, the GEV-distribution gives mostly slightly lower discharges for the same recurrence times than the Log-Pearson Type III distribution for the first method. By using the method of the top extreme peak discharges, it is the other way around. Although these distributions look very similar, both distributions fit not very well. Especially for the highest measured peak discharges for each station the distributions do not follow the trend in the data accurately.
Both figure show also a wide range of extreme discharges at a recurrence time of once in 100 years and even more at once in 1000 years. For example, by looking at the stream gauging station F300-R it can be seen that by applying the Gumbel distribution to the annual peak discharges (first method) the peak discharge at a recurrence time of once in 1000 years is estimated at about 750 m^3/s, while by applying the GEV-distribution the peak discharge once in 1000 years is estimated to be about 1620 m^3/s which is almost 900 m^3/s higher. There are even much more extreme examples, which can be seen also in the Figure 18 and Figure 19. Although a distribution type has to be chosen, it is clear that with each distribution type the results will have a high degree of uncertainty.
By comparing both figures it is visible that for each stream gauging station the Generalized Extreme Value distribution, applied by using the annual peak discharges and by using the top extreme discharges, are quite similar for both methods. This is the case for the Gumbel distribution too. However, the Log-Pearson Type III distribution give quite different results in applying the different methods. This shows that there is also a certain degree of uncertainty in the results by choosing a method for selecting the extreme discharges for the frequency distributions, especially for the Log-Pearson Type III distribution.

To choose a frequency distribution and a method for selecting extreme discharges the coefficient of determination (R^2) and the root-mean-square error (RMSE) is calculated for all distributions and methods. The R^2 is a frequently used measure of the goodness of fit of a distribution. The R^2 is calculated with the following formulas:

$$R^2 = 1 - \frac{SS_{res}}{SS_{tot}} \quad (15)$$

$$SS_{tot} = \sum(y_{obs} - y_{mean})^2 \quad (16)$$

$$SS_{res} = \sum\left(y_{obs} - y_{pred}\right)^2 \quad (17)$$

in which y_{obs} are the observed values of annual peak discharges (first method) or top extreme discharges (second method), y_{mean} is the mean of the observed data and y_{pred} are the predicted values by the different distributions. A value of 1 for the R^2 is a perfect fit, so the closer the value for R^2 to 1, the better the distribution fits the observed values.
The RMSE is a frequently used measure of differences between the predicted and observed values, and is calculated by the following formula:

$$RMSE = \sqrt{\frac{1}{n} * \sum\left(y_{pred} - y_{obs}\right)^2} \quad (18)$$

in which y_{pred} are the predicted values by the different distributions and y_{obs} are the observed values of annual peak discharges (first method) or top extreme discharges (second method). The lower the RMSE the better the distribution predicts the observed values.
Table 4 shows the R^2 and RMSE values for the distributions for each stream gauging station and for each method of selecting extreme discharges.

TABLE 4: R^2 AND RMSE FOR THE FREQUENCY DISTRIBUTION TYPES FOR EACH STREAM GAUGING STATION AND FOR BOTH METHODS OF SELECTING EXTREME DISCHARGES

Coefficient of determination (R^2)

	Annual peak discharges			Top extreme discharges		
Station	**Gumbel**	**GEV**	**LPIII**	**Gumbel**	**GEV**	**LPIII**
A	0.962	0.964	0.968	0.958	0.962	0.953
B	0.902	0.970	0.971	0.899	0.969	0.973
C	0.938	0.951	0.945	0.935	0.947	0.957
E	0.903	0.957	0.959	0.911	0.939	0.952

Root Mean Square Error (RMSE)

	Annual peak discharges			Top extreme discharges		
Station	**Gumbel**	**GEV**	**LPIII**	**Gumbel**	**GEV**	**LPIII**
A	16.42	15.96	18.84	14.02	13.62	17.73
B	39.23	28.70	27.35	35.96	26.54	26.13
C	46.46	43.83	51.37	39.66	37.75	39.75
E	114.83	90.97	87.55	98.99	89.74	87.02

For most of the stations and with both methods the Gumbel distribution fits the worst according to the R^2 and RMSE. This distribution type gives also the most different results with respect to the other distribution types. The other two distribution types give almost the same results for the R^2 and RMSE. However, by comparing the R^2 and RMSE values of both distribution types to each other it can be concluded that the Generalized Extreme Value distribution using the method of selecting annual peak discharges fits the best to the extreme discharges observed. Therefore, the GEV-distribution based on annual peak discharges is chosen to be used later on in this study.

Finally, we want to emphasize again that the extreme discharges used for the extreme value distributions are daily averaged discharges. The extreme value distributions based on the daily averaged discharges and probably will have a different shape and will give different results than when it is based on the hourly averaged discharges or on based on the real peak discharges. This is due to the different shapes of the hydrographs, which has been explained in section 3.3.3. Due to this fact and due to the other uncertainties mentioned above, the distributions used for this study have a high level of uncertainty. This indicates also the difference in magnitude of the return times between those determined with the extreme value distribution and those used in the Feasibility Study of the USACE (2013b), which are also shown in Appendix C: Frequency discharges used in the Feasibility Study of the USACE, because the return times used by the USACE are determined with real peak discharges. Those latter return times vary on average between once in 10 years and once in 50 years for the reach of the river between station B and station C. It is not known by us if the river has been flooded in the period of which the extreme discharges are taken for the extreme value distributions and also not on which locations this happened. Other differences between the return times found in this study and the return times used in the study of the USACE will be discussed in section 6.3.

4 SETTING UP THE MODEL

In this chapter the model set up is described, the assumptions made for this model are described as well as the calibration and validation of the model. For setting up the model the data as described in the previous chapter is used.

4.1 MODEL DESCRIPTION

For this study a two-dimensional model is set up to predict the flow characteristics of an event flowing through the river. We believe that a two-dimensional model is better able to simulate the LA River. Also the USACE recommended in their study to set up a two-dimensional flow model to simulate more accurately the proposed alterations in and adjacent to the channel (USACE, 2013b). For this study the model Delft3D is used, developed by Deltares. It is a two and three dimensional modelling suite to investigate hydrodynamics, sediment transport, morphology and water quality for fluvial, estuarine and coastal environments (Deltares, 2015a). The model solves the unsteady two and three dimensional shallow-water equations to predict the flow for shallow seas, coastal areas and river systems. This model has the advantage of having an easy coupling with Geographic Information Systems (GIS), which is convenient for this project. For this study the two dimensional (depth-averaged) option of the module Delft3D-FLOW is used to investigate the hydrodynamics. The morphology is neglected in this study. In order to prepare the model, also some other tools provided with Delft3D are used, namely the grid generation module RGFGRID and the data interpolation module QUICKIN. The next sections describe the most important steps and the associated assumptions during the preparation of the model.

4.1.1 Staggered grid

The module Delft3D-FLOW uses a numerical method based on finite differences. Therefore, the model area is covered by a grid. To discretize the shallow water equations, the variables water level and velocity (u, v, w) are arranged in a special way on the grid. The pattern of this grid is called a staggered grid. In this staggered grid the water level points are defined in the center of a cell and the velocity components are perpendicular to the grid cell faces where they are situated (Deltares, 2014a). Figure 20 shows the location of the variables in a grid cell.

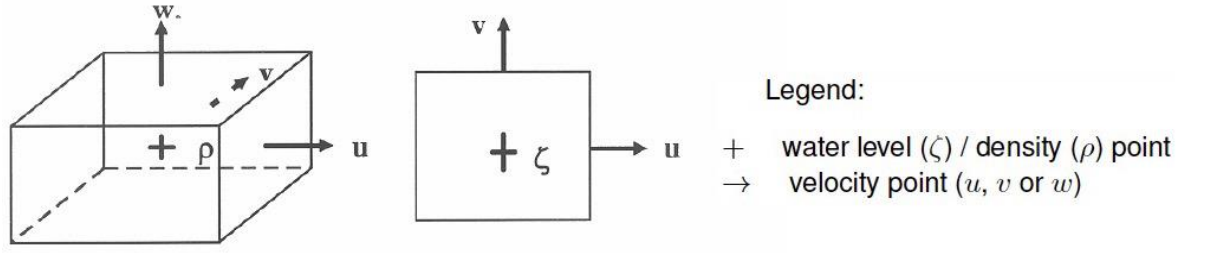

FIGURE 20: GRID STAGGERING, 3D VIEW (LEFT) AND TOP VIEW (RIGHT) (DELTARES, 2014A)

In the staggered grid system, the grid numbering and the definition of the computational control volume is different. This is made visible in Figure 21. In part (a) of the figure the staggered grid is given with the numbering, indicating which water level, velocity components and depth have the same number in m- and n-direction in the computational code. The numerical grid is drawn through the depth points, because these are the points defined at the corners of the computational control volume, which can be seen in part (b) of Figure 21. Depth is the technical term used in Delft3D, which means the bottom depth with respect to the reference depth. In this study the reference depth is the mean sea level, so the depth points higher than the reference depth, which is the case almost everywhere in the grid, will appear as negative values. In the staggered grid the

numerical grid is the same as the morphologic grid (Figure 21 part (c)). This means that the morphologic parameters are calculated in the depth points, the points on the corner of the grid. The water level points are calculated on a different place than the depth points. This means that the hydrodynamic grid is different than the numerical grid. This is shown in Figure 21 part (d). On the corners of the hydrodynamic grid the water level is calculated.

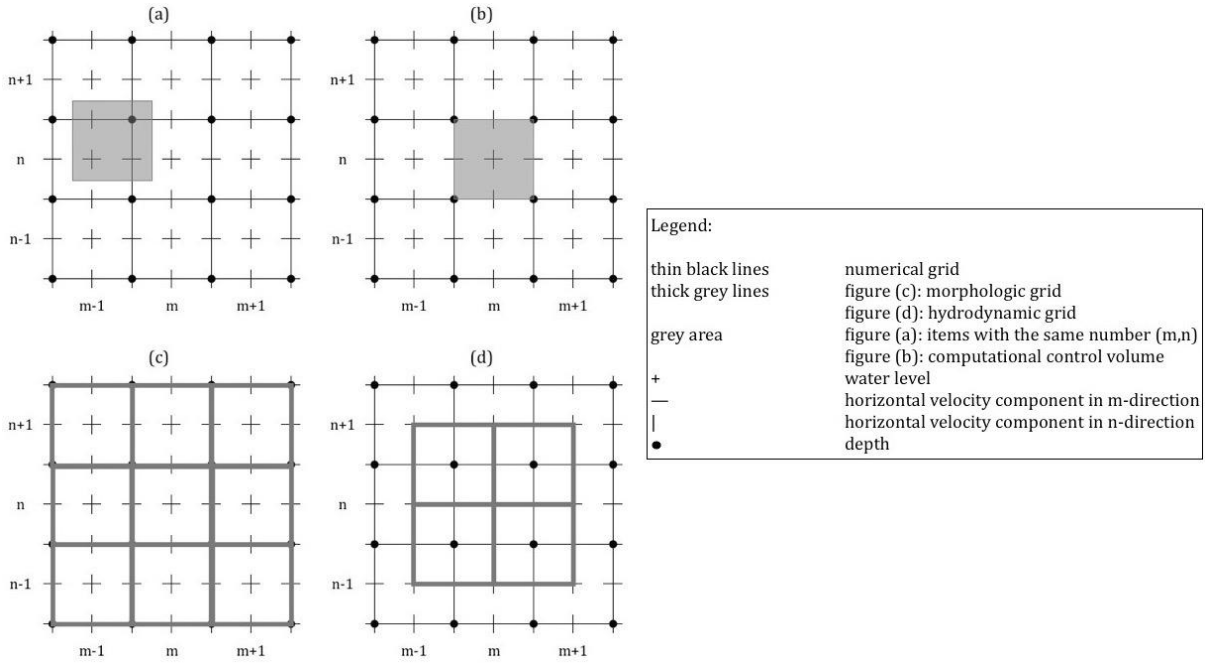

FIGURE 21: TOP VIEW OF STAGGERED GRID: (A) ITEMS WITH SAME NUMBER (M,N); (B) COMPUTATIONAL CONTROL VOLUME; (C) MORPHOLOGIC GRID; (D) HYDRODYNAMIC GRID

4.1.2 Grid generation

The grid used for this model is a curvilinear grid in a Cartesian coordinate system, which is built with the module RGFGRID. This kind of grid has the advantages to allow curves along the channel or land boundaries without having 'stair-case' boundaries and to provide low grid resolution at places of low interest and high grid resolution at places of high interest (Deltares, 2014c). However, to get accurate results in the simulation, the curvilinear grids have to fulfill some requirements. Therefore, the step of making a grid is a very important but also time-consuming task.

Each part of the LA River that has to be taken into account for this study needs to be covered by grid cells. By covering the river by grid cells some rules have to be taken into account. The smaller the grid cells and thus the larger the amount of grid cells the higher the degree of accuracy. On the other hand, the larger the amount of grid cells the more computing time is needed. A balance has to be found between the accuracy of the model and the computing time needed for the simulations. The following decisions were made with regard to this balance. (1) During this study it was discovered that discharge data for the part of the river upstream of the Sepulveda Dam, the reaches 1 and 2 in Figure 4, was almost not available. Therefore, the part of the river upstream of the Sepulveda Dam is not included in the model. (2) Only the places adjacent to the river at which measures will be taken that are investigated in this study are covered by grid cells. (3) To observe when the river is flooding, also the floodplains along the river are modelled. However, the size of the floodplains covered by grid cells, is limited to 2 grid cells.

In this model it is tried to cover the Los Angeles River by 8 grid cells on each cross section. The floodplains on both sides are covered by two grid cells. This makes a grid of 12 cells per cross section, apart from the places where measures are planned. In practice this goal is not achieved completely, due to a very sinuous river at some places, especially in the part of the river between Sepulveda Dam and the 90-degree corner at Griffith Park, which are the reaches 3 and 4 in Figure

4. This means that each cross section is covered by 12 grid cells, but not each cross section consists of 8 cells for the river and 4 cells for the flood plains. The minimum amount of cells covering the river in a cross section is 4. This together gives quite a large grid with a length (M-direction) of 2199 grid cells, a maximum width (N-direction) of 63 cells (at the Piggyback Yard) and in total almost 29,000 grid cells. The grid generated with RGFGRID for the Los Angeles River is shown in Figure 22.

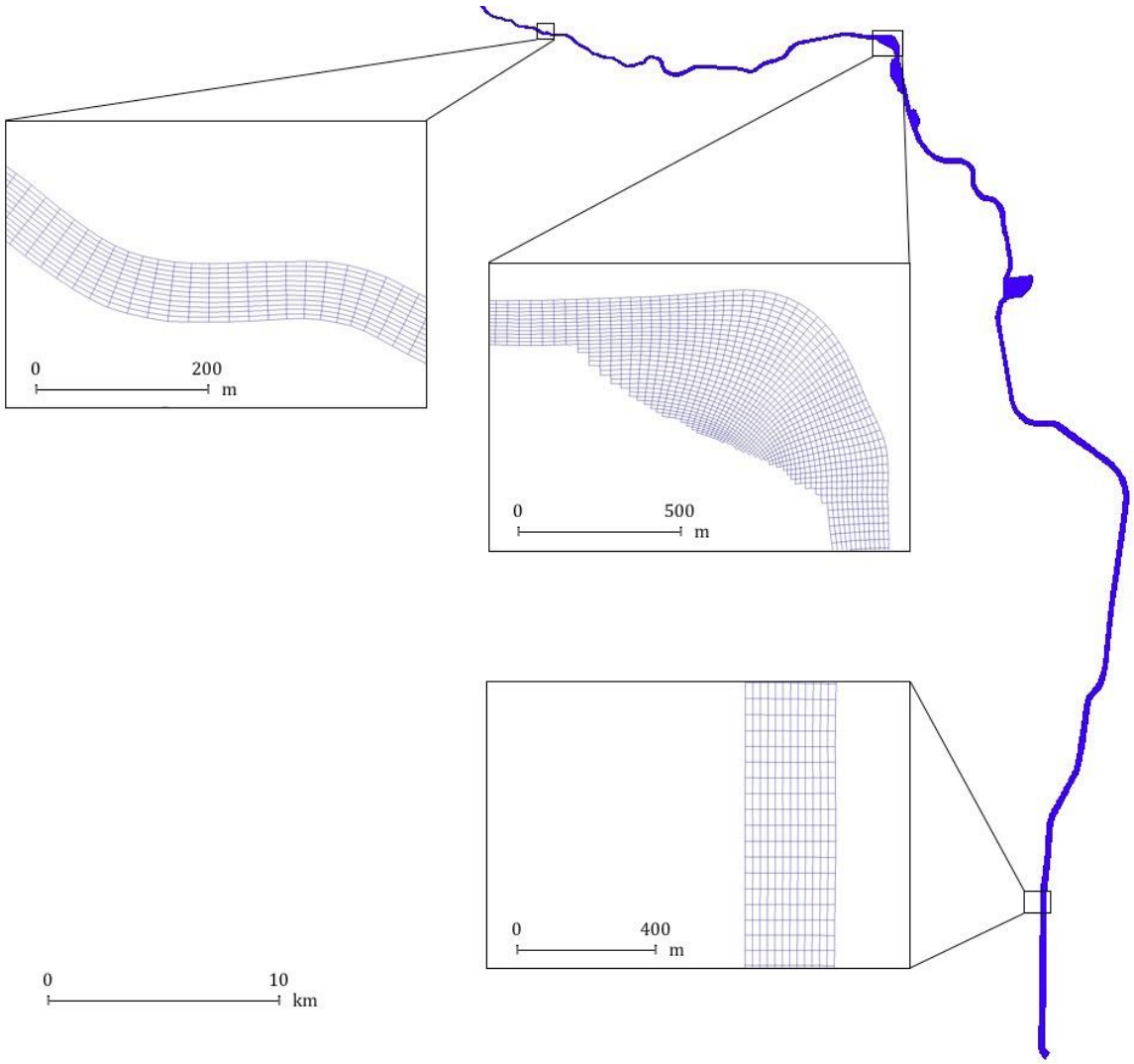

FIGURE 22: GRID OF THE LOS ANGELES RIVER GENERATED WITH MODULE RGFGRID OF THE SUITE DELFT3D

The grid has to fulfill some criteria set by the software developer Deltares to reach a certain grid quality, namely the orthogonality, smoothness and aspect ratio. The meanings of these criteria are explained below.

Orthogonality

The grid has to be orthogonal, which means the grid lines must intersect perpendicularly. The orthogonality of the grid cells is measured by the cell-centered cosine value. It is recommended to have this value less than 0.04 in the model area of high interest. In the model area of lower interest, a value of up to 0.10 can be tolerated (Deltares, 2015b). Deviation of the cosine from zero will result proportionally in errors in the direction of the pressure gradient in the module Delft3D-FLOW. Having a curvilinear grid makes it more difficult to get the grid lines intersect perpendicularly, especially in the sharp bends of the river. In the generated grid used for this study the orthogonality in the area of high interest, which is the river itself, is less than 0.04. In the floodplains the orthogonality is in some places higher, especially in the sharp corner near

Griffith Park. However, the value of orthogonality at these places is everywhere lower than 0.10, except for the last row of grid cells at the Pacific Ocean, where the orthogonality is at maximum 0.11. This will lead to less accurate results for the very last part of the model, however, the results of this part of the river are not relevant for this study.

Smoothness
The grid needs also to vary smoothly. Therefore, the smoothness of the grid in the M-direction and the N-direction needs to be sufficient. This smoothness is measured by the ratio of neighboring grid cell dimensions. The value of smoothness of each cell is recommended to be less than 1.2 in the area of interest and can be up to 1.4 further away (Deltares, 2014c, 2015b). The grid of this model has smoothness values in the M-direction of less than 1.2. The highest value is in the sharp corner at Griffith Park, namely 1.18. The smoothness values in the N-direction are less than 1.2 in the area of high interest, which is the Los Angeles River. In some floodplain areas, especially in the corner at Griffith Park and in the Piggyback Yard, the smoothness values are a bit bigger, but the maximum smoothness value is 1.4 exactly, which is just inside the range of the smoothness criterion.

Aspect ratio
The aspect ratio is the measured ratio of grid cell dimensions in M-direction and N-direction. This value is recommended to be in the range of 0.5 to 2, but in case of one-directional flow phenomena also a larger value of up to 5 is allowed (Deltares, 2015b). The generated grid for this research project is for river flow, which is mainly in one direction, namely downstream. In the grid for this study all aspect ratio values are less than 5.

The grid meets the requirements set for the orthogonality, smoothness and aspect ratio. The ranges of the required orthogonality, smoothness and aspect ratios are recommended ranges for which it is recommended to be at the lowest side of the recommended ranges of these ratios. However, these ratios are counteracting each other, which means the process of grid generation is an iterative process in which a balance has to be found between the values of the different ratios. Especially in the river bends it is not possible to have the lowest ratio values for each criterion. As a result of some higher values for the different criteria ratios the results are influenced by the limitations of a grid.

4.1.3 Bathymetry
Each of the grid cells needs to have a depth value for each grid cell point. As already stated in section 4.1.1 is the reference depth the mean sea level, defined at the elevation level of 0 meter. This means that almost all depth values are negative, because almost all of them are higher than mean sea level. In practice the elevation at every place is multiplied by -1 to get the depth value. The elevations along the river, referred to as the bathymetry, is obtained from a Digital Elevation Map (DEM) of the Los Angeles County. This DEM is acquired as part of the Los Angeles Regional Imagery Acquisition Consortium (LAR-IAC) in 2006, and is made public within the partnership of the US Geological Survey (USGS) (Los Angeles County, 2011). This DEM contains the elevation in feet of the landscape and includes buildings, vegetation, bridges, roads and also water levels. The publicly available DEM has a resolution of 10 foot (3.048 meter) and is converted from feet into meters for the purpose of this research project. The DEM was obtained by use of LIDAR, which stands for Light Detection and Ranging. It is a remote sensing technique that measures variable distances to the earth by using pulsed laser. These light pulses generate precise, three-dimensional information about the shape of the earth (NOAA, 2015b).
The DEM is converted from a GIS-format to an XYZ-format to be able to be combined with the grid. This is done with the Delft3D module QUICKIN. Most of the grid cells consist of more than one sample point, and to allocate a depth value to each grid cell point the tool 'Grid Cell Averaging' in QUICKIN is used. This tool averages the samples in the vicinity, which is the area covered by an 8-point polygon surrounding the grid point. Four points are the cell centers of the four

surrounding grid cells and the other four point are the points halfway between the grid point and its neighboring grid points (Deltares, 2014b).
With this technique the problem arises that in the DEM the elevation of the bridges is given, but not the elevation of the river below the bridges. The water can flow underneath the bridges, so these bridges in the bathymetry are removed by linear interpolating the depth values upstream of the bridges with the depth values downstream of the bridges. In the DEM also the elevation of the vegetation in the river is given instead of the elevation of the bottom of the river. This vegetation is also removed from the DEM by linear interpolation and is taken into account in the roughness file, which is explained in the next section.
Another problem of this LIDAR technique is that the elevation of the water level is measured and not the bottom elevation of the river below the water surface. However, an advantage of the Los Angeles River for this study is that most of the time the river is almost empty. To check if the river was empty during the measurements with the LIDAR technique, the bathymetry on several locations along the river is compared with the cross sections used for the one-dimensional HEC-RAS model of the Los Angeles River, used for the Feasibility Study of the USACE (2013b). Especially the bottom elevation of the river in the DEM is compared with the bottom elevation of the cross sections used in HEC-RAS model. On about 80% of the cross sections the elevation given by the DEM was equal to the elevation given by the cross sections of the HEC-RAS model, which means that the river at these places was empty during the measurements. On some places the difference was less than 0.5 meter and especially near the estuary the elevation given by the DEM differed up to 3 meter from the elevation given by the cross sections of the HEC-RAS model. The bottom elevation given by the cross sections of the HEC-RAS model is seen as leading and the bathymetry generated for this research project is corrected accordingly.
The slopes of the river walls are assumed as being correctly measured by the LIDAR method to generate the DEM. However, due to the resolution of the DEM and moreover, due to the grid size it is impossible to implement the slopes of the river walls 100% correctly. Therefore, this is also one of the limitations of the grid. At some places along the river the walls are vertical, but on other places the walls have a certain slope. In the model these slopes are represented as a staircase.
One last aspect to mention about the bathymetry is the way in which the depth values are used. The depth values can be defined at the corners or at the centers of the grid cells. Defining them at the corners of the grid cells is the default option of module QUICKIN, and therefore this method is used, as can be seen in Figure 21. However, the water level is calculated in the cell center of the grid cell. To calculate the water level in a grid cell the four depth values at the corners of the cell are used to determine one depth value for each grid cell, to be used in the calculations. In the module Delft3D-FLOW different methods of determining these depth values are possible. It is possible to pick the maximum, minimum or mean value of those four depth values. Each method will give different results, because the river will be wider by picking the minimum values or smaller by picking the maximum values. The method of picking the maximum value of the four depth values is the default and recommended method (Deltares, 2014a). However, it became clear during setting up the model that the river in the model would become smaller than in reality by using this method. Therefore, the method of calculating the mean value of the four depth values at the corners is used.

4.1.4 Roughness

In the 20th century the Los Angeles River is changed into a concrete river. This concrete ensures a low roughness of the river bottom and walls. However, on some places vegetation has established on the bottom of the river, which has a higher roughness. Also the floodplains have a higher roughness. Therefore, a roughness file is made to be able to define different roughnesses along and across the river. This is done also with help of the QUICKIN module of Delft3D, in which to every grid cell a roughness coefficient is assigned. These roughness coefficients are defined at the velocity points of the grid cell. This means that the roughness files consist of roughness values

in M-direction and in N-direction. For this case the roughnesses are equal in both directions, so the roughness for a grid cell is in M-direction the same as in N-direction.
The roughness coefficients in Delft3D-FLOW can be expressed with different roughness formulas, namely Chézy, Manning or White-Colebrook. In the Feasibility Study by the USACE (2013b) the roughness formula of Manning is used. Because of the ease to use the same roughness values, the roughness formula of Manning is chosen also for this research.
The different roughness coefficients are classified into 6 categories (I – VI, see Table 5), which correspond with 6 types of surfaces. Category I is the concrete walls and bottom of the channel, which is almost the entire channel. In the next category some grouted riprap sides and bottoms are classified. This grouted riprap are stones with casted concrete over it. This has a slightly higher roughness than the concrete itself. The Manning coefficients for the first two categories are taken from the Feasibility Study Appendix E (USACE, 2013b). Category III represents the sandy bottom. This type of bottom appears only in the very downstream part of the river, near the estuary. Category IV is the surfaces with stones on the bottom, which appears mainly in river reach 5 (Figure 4). The Manning coefficients for category III and IV are estimated with help of Manning's n values table (Chow, 1959). Category V is the category for the floodplains. For this project a uniform value has been chosen for all floodplains with help of the coefficient used in the Feasibility Study, Google Earth and the Manning's n values table. The last category, for which the coefficient is estimated with the Manning's n values table, Google Earth and own observations, represents the vegetation in the river. This is also a uniform value for all the vegetation in the river, which is classified as 'light brush and trees in summer' in the Manning's n values table. The roughness categories with their corresponding descriptions and values for Manning's n are given in Table 5.

TABLE 5: ROUGHNESS CATEGORIES

Category	Description	Manning's n value
I	Concrete walls/bottom	0.014
II	Grouted riprap walls/bottom	0.02
III	Earth bottom	0.03
IV	Bottom with stones	0.035
V	Floodplains	0.045
VI	Vegetation	0.06

4.1.5 Boundary conditions

For modelling the LA River different boundary conditions have to be defined in the model. In the following sections the different boundary conditions and the input used for these conditions are explained and discussed.

4.1.5.1 Upper boundary condition

The river has a source, namely the confluence of the rivers Arroyo Calabasas and Bell Creek. This point would have been the upper boundary condition of the river in the model. Unfortunately, there is a lack of discharge data for the part of the river upstream of the Sepulveda Dam and for the tributaries joining the river in this upper part of the river. Due to this lack of information the location of the stream gauging station near the Sepulveda Dam (location A in Figure 11) is used as the upper boundary condition. In the model for the LA River the input of the upper boundary condition caused some problems, which resulted in errors in the calculations. To prevent the model for these errors, the upper boundary condition has been modelled as an operation. This means that the discharge is released in the midpoint of the cross section and that the flow is distributed across the river profile over time. The disadvantage of this method is that it requires some distance for the river flow to adapt to the profile. Therefore, the point of discharge release as the upper boundary condition is set about 500 meter more upstream than stream gauging station A. This 500 meter is considered sufficient for the river flow to adapt to the river profile.

4.1.5.2 Lateral inflows

The river has also different lateral inflows, which all need to be modelled. The main lateral inflows are the tributaries, which can be considered as boundary conditions also. These boundary conditions are modelled as operations too, as explained in the previous section. To estimate the boundary conditions, hourly data of the hydrological years 2009 to 2012 is collected of the stream gauging stations of the six tributaries (Los Angeles County - Department of Public Works (LACDPW), 2015b). The stream gauging stations of these tributaries are described below and the locations of these stations belonging to the tributaries are given in Figure 23.

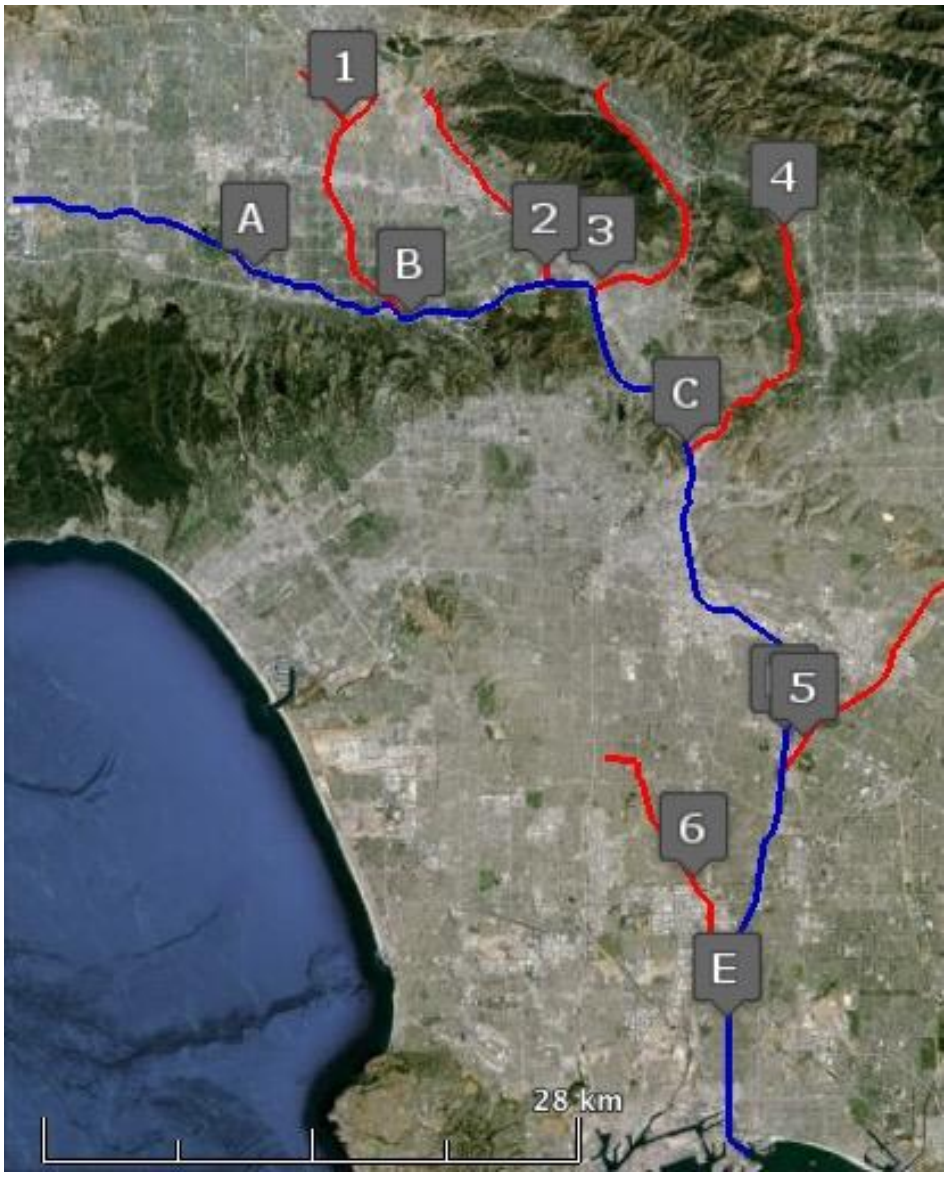

FIGURE 23: SATELLITE MAP OF LOS ANGELES COUNTY WITH THE LOS ANGELES RIVER (BLUE), THE MAIN TRIBUTARIES (RED) AND THE LOCATIONS OF THE STREAM GAUGING STATIONS, ADAPTED FROM (Google Earth, 2015)

1. *Pacoima Diversion at Branford Street (F305-R)* (this station is located at the end of the Pacoima Wash, just before it joins the Tujunga Wash; the Tujunga Wash has no stream gauging stations; discharge from this station reaches the LA River in less than one hour)
2. *Burbank Western Storm Drain (E285-R)* (station located just before the confluence of the Burbank Western Channel with the LA River)
3. *Verdugo Wash at Estelle Avenue (F252-R)* (station located just before the confluence of the Verdugo Wash with the Los Angeles River)

4. *Arroyo Seco below Devil's Gate Dam (F277-R)* (station located more upstream of the Arroyo Seco; discharge from this station reaches the LA River in about one hour)
5. *Rio Hondo above Stewart and Gray Road (F45B-R)* (station located just before the confluence of the Rio Hondo with the LA River)
6. *Compton Creek near Greenleaf Drive (F37B-R)* (station located more upstream of the Compton Creek; discharge from this station reaches the LA River in less than one hour)

These tributaries are the main lateral inflows of the LA River. However, the river has several storm drains joining the river of which no discharge data is available. To compensate for these storm drains in the model, just before three stream gauging stations in the LA River (station B, C and E) an operation point for the residual discharge is defined. For these residual points the data of the stream gauging stations in the LA River and of the tributaries joining the river between these stations is used. So for example, the discharge data used for the residual discharge between stations A and B is the data at stream gauging station B minus the data of stream gauging station A and the data of stream gauging station at Pacoima Wash. In doing this a strange phenomenon is found, where the data for the residual point between stations A and B, and to a lesser extent for the residual point between stations B and C, consists of negative values for mainly the base flow (in the case of an event the flow has mainly positive values). This means that water is lost or extracted from the river, but as far as known this has not happened. Another possibility could be the evaporation of the water from the river, but this is also not likely, because of the short travel times of the water in the river. In conclusion, this phenomenon is remarkable and cannot be explained.
All tributaries are independent of each other, which means that the input varies for each lateral inflow point. To make this discharge input for the model less variable, we try to find a relation between the discharge of each tributary and the discharge near the Sepulveda Dam, at point A. To find these relations, the hourly discharge data of each tributary and of each residual flow point is plotted against the hourly discharge data of point A. This is done by taking into account the travel times found in section 3.3.4. With help of a linear trend line through the origin the relation between the discharges is estimated. Two examples of applying this method are given in the figures in Appendix D: Determining relations between station A and lateral inflows. For this purpose, the hourly data for the 4 collected hydrological years 2009 to 2012 is split in two. The first 2 years are used to derive the relations, which can be seen as a calibration, and the second 2 years are used to validate the derived relations. The relations are assessed with help of two criteria: the Nash-Sutcliffe coefficient (NS) and the Relative Volume Error (RVE). The formulas for these criteria are given below. A value for NS can be up to 1, which is a perfect relation between the measured and estimated discharge series, but a value for NS of 0.7 means that the relation is considered accurate. A value for an RVE of 0% means a perfect relation and a relation is considered accurate for values between -5% and 5%.

$$NS = 1 - \frac{\sum_{k=1}^{k=N}[Q_{est}(k) - Q_{obs}(k)]^2}{\sum_{k=1}^{k=N}[Q_{obs}(k) - \overline{Q_{obs}}]^2} \quad (19)$$

$$RVE = 100 \cdot \frac{\sum_{k=1}^{k=N}[Q_{est}(k) - Q_{obs}(k)]}{\sum_{k=1}^{k=N} Q_{obs}(k)} \quad (20)$$

in which Q_{est} are the estimated discharges and Q_{obs} are the observed discharges.

The results of this method explained above are given in Table 6. The table gives the factors of the discharge series at station A estimated to predict the discharge series at the different tributaries and the residual flow points. Also the results for the NS and RVE are given for the first 2 years that are used to derive the relations, which can be seen as a calibration, and for the second 2 years that are used to validate the derived relations. These criteria are applied also to the stream gauging stations in the river, where the estimated discharges are the sum of the discharges estimated upstream of the station.

TABLE 6: RESULTS OF DERIVED RELATIONS BETWEEN DISCHARGE SERIES OF THE TRIBUTARIES AND RESIDUAL FLOWS AND THE DISCHARGE SERIES OF STATION A TO ESTIMATE THE BOUNDARY CONDITIONS FOR LATERAL INFLOW

Station	Factor relative to A	CALIBRATION		VALIDATION	
		NS	RVE	NS	RVE
Station A		**1.00**	**0.000%**	**1.00**	**0.00%**
Pacoima Diversion at Branford Street (F305-R)	0.063	0.33	23.59%	0.25	-37.60%
Residual flow A-B	0.048	0.03	6.41%	0.00	-85.84%
Station B		**0.92**	**1.36%**	**0.82**	**-22.81%**
Burbank Western Storm Drain (E285-R)	0.123	0.37	-17.66%	0.37	-39.17%
Verdugo Wash at Estelle Avenue (F252-R)	0.117	0.33	8.22%	0.18	-19.15%
Residual flow B-C	0.230	0.20	39.73%	0.04	-216.12%
Station C		**0.86**	**4.13%**	**0.76**	**-1.01%**
Arroyo Seco below Devil's Gate Dam (F277-R)	0.076	0.11	-30.46%	0.14	-61.74%
Rio Hondo above Stewart and Gray Road (F45B-R)	0.194	0.21	27.63%	0.06	-43.79%
Compton Creek near Greenleaf Drive (F37B-R)	0.051	0.11	-4.08%	0.21	1.80%
Residual flow C-E	0.668	0.22	37.44%	0.14	-20.40%
Station E		**0.71**	**10.85%**	**0.55**	**-15.11%**

The NS values for all the estimated tributaries and residual flows are all very low, and the RVE values are almost all out of the range of -5% to 5% to consider an accurate relation. This means that the estimated relations for the tributaries and the residual flows are poor. However, these are the best results that can be obtained in a simple way. It is possible to use other types of relations, such as for example a polynomial relation, but it is found that this does not improve the results of the criteria significantly. Besides, using polynomial relations makes the model much more difficult. Therefore, it is decided to use these relations, especially since the discharges at the stream gauging stations in the LA River are estimated reasonably well with the relations found for the tributaries and residual flows. Because the LA River is being studied and not the tributaries, the linear relations found are useful enough to set the boundary conditions for the lateral inflows of the river.

4.1.5.3 Downstream boundary condition

The boundary condition in the estuary, at the mouth of the river at the Pacific Ocean is modelled as an astronomic water level boundary condition. This means the water level at this boundary is modelled with the harmonic constituents of the Pacific Ocean. For this study the major constituents 'Principal lunar semidiurnal constituent' (M2) and 'Principal solar semidiurnal constituent' (S2) near the Los Angeles coast are used. This data is taken from the tides and currents observation station Long Beach, Terminal Island CA (NOAA, 2015b). This station is the observation station closest to the estuary of the LA River. The constituent at the estuary itself will have small differences, but it will not influence the calculations much. Table 7 shows the amplitudes and phases of the constituent at this place. The phases are referenced to the local time zone.

TABLE 7: HARMONIC CONSTITUENTS AT LONG BEACH

Constituent's name	Amplitude (m)	Phase (deg)
M2	0.526	273.7
S2	0.208	260.8

4.1.6 Other input parameters

There are some other parameters than discussed already that can be set in the FLOW module. All of these parameters are set already in a default value. For most of these parameters it is chosen not to change these parameters, but to keep them in the default. This is done to keep the model as simple as possible and not making it more complex for this study. For example, the horizontal eddy viscosity is set to a default uniform value of 1 m^2/s and the salinity, temperature and wind speed are not taken into account. Also some parameters are kept in the default value because the exact parameter value for this river is not known.

There are 3 input parameters that still need a small explanation. (1) The initial condition is set to a uniform value of a water depth of 0 meter. This means that the initial condition is an empty river. This is chosen because the river has almost no base flow in reality, so in reality the river is almost empty too. (2) The time frame of the simulations for each simulation is set to a beginning time at January 1, 2015 at 00:00:00. This is kept the same for all simulations to be consistent in the time. This is mainly important for the ocean boundary condition, where the harmonic constituent is dependent of the time. (3) The time step in the simulations is set to 0.1 minutes, low enough to get accurate results but high enough to get acceptable computing time. The output is given in time steps of 5 minutes, also low enough to get accurate results and high enough to limit the storage space of the results.

4.2 CALIBRATION AND VALIDATION

With these input parameters the model is almost ready to start a simulation. The last steps in setting up the model is to calibrate and validate the model. The calibration will be done by varying the roughness coefficients of the river. To execute a proper calibration another type of flow data is needed. The flow data used as input for the model is the discharge data of the different stream gauging stations. To calibrate the model properly, another data type is needed, for example data of the water depth or flow velocity from the stations. However, only for one station water depth data is collected for some years, namely for station A (USGS, 2015). This means there is almost no data to calibrate the model, and the data available is only for the very upstream part of the river. Nevertheless, the model is calibrated with this water depth data and besides this, it is calibrated too with the discharge data of all stream gauging stations located in the LA River. This makes this process of calibration less proper than desirable, due to having almost only one type of data.

To calibrate the model 4 peak events are selected from the same hourly data sets that have been used for the calibration of the relations for estimating the tributaries (section 4.1.5.2). This means that the data sets for the hydrological years 2009 and 2010 are used to select 4 representative peak events. The following peak events are selected: (1) November 26, 2008 at 0:00 to November 26, 2008 at 23:00, (2) February 16, 2009 at 3:00 to February 17, 2009 at 2:00, (3) January 17, 2010 at 18:00 to January 19, 2010 at 5:00 and (4) April 11, 2010 at 23:00 to April 12, 2010 at 10:00. These peak events are placed one behind the other in order to create a discharge series. This series, which can be seen in Figure 24 (blue line, hidden behind the red line for the figure 'Discharge at Station A'), has a length of 96 hours, and is used as input data for the upper boundary condition and for the lateral inflow boundary conditions. Figure 24 shows the results of simulating this discharge series. It shows the simulated water depth at station A and the simulated discharges at each stream gauging station in the river (except for station D, according to the conclusions in section 3.3.2). In the figures in which the line of the discharge before calibration (initial) is not visible, the line is hidden just behind the red line, which is the calibrated discharge. By interpreting the results of the simulation only by help of the figures, the following three aspects are noticeable. (1) The simulated water depth at station A is overestimated quite a lot for the measured peaks. (2) The simulated discharge at station A is almost the same as the measured discharge, which is as expected, because the discharges are released just before this station. (3) On first sight the simulated discharges for the other stream gauging stations are estimated quite well, but a delay in travel time can be observed.

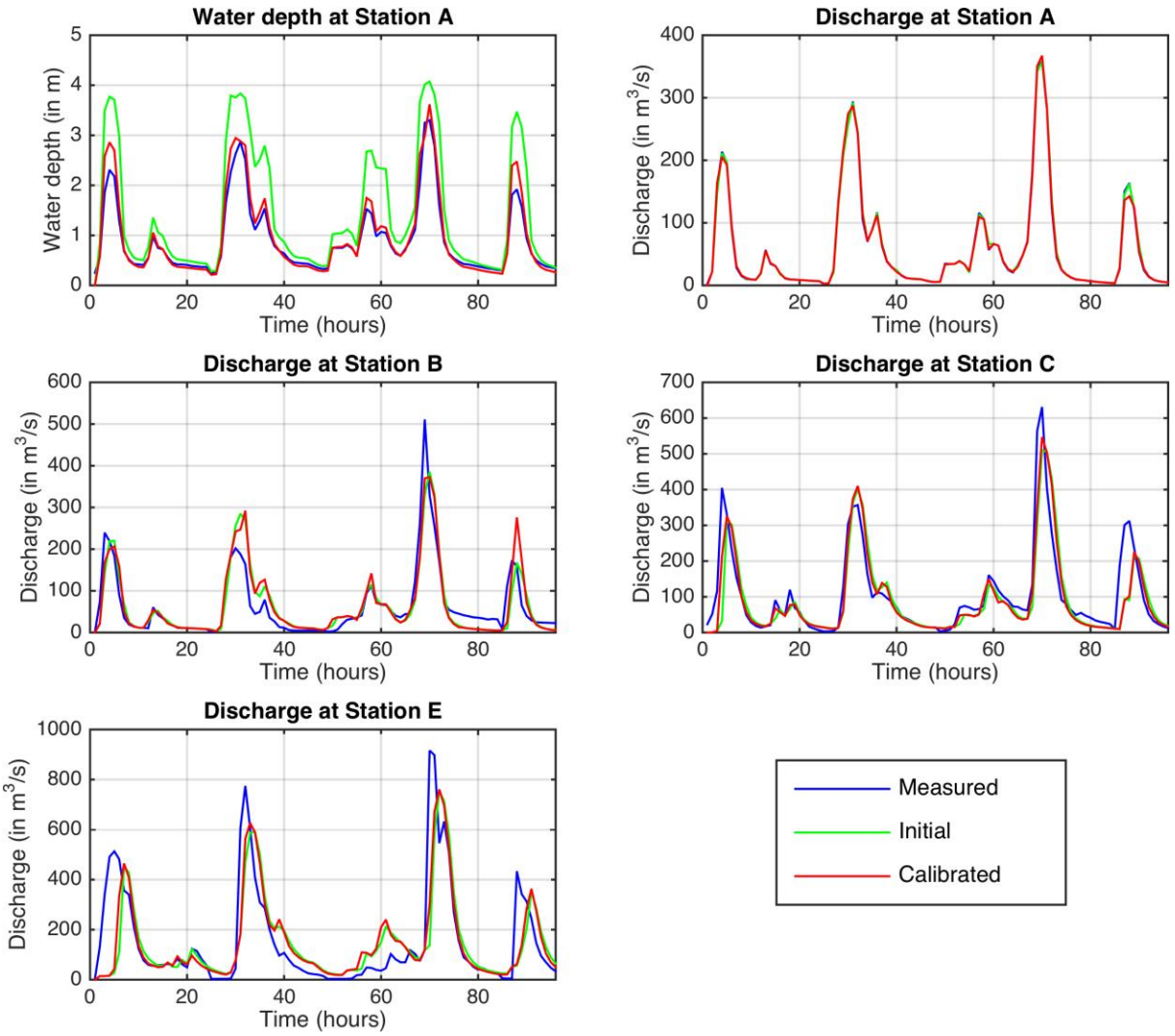

FIGURE 24: MEASURED, INITIAL AND CALIBRATED WATER DEPTH FOR STATION A AND DISCHARGES FOR ALL STATIONS

To assess the results of the first simulation in a more scientific way, the results are tested with the criteria Nash-Sutcliffe coefficient and Relative Volume Error, formulas (19) and (20), which are explained in section 4.1.5.2. The results of the simulation are tested with respect to the measured values. The results of these tests are given in Table 8. The NS-coefficient shows quite good results for the water depth at station A and the discharges for stations A and B. However, the RVE shows very bad results for the simulated water depth at station A. It shows a huge overestimation of the water depth, which already was observed in the figures. By knowing the results of these tests the calibration is started.

TABLE 8: RESULTS OF TESTS BEFORE AND AFTER CALIBRATION

	test	Water depth	Discharge			
		A	A	B	C	E
Before calibration	NS	0.91	1.00	0.78	0.67	0.45
	RVE	55.33%	0.53%	2.78%	-10.03%	-4.04%
After calibration	NS	0.97	1.00	0.81	0.79	0.56
	RVE	6.97%	0.12%	6.53%	-9.87%	-2.90%

The simulated water depth at station A has large discrepancy. The station is located just after the upper boundary condition, which makes that the river flow has not changed much, when measured at station A. Unfortunately, no other stream gauging station has recorded water depth, so this result cannot be compared with other locations. However, some research has been done to the question if the simulated water depth meets the expectations of the water depth at station A and at other locations. This is done by taking the widths and the elevations of the grid cells of the cross section at several locations out of the model and by calculating the Q-h relations at these stations manually, by using simplified equations. It turned out that for most locations the simulation meets the expectation quite well, except for locations between stations A and B. This is caused by the grid at these locations. Between the stations A and B the river is very narrow. In generating the grid for the river, it resulted in a river covered by about 4 cells instead of 8 cells, mainly between stations A and B, which already has been stated in section 4.1.2. This means that the grid is probably too coarse. Because the river is already quite narrow at these locations, the water depth increases too much, as can be seen in Figure 24. To compensate for the density of the grid at the locations between stations A and B, we decided to make a distinction between the roughness of the concrete river bed between stations A and B and the concrete river bed for the remaining part of the river. In this way a lower roughness coefficient of the concrete river bed between stations A and B was defined, which causes higher flow velocities resulting in a lower water level for the same discharge.
As already stated before the calibration is done by varying the values of the roughness coefficients of the different roughness categories. The values for the roughness coefficients given in Table 9 are the final values as a result of the calibration. The results of the calibration can be seen in Figure 24 and Table 8. The figure as well as the table show a much better result for the simulated water depth at station A. For the water depth the RVE is close to the acceptable value for the RVE, as stated in section 4.1.5.2. Although the RVE for the discharge at station B and station C and the NS for the discharge at station E are still not inside the range set for these criteria, it has to be concluded that the results of the simulation are sufficient.

TABLE 9: MANNING'S N VALUES FOR THE DIFFERENT ROUGHNESS CATEGORIES BEFORE AND AFTER CALIBRATION

Category	Description	Manning's n value before calibration	Manning's n value after calibration
I.a	Concrete walls/bottom between A and B	0.014	0.0077
I.b	Concrete walls/bottom at other locations	0.014	0.011
II	Grouted riprap walls/bottom	0.020	0.017
III	Earth bottom	0.030	0.025
IV	Bottom with stones	0.035	0.028
V	Floodplains	0.045	0.045
VI	Vegetation	0.060	0.048

After the calibration the model was validated to check if the model simulates well with other peak events too. Therefore, from the data sets with the hourly discharge series the hydrological years 2011 and 2012 are used to select 4 representative peaks from. The following peak events are selected: (1) February 18, 2011 at 16:00 to February 19, 2011 at 15:00, (2) March 20, 2011 at 3:00 to March 22, 2011 at 2:00, (3) November 20, 2011 at 11:00 to November 21, 2011 at 10:00 and (4) April 13, 2012 at 8:00 to April 14, 2012 at 7:00. To create a discharge series these peak events are placed one after another, which resulted in a series of 120 hours. The results of the simulation of this series are given in Figure 25 and the results of the tests of this simulation are given in Table 10. The second peak of this series is an extreme and somewhat different shaped peak. The peaks are estimated quite well, but the volume of the wave is estimated less good, in particular at stations C and E. As the event is measured more downstream the simulation becomes less accurate, but in general the results are acceptable, in particular for the height of the peaks tested with the Nash-Sutcliffe coefficient. The Relative Volume Error is quite high for the stations

C and E. This is due to the incorrect water balance due to the estimated lateral inflows. It is possible to limit the RVE by calibrating the lateral inflow by adapting the derived relations. However, this is not done in this study.

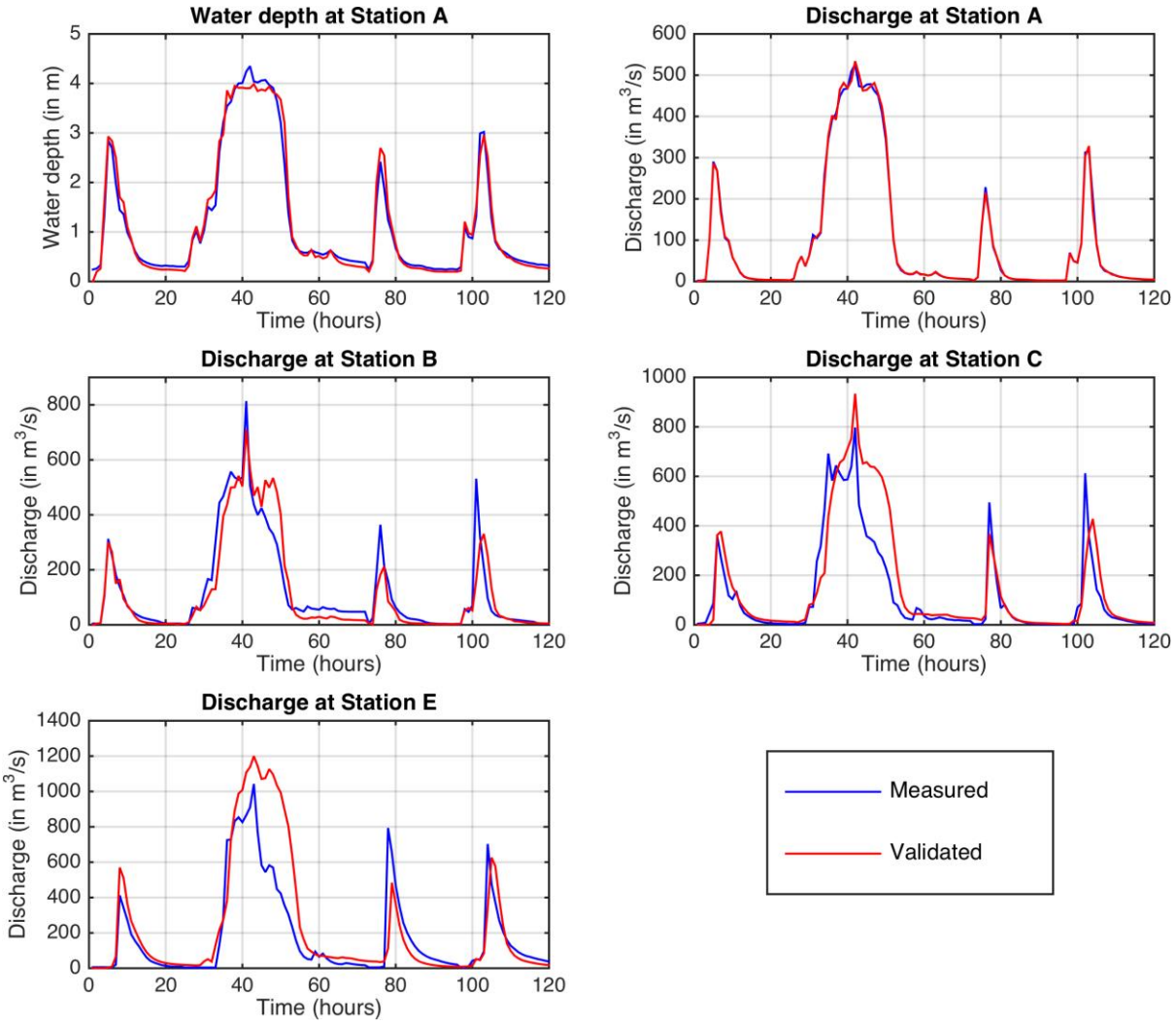

FIGURE 25: MEASURED AND VALIDATED WATER DEPTH FOR STATION A AND DISCHARGES FOR ALL STATIONS

TABLE 10: RESULTS OF TESTS FOR VALIDATION

	test	Water depth	Discharge			
		A	A	B	C	E
Validation	NS	0.98	1.00	0.89	0.82	0.76
	RVE	1.11%	0.52%	-6.74%	26.59%	33.88%

5 SCENARIOS

With the model described in chapter 4 different situations can be simulated. For this study four scenarios are defined. The first scenario is the reduction of discharge in the river by storing the water before it flows into the river. In the second scenario two side channels, planned in the Feasibility Study of the USACE, is implemented, and in scenario 3 a retention basin is implemented in the Piggyback Yard. Scenario 4 is about the change in precipitation due to climate change. All these scenarios are investigated to get more insight into the effects of measures in and around the LA River on the flood safety of the city. In this chapter these scenarios will be explained and the results of the simulation will be presented and discussed. First the hydrograph to be used in each scenario is defined and the flood risks in the current situation is estimated as a reference situation.

5.1 REFERENCE SITUATION

To model the reference situation first a typical hydrograph as input for the upper boundary condition is defined. To define a typical hydrograph 15 representative peak events with a length of 24 hours are chosen from the hourly discharge series recorded at station A. These peak events are scaled to get dimensionless hydrographs. The scaling is done by dividing each hydrograph by its average over 24 hours. This is done because of the way in which the peak distributions, presented in section 3.4, are calculated, namely as daily averaged peak discharges. By using daily averaged peak discharges for the hydrographs too, the return times of the peaks can be calculated easily with help of the extreme distribution graphs. The hydrographs used to determine a typical hydrograph are shown in Figure 26.

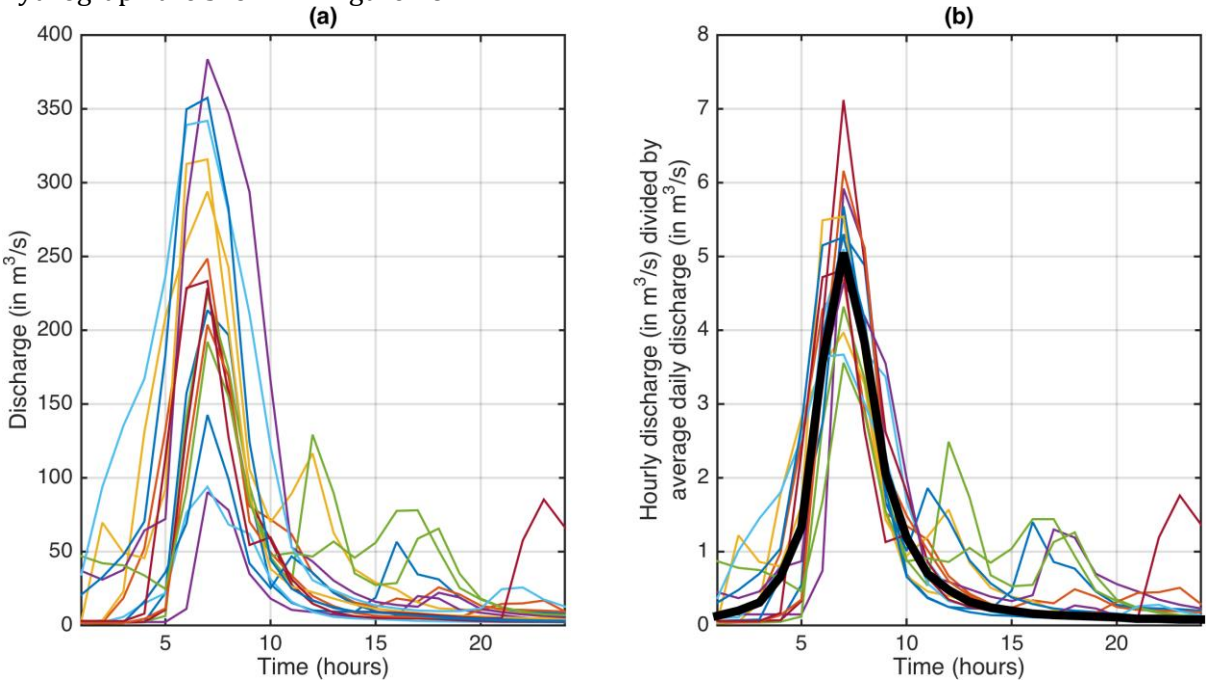

FIGURE 26: (A) HYDROGRAPHS OF PEAK EVENTS RECORDED AT STATION A, (B) DIMENSIONLESS HYDROGRAPHS OF THE PEAK EVENTS MEASURED AT STATION A, WITH IN BLACK THE TYPICAL DIMENSIONLESS HYDROGRAPH RESULTING FROM AVERAGING ALL PEAKS (WEIGHTED AVERAGE)

This typical dimensionless hydrograph, which is the weighted average of all peaks and is the black graph in Figure 26 (b), is then multiplied with an average daily discharge, generating a typical hydrograph corresponding to this average daily discharge. However, by using the typical

dimensionless hydrograph a problem arises. By checking whether this method works for the most extreme peaks as are used to define the extreme peak distributions, it turns out that the peak will be quite overestimated. For example, the most extreme average daily discharge of 2011 was on March 20, i.e. 254 m^3/s. By using the method of the typical dimensionless hydrograph an hourly averaged peak discharge of 1283 m^3/s is estimated. In reality, this hourly averaged peak discharge was 'only' 527 m^3/s, which is more than two times lower than estimated by the typical dimensionless hydrograph. There is no information known by us that the river was flooding on this day, so it is assumed that the river did not flood. Since higher daily averaged discharges are expected, the part of the distribution graph for daily averaged discharges higher than 254 m^3/s is interesting for this study. Therefore, we decided not to use this typical dimensionless hydrograph, for high peaks but only for relatively low daily averaged discharges. Instead of this, the extreme hydrograph, which appeared on March 20, 2011 is used, which was one of a kind. It has a high daily averaged discharge with a relatively low peak, as can be seen in Figure 27 (a). This hydrograph represents the most extreme peak event in the years for which hourly data is available. To use this hydrograph for the simulations, this hydrograph is made dimensionless in the same way and shown in Figure 27 (b). The first hours of this dimensionless hydrograph are smoothened to create a complete hydrograph just within the 24 hours, zo it starts near zero.

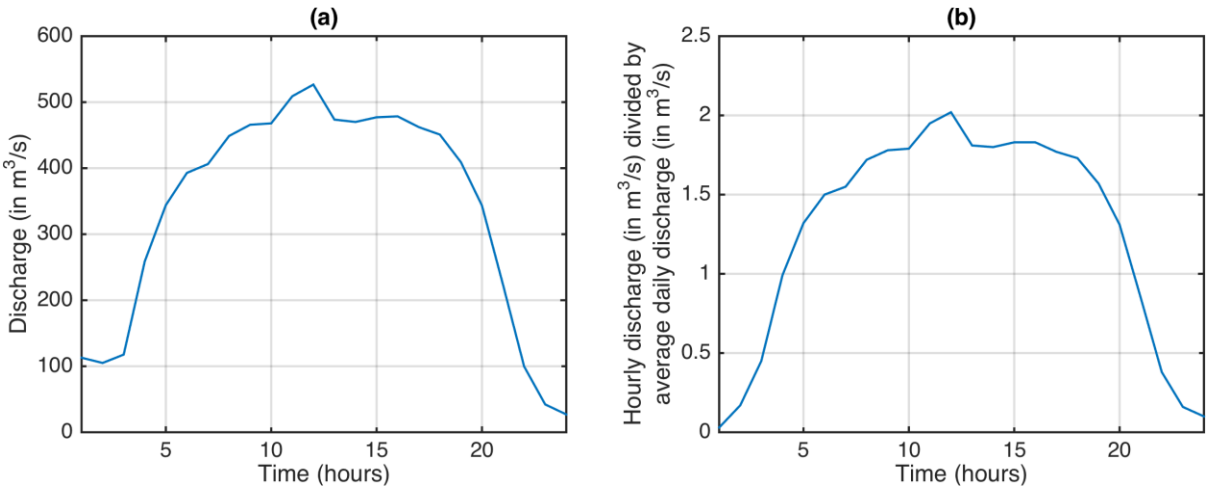

FIGURE 27: (A) HYDROGRAPH OF THE MOST EXTREME PEAK EVENT RECORDED AT STATION A ON MARCH 20, 2011, (B) DIMENSIONLESS HYDROGRAPH OF THIS MOST EXTREME PEAK EVENT

With the help of this extreme dimensionless hydrograph the simulations will be done. By multiplying the hydrograph with an average daily discharge the input for the upper boundary condition is calculated and with this the boundary conditions for the lateral inflows are calculated using the multiplication factors in Table 6. To determine the discharge and the corresponding return time at which the LA River is flooding, different simulations are done with different daily averaged discharges.

It turned out that for a daily averaged discharge of 535 m^3/s at station A, the river is just not flooding. With a discharge higher than 535 m^3/s the river is flooding for the first time on a location between station A and station B. However, in the plans of the USACE the measures, of which some will be investigated in this study, are not planned between stations A and B but mainly between stations B and C. Due to the steepness of the river profile and subsequent large velocities in the river, the influence of these measures on the water level between stations A and B will be very low. Also, the bathymetry of the river based on the DEM is modified significantly between stations A and B due to trees and bridges and also due to the narrowness and sinuosity of the river between these two stations. Therefore, it is decided to raise the levees of the river between stations A and B so that the river will not flood between these two stations. This enables us to study floods between stations B and C and the influence of the measures on these floods, without the possibility that the discharge wave is influenced by flooding upstream.

To determine the return times of a new critical flood between stations B and C, two different criteria are used. The return time is determined for the daily averaged discharge at which the river is just not flooding somewhere between stations B and C. Besides this, the return time is also determined for the average daily discharge at which the river is just not flooding near station B. The river is just not flooded somewhere between stations B and C when the daily averaged discharge of the wave is 841 m^3/s at station B and 1201 m^3/s at station C. The increase in daily averaged discharges measured at the subsequent stations is due to the several lateral inflows in the river. The daily averaged discharges correspond to a return time of once in 154 years for station B and to once in 166 years for station C, according to the Generalized Extreme Value distribution fitted to the annual extreme peak discharges (Figure 18). Besides this, the river is just not flooding near station B with a daily averaged discharge of 1351 m^3/s at station B and 1935 m^3/s at station C. These average daily discharges correspond to a return time at station B of once in 583 years and at station C to once in 859 years. The so-called daily averaged discharge is calculated without taking into account the travel time of the event. This means that the average discharge for each station is measured between January 1, 2015 at 0:00 and January 2, 2015 at 0:00.
In the model results the river is flooding quite a lot in the downstream part between station E and the downstream boundary condition, defined as a harmonic constituent. The flooding in the downstream part of the river is probably due to the influence of the ocean on the river flow. It is assumed that these floods due not influence the model results upstream in the parts of the river in which the measures are planned.

5.2 Scenario 1

For the first scenario it is assumed that during events part of the discharge is stored outside the LA River, before it flows into the river. This means that the precipitation is stored in local storage points. For example, by building some (underground) storage basins next to the tributaries of the LA River. Also individual storage points can be built, for example investing in green roofs on houses to store the precipitation. Also enhancing infiltration next to the the streets is an option. The consequences of storing the water is to reduce or delay the lateral inflow in the LA River. This reduction is simulated in the model as the first scenario.
In the model this measure is implemented by reducing the discharge as input for the upper boundary condition with 5%, 10% and 15%. It is not known whether a reduction of these percentages is achievable, but it gives an insight in the consequences of reducing the lateral inflow. As a result of reducing the upper boundary condition in the model, also the lateral inflows are reduced by 5%, 10% and 15%, due to the dependence on the upper boundary condition. This means that the reduction of 5%, 10% and 15% is a reduction of discharge in the whole Los Angeles River catchment. In reality the percentages of reduction will vary per tributary, but this scenario is only to give some insight in the consequences of this measure, as already stated before.
The extreme value distribution will change due to this measure. The example of a reduction of 15% in determining a daily averaged discharge at which the river is just not flooding, is used to explain this change in distribution. The same event as used for the reference situation is simulated, however, with a reduction of 15%. This results in a lower daily averaged discharge in the river, namely a discharge of 712 m^3/s instead of 841 m^3/s in the reference situation. This discharge has the same return time as in the reference situation, however, the river is now not close to flooding. To determine when the river is just not flooding in this case, the graph of the GEV-distribution used for the reference situation is shifted downwards, to have the same return time for 712 m^3/s for scenario 1 as for 841 m^3/s for the reference situation, which is shown in Figure 28. After doing this the new return time for when the river is just not flooding, at a daily averaged discharge of 841 m3/s, can be determined, which occurs now once in 228 years. This is an improvement of about 50%. The same approach is followed for each simulation, so for 5%, 10% and 15%, but also for determining the discharge and return time at which the river is just not flooding somewhere between stations B and C and at which the river is just not flooding near

station B. This is done too for the GEV-distribution for station C. The shifted graphs of the GEV-distributions are shown in Appendix E: Extreme value distributions for scenario 1.

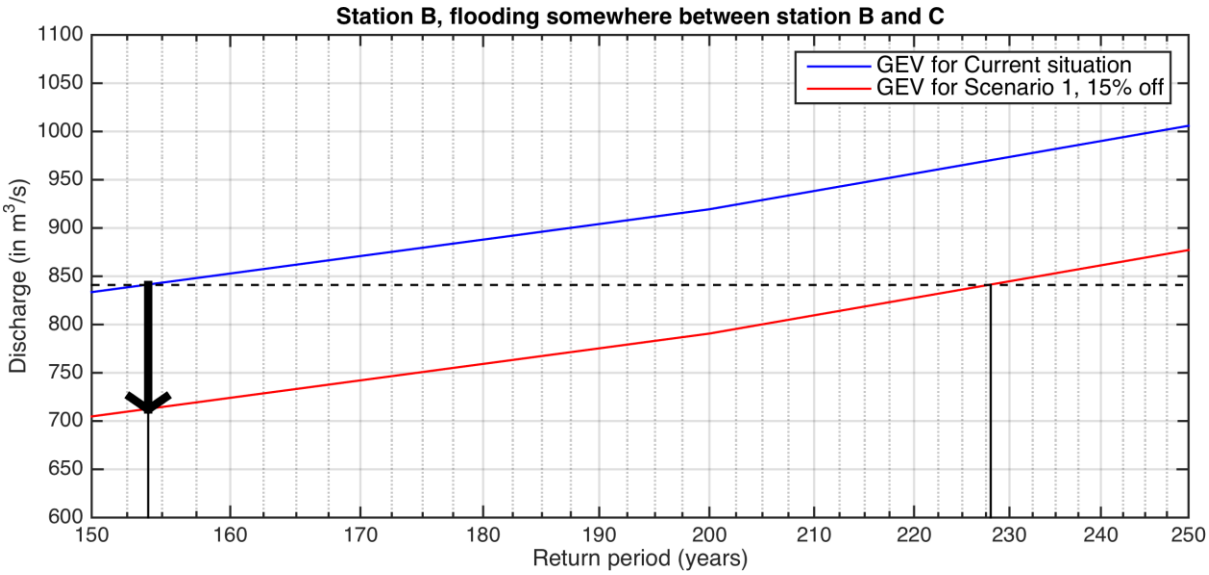

FIGURE 28: METHOD OF DETERMINING RETURN TIMES FOR SCENARIO 1, WITH A LOGARITHMIC X-AXIS

Table 11 contains the results of the determination of the return times for the daily averaged discharges of scenario 1, accompanied with the return times for the reference situation. For the criterion when the river is just not flooding between stations B and C the water level reduces by about 15 centimeters on average between the stations with 5% less discharge and with 15% less discharge the water level reduces by more than 40 centimeters on average. This means that a river with 5% less discharge is about 15% safer than in the reference situation and a river with 15% less discharge is about 50% safer. By looking at the other criterion, when the river is just not flooding near station B, the water level reduces by about 15 centimeters on average between stations B and C with 5% less discharge. With 15% less discharge the water level reduces by about 80 centimeters on average. This corresponds to a 20% safer river with 5% less discharge and a 60% safer river with 15% less discharge, based on the determined return times.

TABLE 11: RETURN TIMES (ONCE IN X YEARS) FOR THE REFERENCE SITUATION AND FOR SCENARIO 1

	Flooding somewhere between stations B and C		**Flooding near station B**	
	Station B	*Station C*	*Station B*	*Station C*
Reference situation	154	166	583	859
Scenario 1, 5% off	180	198	677	1028
Scenario 1, 10% off	207	231	746	1196
Scenario 1, 15% off	228	268	902	1372

5.3 SCENARIO 2

In the Integrated Feasibility Study of the USACE (2013a) four main alternatives with each different combinations of measures are described and analyzed. Two of these measures, which are implemented in most of the alternatives, are side channels. Both channels are planned in reach 5 of Figure 4. The first side channel is planned to shortcut the 90-degrees corner at Griffith Park. This side channel is implemented in three of the four alternatives and is mainly intended to support a riparian fringe. The second side channel is planned also in Griffith Park, approximately 1 kilometer downstream of the 90-degrees corner and is implemented in all four alternatives.

This side channel is meant also to create a riparian environment and also to be a hydrological connection during excessive storm events. Both side channels are schematized in Figure 29. To study the effects of the side channels at these locations on the safety of the city, the side channels are implemented in the model and simulated. From the report of the Feasibility Study (2013a) only some descriptions and figures of these side channels are available. Therefore, we decided to implement those side channels only roughly in the same way as has been described in that study. This means that an own version of the side channels is implemented. The bathymetry of the side channels created for this scenario is shown in Appendix F: Bathymetry of river at location of measures for scenario 2. The roughness coefficients are not changed for the profile of the side channels, so the roughness coefficient of the floodplains (0.045) is used. This is done because the profile of the side channel will not be made of concrete, but it is not yet known what roughness it will have exactly. The roughness coefficient for the floodplains is already an average coefficient for several profiles, so this coefficient is used.

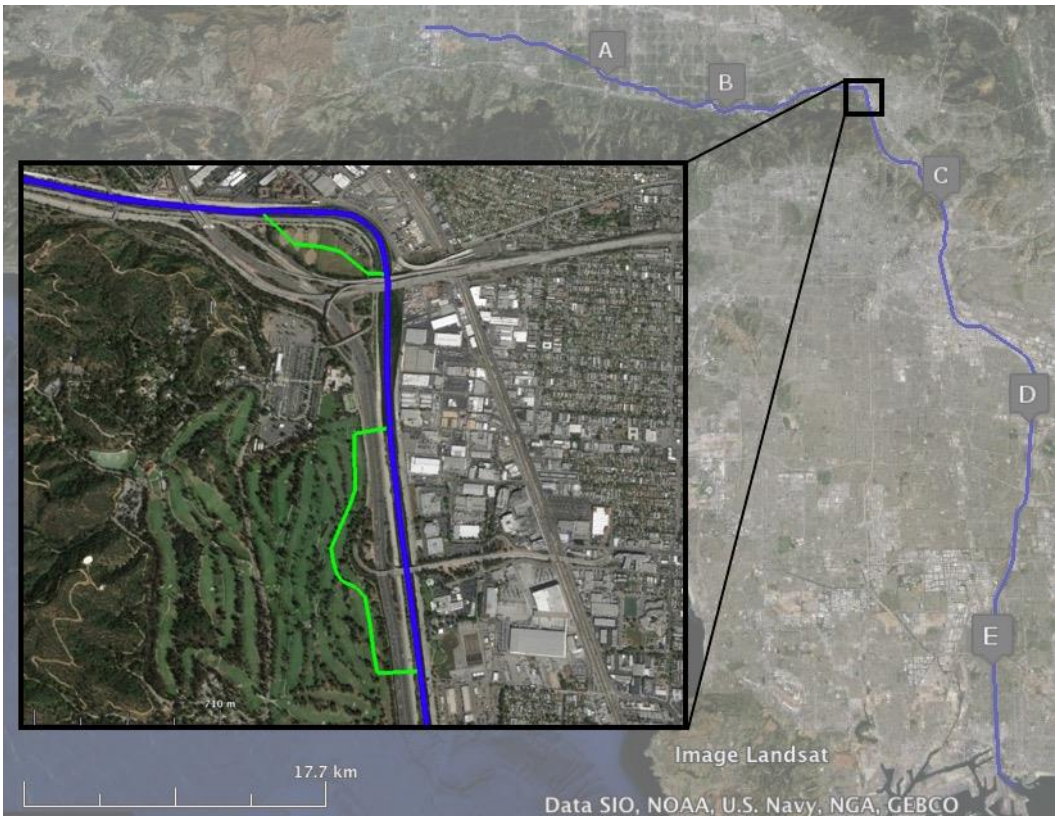

FIGURE 29: SCHEMATIC REPRESENTATION OF THE LOCATION OF THE SIDE CHANNELS (GREEN) NEXT TO THE RIVER (BLUE), ADAPTED FROM (Google Earth, 2015)

By looking at the return times which are calculated with the distribution of the daily averaged discharge, the implementation of the side channels will hardly have an effect on the safety in the city. This is because the daily average discharge is hardly influenced by the side channels. For station B the daily averaged discharge is reduced by 4 to 5 m^3/s, and for station C the average daily discharge is about 0.5 m^3/s lower than in the reference situation. These differences are negligible small, due to the uncertainties in the simulations as have been discussed already.
To assess the local effects of these measures, first the maximum water level of the reference situation and of the situation of scenario 2 are plotted in a graph, which is given in Figure 30. The locations of both side channel is shown in the same figure. The distance between grid cell number 1290 and 1400 is about 3.5 kilometer. The fall and rise of the water level in the reference situation between grid cells 1325 and 1340 is due to the fact that the Verdugo Wash is joining the river at this point, after which the river becomes wider between those grid cells. The graph shows some differences between both situations, which means the implementation of these side channels has

some effect on the local water levels. It can be seen that there is a local reduction of the water level in the main river at the inlet of both side channels of about 1 meter, but a local rise of the water level in the river at the outlet of the side channels of about 0.5 meter. Between the inlet and outlet of the first side channel the water level reduces by on average 40 centimeters and for the second side channel by on average 25 centimeters. Soon after the outlets of the side channels the water level of the river returns to the same water level as in the reference situation. It can be concluded that the measure of implementing a side channel at these locations and of these size only have very local effects on the water level. This is also visible by the short backwater curves for both side channels. These short backwater curves are due to the steep slope and small friction of the river, which causes flow velocities of up to 15 m/s.

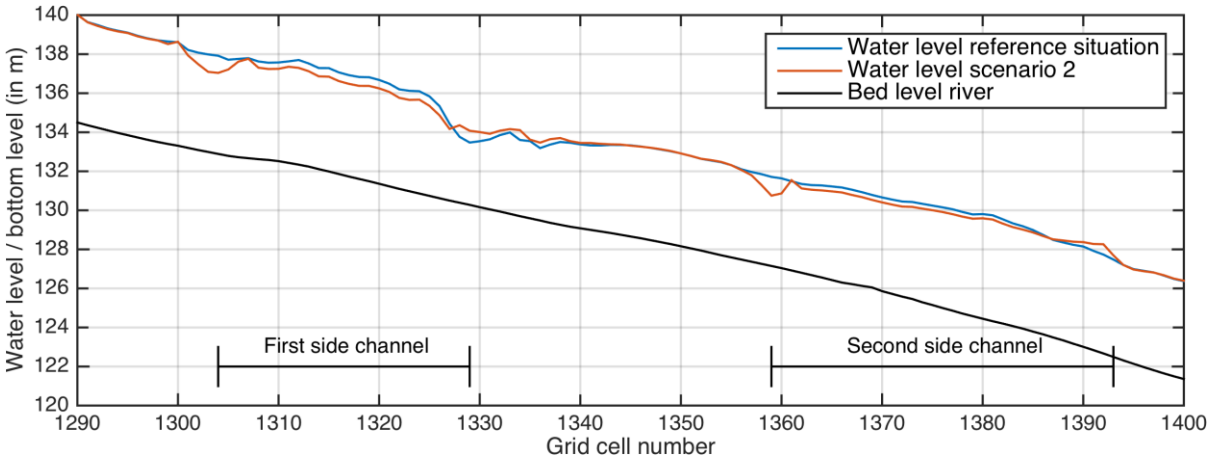

FIGURE 30: MAXIMUM WATER LEVELS AND BED LEVEL OF THE MAIN RIVER AT THE LOCATION OF THE MEASURES FOR SCENARIO 2, WITH THE REFERENCE SITUATION AND THE SITUATION IN SCENARIO 2, FOR AN EVENT THAT IS JUST NOT FLOODING BETWEEN STATIONS B AND C

Due to the short backwater curves, the side channels have negligible effect on the discharge upstream and downstream, so the return times of the discharges at stations B and C remain the same, as already stated above. However, to get an indication of the increase in safety in terms of return times for the stretch of the river where the side channels are planned, the return times for stations B and C are extrapolated to these parts of the river. By doing this the tributaries are taken into account, by adding and subtracting the daily averaged discharges of the tributaries before or after the river part of interest. For example, to determine the return time for the river next to the first side channel with the extreme value distribution for station B, the daily averaged discharge of the Burbank Western channel, which is 92.5 m^3/s in the situation where the river is just not flooding between stations B and C, is subtracted from the daily averaged discharge in the main river next to the first side channel, which is 810.3 m^3/s in the same situation. So it is assumed that in the reference situation the daily averaged discharge of 717.8 m^3/s at station B would lead to a daily averaged discharge of 810.3 m^3/s in the river part where next to it the first side channel is planned. The return time for this discharge are determined with the same method as described in section 5.2, i.e. by lowering the GEV-fit.

The results of extrapolating the return times of stations B and C to the parts of the river next to the side channels are given in Table 12. The table shows an increase in safety for the city at the specific locations by implementing both side channels. The safety of the river next to the first side channel increases by 40 to 50%, depending on which station and which situation of flooding is used to determine the return times. For the second side channel the increase in safety of the river next to it is between 30 and 40%, also depending on which station and which situation of flooding is used to determine the return times. The degree of increase in safety is quite uncertain, due to the assumptions in determining the return times and in implementing the side channels into the model. However, it can be concluded that the river parts with side channels next to it will become much safer by implementing these side channels.

TABLE 12: RETURN TIMES (ONCE IN X YEARS) FOR THE REFERENCE SITUATION AND THE EXTRAPOLATED RETURN TIMES FOR SCENARIO 2

	Flooding somewhere between stations B and C		**Flooding near station B**	
	Station B	*Station C*	*Station B*	*Station C*
Reference situation	154	166	583	859
Scenario 2, first side channel	224	232	873	1255
Scenario 2, second side channel	213	222	784	1149

5.4 SCENARIO 3

For the third scenario a retention basin is implemented next to the LA River. The location of this retention basin is at the Piggyback Yard, which is located just after stream gauging station C, as is shown in Figure 31. This Piggyback Yard is nowadays an intermodal rail facility where the freight containers are transitioned from railcar to truck and is known as the Los Angeles Transportation Center (USACE, 2013a). In earlier times, before the channelization of the LA River, the river was flowing through this area and was flooding in this area during big storm events. In the Feasibility Study of the USACE (2013a) the Piggyback Yard is implemented in all four alternatives, but in two different ways. The main purpose of both alternatives is to recreate a riparian habitat in the Piggyback Yard. In both alternatives the bottom of the Yard is lowered and a riparian environment is established. Also the historical wash in this area is restored. In the first alternative the river channel is not changed, but the water is allowed to flow through the existing storm drains into the historical wash in the Piggyback Yard and out again through the same storm drains. In the other alternative the levee, that separates the river and the Piggyback Yard from each other, is taken away, so that the river can flow into the wash in the Piggyback Yard, but also flow directly into the Yard (USACE, 2013a).

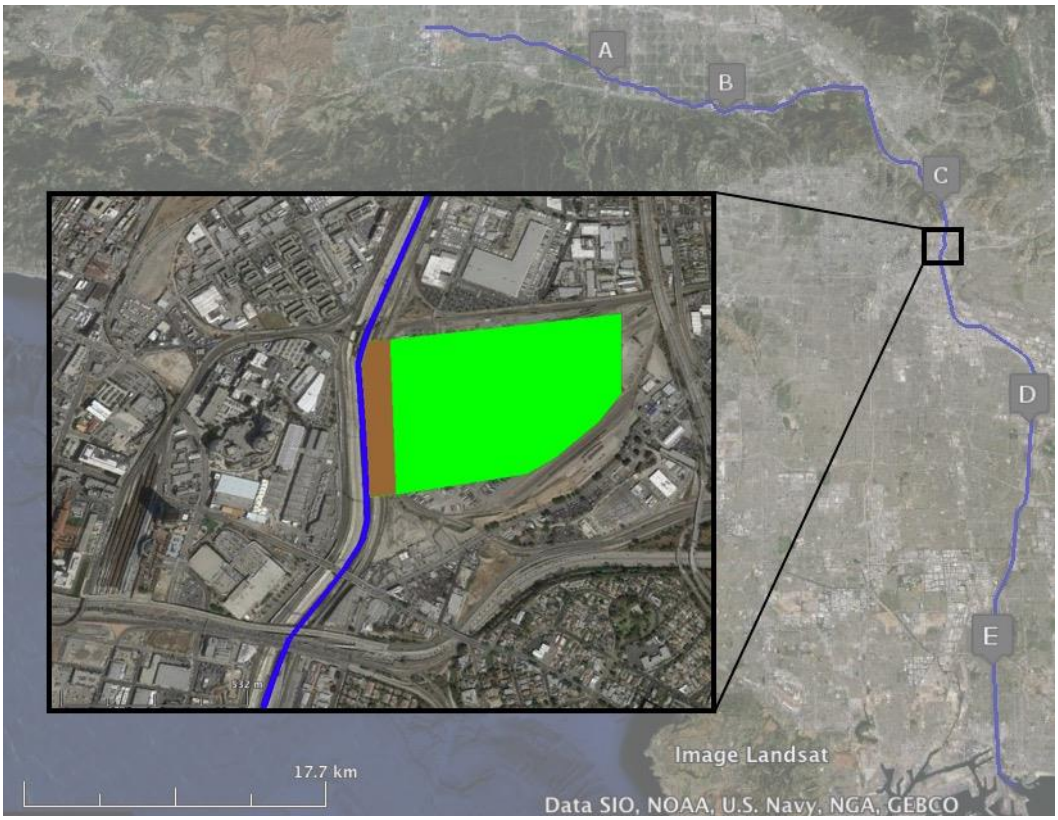

FIGURE 31: SCHEMATIC REPRESENTATION OF THE LOCATION OF THE RETENTION BASIN (GREEN) AND (POSSIBLE) DIKE (BROWN) NEXT TO THE RIVER (BLUE), ADAPTED FROM (Google Earth, 2015)

These types of measures do very much look like the side channels investigated in scenario 2. However, the location of the Piggyback Yard still is studied, because of the possibility to create a retention basin due to the space available, which is not available on other places next to the river. Therefore, the first alternative defined in the Feasibility Study is adapted a bit, so that the Piggyback Yard can be used as a retention basin. This can be done by closing the existing storm drains between the river and the Piggyback Yard during excessive storm events and reopen it after the event is passed. When the water level is high enough it can flow over the existing levees into the Piggyback Yard, which then functions as a retention basin. The bathymetry used as input for this alternative is shown in Figure G 1 of Appendix G: Bathymetry of river at location of measures for scenario 3. The second alternative, which is in fact some extra space for the river to flow, is also simulated. Apart from these two alternatives, another alternative is defined to be investigated in this third scenario. This third alternative is mainly the same as the first alternative, only the levee has been lowered by 6 meters to a level of 85 meter above main sea level. This lower levee will cause earlier flooding into the Piggyback Yard than in the first alternative. The cross sections of the Piggyback Yard for the reference situation and the different alternatives for scenario 3 are given in Figure G 2 of Appendix G: Bathymetry of river at location of measures for scenario 3.

With the alternatives in scenario 3 the same happens as with the side channels of scenario 2: the return times at stations B and C will not change, because the daily average discharge is almost the same as in the reference situation. The little differences for the alternative with a lowered levee is quite obvious, according to the low capacity of the retention basin due to the low levee. The capacity of the retention basin with a levee at 85 meter above main sea level is roughly estimated to be 300,000 m^3. This means that the daily averaged discharge will be influenced hardly, because this can be at maximum a lowering of 3.5 m^3/s. For the first alternative the retention basin has a higher capacity of about 2.3 million m^3, however, the river is not flooding at this point, because the levee is too high to be flooded. Without a levee the daily averaged discharge remains the same, because the discharge is not stored, but only delayed for a while.

Although the daily averaged discharge is almost the same as in the reference situation, the implementation of a retention basin has effects on the water level. Figure 32 shows the maximum water levels for the reference situation and four all alternatives during an event which causes just not a flood at station B, accompanied with the bottom level of the river. The location of levee between the levee and the Piggyback Yard (for the alternatives in which a levee exists) is given in the same figure. In this figure the water levels for the reference scenario are the same as for the alternative with the current levee, because the levee is too high to be flooded. The rise in water level in the reference situation between grid cell numbers 1710 and 1715 is due to a bit narrower river in the model. This is due to a difficulty in the translation of the bathymetry to the grid, due to the extension of the grid with the Piggyback Yard. In reality the river is not narrower on this

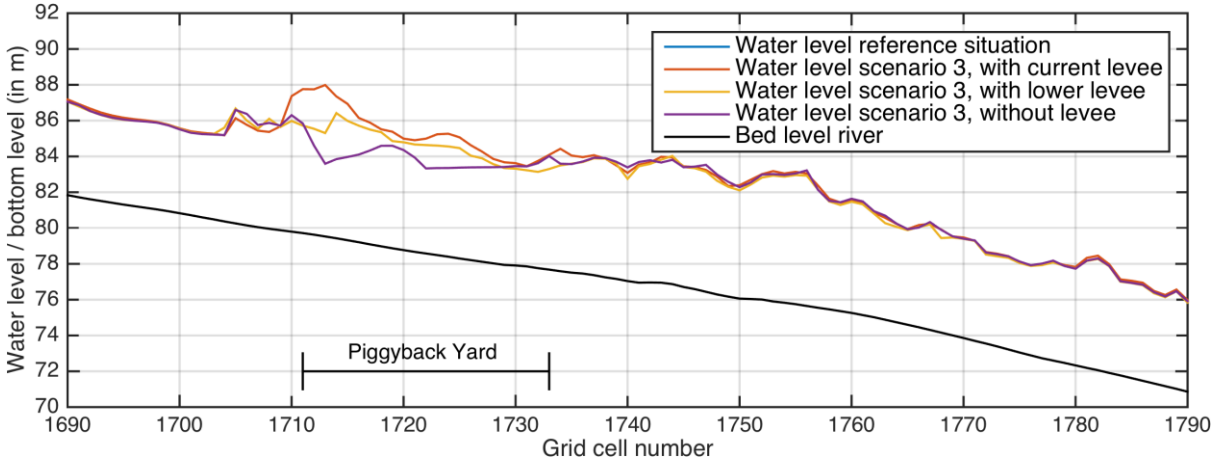

FIGURE 32: MAXIMUM WATER LEVELS AND BED LEVEL OF THE MAIN RIVER AT THE LOCATION OF THE ALTERNATIVES FOR SCENARIO 3, WITH THE REFERENCE SITUATION AND THE SITUATION IN THE DIFFERENT ALTERNATIVES OF SCENARIO 3, FOR AN EVENT THAT IS JUST NOT FLOODING AT STATION B

place, so the maximum water level in reality will be lower than given in the figure. For the other two alternatives it can be seen that the water level is lower at the location where the retention basin is, with a much lower water level for the scenario without a levee. However, quickly after the Piggyback Yard the water level is again almost the same as in the reference situation. By zooming in the figure it looks like the water level in the situation with a lower levee is a little bit lower than in the reference situation after the basin, but this is in the order of less than 10 centimeters, which could also occur due to the uncertainties in the model. The maximum water levels for the different alternatives are very much the same as in the reference situation, which means that the implementation of a retention basin has no influence on the water level upstream of the Piggyback Yard. This is also due to the steep slope and the small friction of the river, which causes only very small backwater curves. By summarizing these observations, it can be concluded that the implementation of a retention basin on this location is not useful if you want to improve safety, because there were already no problems due to flooding after the stream gauging station C.

To get an indication of the increase in safety in terms of return times for the stretch of the river next to the Piggyback Yard, the return times for station C are extrapolated to these parts of the river in the same way as described in the previous section. This is done only for stream gauging station C because the other stations are much further away from the Piggyback Yard. The results are shown in Table 13. It shows that the Piggyback Yard with a levee has almost no effect on the safety in the city. Only the alternative without a levee has more effect on the safety of the city, because implementing this measure, will increase the safety by 12 to 16% at maximum on this location, depending on which situation of flooding is used to determine the return times. Also for this scenario the degree of increase in safety is uncertain, due to the assumptions made in implementing in the model and determining the return times. However, implementing the Piggyback Yard without a levee will locally increase the safety in the city.

TABLE 13: RETURN TIMES (ONCE IN X YEARS) FOR THE REFERENCE SITUATION AND THE EXTRAPOLATED RETURN TIMES FOR SCENARIO 3

	Flooding somewhere between stations B and C	**Flooding near station B**
	Station C	*Station C*
Reference situation	166	859
Scenario 3, with current levee	166	859
Scenario 3, with lower levee	167	870
Scenario 3, without levee	193	964

5.5 SCENARIO 4

In section 3.1 the data of the precipitation in the LA River catchment is investigated to get an insight in the climate in the Los Angeles area. It is clear that the catchment has a very dry climate with dry summers and not much precipitation in winter. However, precipitation events in the winter can be extreme with high peaks. It is mentioned in section 3.3.5 that a quantitative relation between the amount of precipitation and the amount of discharge is hard to find, because it depends very much on where the precipitation falls and on the intensity of the precipitation at these locations. However, the precipitation is very important for the LA River, because without precipitation there is no river flow. For restoring the river without decreasing the safety of the river for the future, it is needed to take into account potential climate change.

Many scientists have researched the climate change for the future. Most of them agree that climate change is occurring and mean temperatures will increase, but the specific degree of this temperature increase cannot be accurately predicted. The predictions of the changes in precipitation are various. Some scientists predict an increase in precipitation, while others

predict a decrease in precipitation for this area (USACE, 2013b). Others predict a change in local mean precipitation, with a large uncertainty on the sign of the change (Berg et al., 2015). In general, a decrease in precipitation will lead to lower discharges in the LA River, which leads to an increase in return times, which leads to a safer river. For an increase in precipitation it is the other way around. However, due to the impossibility to derive an accurate and quantitative relation between precipitation and discharge, but also due to the uncertainty of the change in precipitation the degree of change in return times cannot be investigated.
Other scientists expect a change in precipitation intensity in the Los Angeles area (Killam et al., 2010). They expect a shorter time period in which the precipitation falls, but with a higher peak. By translating this type of precipitation intensity to a hydrograph it can be expected that on average the daily discharge will remain the same, however, the peak of this event is higher. This will lead to earlier flooding with the same daily averaged discharges. Therefore, it is expected that the typical hydrograph as obtained in section 5.1 will occur more often with even higher peaks and that the extreme hydrograph as used for this research will occur less often.

5.6 COMPARING SCENARIOS

In Table 14 the return times for the reference situation and the scenarios are given in one table to be compared to each other. It can be concluded that storing water in the catchment before it flows into the river is the most effective measure for the entire river stretch. However, it is not known whether a reduction of 5 to 15% of the river discharge is achievable. Implementing side channels or retention basins have only local effects on water levels and discharges, for which constructing the side channels, the largest increase in the safety of the city can be reached. Implementing a retention basin in the Piggyback Yard has very small effects on the safety in the city. Only without a levee between the river and the basin the safety will be increased locally.
Finally, it needs to be clear that this study has investigated the effects of human constructed measures on the safety of the city. In the project of restoring the LA River, this is only one of the objectives, although a very important objective. There may be lots of other good reasons to implement a side channel or a retention basin, but these are out of the scope of this study.

TABLE 14: RETURN TIMES (ONCE IN X YEARS) FOR THE REFERENCE SITUATION AND SCENARIO 1 AND THE EXTRAPOLATED RETURN TIMES FOR SCENARIOS 2 AND 3

	Flooding somewhere between stations B and C		**Flooding near station B**	
	Station B	*Station C*	*Station B*	*Station C*
Reference situation	154	166	583	859
Scenario 1, 5% off	180	198	677	1028
Scenario 1, 10% off	207	231	746	1196
Scenario 1, 15% off	228	268	902	1372
Scenario 2, first side channel	224	232	873	1255
Scenario 2, second side channel	213	222	784	1149
Scenario 3, with current levee		166		859
Scenario 3, with lower levee		167		870
Scenario 3, without levee		193		964

6 DISCUSSION

In the previous chapters a model has been set up to investigate the flood risks of the Los Angeles River and the change of these risks after revitalizing the river by taking some measures. In this study a lot of assumptions and choices have been made, which have been described and partially discussed in the previous chapters, in order to make this kind of study realizable and to keep the model as simple as possible. In this chapter the assumptions and choices made in setting up this model which cause the highest uncertainties in the results are reflected and discussed. Secondly, some general discussion about the model results is done. And finally, the differences between the return times found in this study and the return times used in the Feasibility Study by the USACE are discussed.

6.1 UNCERTAINTIES DUE TO MODEL SET UP

The uncertainties due to the model set up are discussed for three of the most important parts of the model, i.e. the grid, the bathymetry and the lateral inflows.

Grid

The first step in setting up the model was to generate the grid. Therefore, a rough sketch of the river was made and with this sketch the grid has been generated. The intention was to cover the cross sections of the river by 8 grid cells and putting 2 other grid cells at each side to represent the floodplains. It is assumed that this subdivision of grid cells is good enough to create an accurate model. Making a grid takes some time and it is of high importance for the model, and therefore quite some time was spent in generating this grid. However, after defining the other parameters for the model and the coupling of the bathymetry with the grid, it turned out that the grid covering the cross section of the river was coarser than desirable for some parts of the river. Especially the grid for the river between stations A and B was too coarse, which caused only 2 to 3 grid cells covering the cross section of the river at these locations. In the first simulations this resulted in more than 2 times higher water levels than measured at station A. After some weeks of trying to find the problem, it turned out that the coarseness of the grid at these locations was causing these problems. This coarseness of the grid was caused by a too rough sketch of the narrow and sinuous river at these locations, which was used as an aid in generating the grid. Creating a complete new grid with 8 grid cells for the cross section of the river profile and 2 grid cells for each floodplain would take too much time. Therefore, only the part between stations A and B is made somewhat finer by reforming the current grid. This resulted in a coverage of at least 3 to 4 grid cells per river cross section. This is still coarser than desirable, however, due to the narrowness and the sinuosity of the river at these places this was the best that could be reached in reforming the current grid. Also, the reforming of the grid lead to more accurate results than before. However, the coarseness of the grid still causes an inaccuracy in the model results.

Bathymetry

Another aspect that causes inaccuracies in the model results, is the bathymetry. The bathymetry is taken from a Digital Elevation Map of the Los Angeles area, which is obtained by LIDAR, a remote sensing technique that uses light pulses. We decided to use a DEM because that was easy to implement in the model and it saved a lot of time. Another option to create a bathymetry map would have been translating the cross sections used in the Feasibility Study of the USACE to the grid, which would have been more accurate for the river profiles than by using the DEM. However, this would take too much time and therefore we decided to use these cross sections only to check the DEM. Due to the fact that this DEM is obtained by using light pulses, the height of the trees hanging over the river was measured instead of the river bottom. Also the bridges and the water

surfaces were measured instead of the river bottom. Therefore, it was needed to adapt the bathymetry given by the DEM. This was done mostly by linear interpolation between the depth value just before the tree or bridge and the depth value just behind it. This is done only for the river profile and not for the flood plains, so at some places the surface level of the flood plains in the model is higher than it actually is. Especially for the part of the river between station A and B, where a lot of trees were hanging over the river, and for the part of the river between station B and C, where trees and bushes grow in the river, the values were adapted significantly. Due to the sinuosity of the river between A and B, due to the fact that a lot of trees are hanging over the river at this location and due to the coupling of the bathymetry with the grid, of which the uncertainty for mainly for this part of the river has been described above, the bathymetry had to be adapted considerably.

Lateral inflow
A last aspect of uncertainty in the model set up is the definition of the boundary conditions for the lateral inflows. The relations between the tributaries and the upper boundary condition at station A are highly uncertain. These relations had to be defined to keep the model as simple as possible, by just varying the upper boundary condition and thereby automatically adapting the boundary conditions for the lateral inflow. This method is also chosen because no data was available of the storm water drains entering the system. However, the simulated discharge series of the boundary conditions for the lateral inflows are sometimes underestimated and sometimes overestimated. In determining these relations, the complete hourly data series of 4 years were taken into account. It would have been better to determine the relations only through the hourly data series of the several peaks, to get a more accurate relation for the peak events. However, this would have taken too much time in the course of this study. Unfortunately, this also gives rise to an uncertainty for these boundary conditions.

6.2 MODEL RESULTS
The aspects of the results of the model are discussed in this section, i.e. the method of determining the point of flooding, the floods in the downstream part of the river and the the high flow velocities of the river.

Determining point of flooding
In this study the simulations for each scenario are done twice, because of different criteria being used to determine the point of flooding. The point between stations B and C at which the river is just not flooding and the point near station B at which the river is just not flooding is determined. It was already known from the study of the USACE that the part of the river between station B and C is the most critical part of the river. Therefore, in this part of the river measures are planned, of which some have been investigated in this study. However, in the first simulations it turned out that the river was flooding somewhere between stations A and B firstly. It was assumed that the measures between stations B and C will have only small influences on the part of the river between stations A and B, because of the high flow velocities due to the steep slope and small friction of the river. This is the reason that in the model the levees of the river between stations A and B are made higher in the bathymetry file, to prevent flooding at these locations and to prevent influence of these possible floods on the river flow downstream of station B.
After adapting the bathymetry between stations A and B, the river floods for the first time between stations B and C. Therefore, the criterion of just not flooding of the river between these stations is used. It turned out that the river first floods at a point a little bit upstream of the confluence of the Burbank Western Channel with the LA River, which is at about one third of the part of the river from station B to C. However, from this point no observed data have been gathered, so no extreme value distribution is available. To determine a return time of the event that the river just not will flood between stations B and C the return times are calculated for station B and for station C, and the return time of the point at which the river just will not flood

will probably lie somewhere in between these two return times. Therefore, also the point at which the river just not floods at station B is determined, to know the return time for flooding at station B. It has to be mentioned that the levees near station B are very high in the model, and therefore a point of just not flooding just beyond station B is chosen. The return time of just not flooding at station C is not determined, because before this happens the river is flooded already at several points between stations B and C, which highly influences a possible flood at station C.
After doing all these simulations another method of determining whether the river is flooding or not was used, other than the method previously used in the study. It now appeared that the river was already flooding a little bit at the point that previously was determined as where the river just was not flooding. However, it has been decided not to simulate the scenarios again with a bit lower discharge event, because this also would take too much time and the results would have been only slightly different.

Downstream flooding

In the model results the river is flooding quite a lot in the downstream part between station E and the downstream boundary condition, defined as a harmonic constituent due to the ocean. This part of the river, namely downstream of the confluence with the Rio Hondo, was already restored some years ago, as mentioned in section 2.2.3. It is assumed that these floods do not influence the model results upstream in the region in which the measures are planned. The flooding in the downstream part of the river is probably due to the influence of the ocean on the river flow. The tides of the ocean also cause tidal flows in the downstream part of the river. The river flow will slow down when it reaches the ocean water, because of contrary flow velocities with a rising sea level due to the tide. It depends on the time of the day how far upstream of the river the river flow is influenced by the tide of the ocean. It is possible that there was a high tide at the moment that the peak of the discharge event was reaching the ocean on the day at which the event is simulated, namely on January 1, 2015. This shows that the actual tide of the ocean can have large influence on the river flow in the downstream part of the river.

Flow velocities

A last aspect to mention about the model results are the high flow velocities in the river. A graph of the depth averaged flow velocities in the river at 12:00 on January 1, 2015, which is a representative graph of the flow velocities during the discharge event, is shown in Figure 33. The velocities for the river between stream gauging stations A and B are up to 15 m/s. After station B the flow velocities are on average between 10 and 11 m/s, but near Griffith Park, the flow velocities reduce to an average of 5 to 6 m/s because of the high roughness due to the vegetation in the river. Just before the confluence with the Arroyo Seco, at stream gauging station station C, where the vegetation in the river stops, the flow velocities are again high, at an average of 12 m/s.

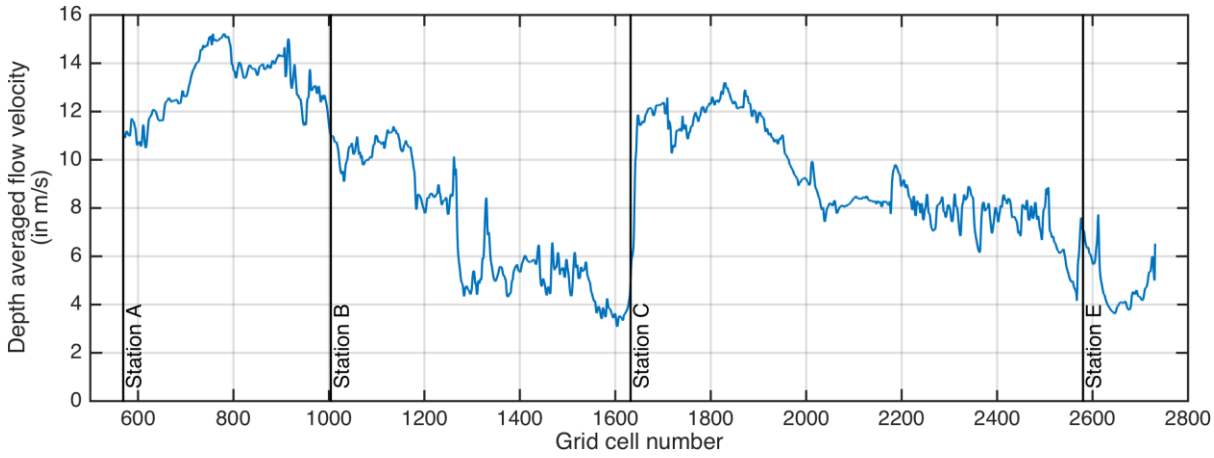

FIGURE 33: DEPTH AVERAGED FLOW VELOCITIES ALONG THE LA RIVER AT 12:00 ON JANUARY 1, 2015, AS A REPRESENTATIVE GRAPH OF THE FLOW VELOCITIES IN THE RIVER

More downstream the flow velocities become lower with on average 8 m/s, and after station E the flow velocities decrease to about 4 to 5 m/s, due to the influences of the ocean. The high flow velocities are of course due to the low friction of the concrete river bottom and due to the steep slope of the river bottom. The high velocities sometimes exceed the design flow velocities of the river channel, which are 11 m/s at maximum (USACE, 2013b). At some places the flow velocities do change very quickly, according to the simulations. This causes a lot of warnings as output of the FLOW module of Delft3D. With each simulation the model reported on the average more than 20,000 warnings for a velocity change of more than 5 m/s between two grid cells. It is unclear why these velocity changes appear exactly, but it probably has to do with the high flow velocities in the river, which causes also supercritical flow conditions with Froude numbers of up to 3. The warnings indicate that the simulations are approaching the limitations of Delft3D with these high velocities and supercritical flow. The model Delft3D might not be suitable anymore, but the same holds for the HEC-RAS model used by USACE (2013b).

6.3 Comparison with the HEC-RAS model

The results of the determination of the return times of flooding in the LA River are different than the return times used in the study of the USACE (Appendix C: Frequency discharges used in the Feasibility Study of the USACE). In chapter 1 it is already mentioned that at some reaches the flood protection level is no more than once in 10 years. To be more specific, the reach of the LA River between the confluence with the Burbank Western Channel (just before the 90-degree corner) and the confluence with the Verdugo Wash (just after the 90-degree corner) has a return time of about once in 10 years (USACE, 2013b). This return time corresponds with a design discharge of about 1130 m^3/s at this location. However, according to this study, the return time of the most critical point between stations B and C, which is located just before the confluence with the Burbank Western Channel and thus just before the most critical reach defined by the USACE, is once in about 160 years with a daily averaged discharge between 841 and 1201 m^3/s and an hourly averaged peak discharge between 1550 and 1950 m^3/s. In this section the similarities and the differences are described and explained as far as possible.

Daily averaged discharges vs. maximum peak discharges

The most important difference is the fact that in this study the daily averaged discharge was used, instead of the maximum peak discharges as used in the study of the USACE. This results in different extreme value distributions. Unfortunately, it is not clear how the return times are coupled to the extreme discharges in the study of the USACE. The frequency discharges used in the study of the USACE (2013b) are taken from the 1992 LACDA Feasibility Study, but this study was not available to us. An extreme value distribution with daily averaged peak discharges will differ from an extreme value distribution with maximum peak discharges, which is already discussed in section 3.3.3. Unfortunately, the hourly averaged peak discharges, which are much closer to the maximum peak discharges than the daily averaged peak discharges are, are only available for 4 years for each stream gauging station. For some stream gauging stations hourly data of 15 years at maximum was available, however, we were not able to investigate all these available data due to the limited time available. These 4 years are too little to determine an extreme value distribution, and even so the 15 years available for some stations are also still too little to determine an accurate extreme value distribution.

To illustrate the differences between the daily averaged peak discharges and the hourly averaged peak discharges for station B, at which hourly data of 15 years was available, the hourly averaged peak discharges are given for the same return period as the daily averaged peak discharges that are used in the extreme value distribution. This shown in Figure 34. It can be seen that the daily averaged extreme discharges do not give any hint to estimate the hourly averaged discharges or even the maximum peak discharges. It may even be the case that for some of these 15 years higher hourly averaged discharges are measured on other days, but which have a lower daily averaged discharge, and therefore do not appear in this extreme value distribution. It would be better if the

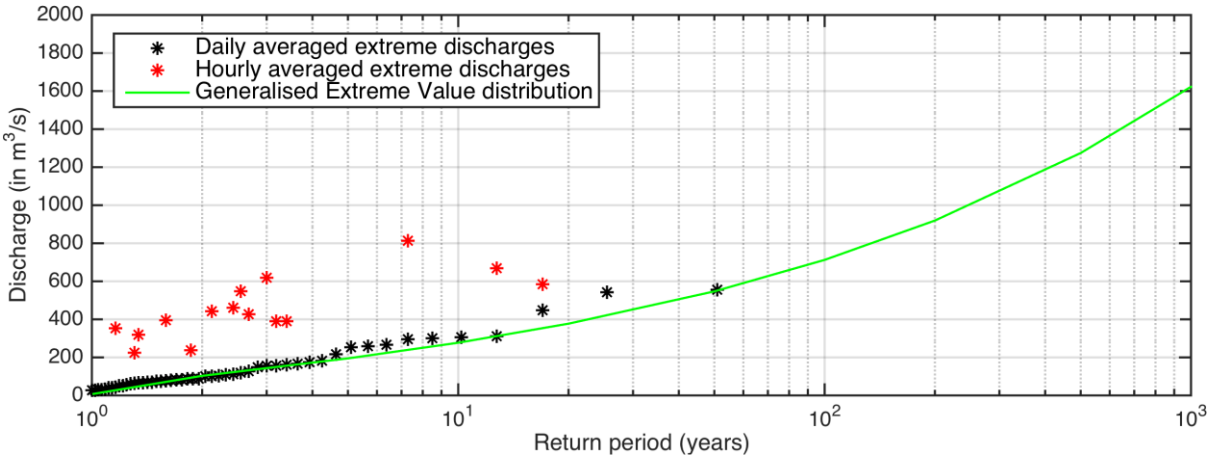

FIGURE 34: EXTREME VALUE DISTRIBUTION FOR STREAM GAUGING STATION B (F300-R) WITH DAILY AVERAGED EXTREME DISCHARGES AND THEIR CORRESPONDING HOURLY AVERAGED EXTREME DISCHARGES (FOR 15 YEARS), WITH A LOGARITHMIC X-AXIS

maximum peak discharges were available for all stream gauging stations and that with these discharges an extreme value distribution was made, but these were not available and that explains the differences between the results of this study and those of the study from the USACE.

Extreme vs. typical hydrograph

The fact of limited availability of hourly data is also the reason to choose the extreme hydrograph instead of the typical hydrograph (section 5.1). As can be seen in Figure 34, some of the hourly averaged extreme discharges are several times higher than the daily averaged extreme discharge, which is also the case for the typical hydrograph. For other daily averaged discharges, which is the case with the extreme hydrograph, is only 2 times higher or even less than 2 times higher, which appears mostly for the highest recorded daily discharges. For this study the highest possible discharge is the most interesting, so the extreme hydrograph is used to execute the scenarios. If the typical hydrograph was chosen, with a peak 5 times higher than the average discharge, a lower daily averaged discharge would have been found for the cases in which the river just not floods between stations B and C or near station B. This means that a higher return time would have been found that is closer to the return times used for the study of the USACE by using the typical hydrograph.

Threshold depth

A final difference between the studies that could explain the differences between the return times, is the fact that the study of the USACE makes use of other threshold depths. In this study the heights of the levees are taken as a threshold depth, which therefore does not take into account a safety level. In the study of the USACE another threshold depth is used, namely a depth some centimeters below the edge of the levee. It was not known by us what criteria were used to set this threshold depth. This difference between the studies means that with a lower threshold depth the maximum discharge that gives no flood is less, so the return times will become lower.

Similarities between studies

Fortunately, there are not only differences between both studies. By looking at the discharge at which the river is just not flooding between stations B and C, which is at a peak discharge of about 1520 m^3/s at that point, this discharge is almost the same as the design discharge for the same point defined in the study of the USACE, namely 1550 m^3/s. The small differences between these values can be explained by the uncertainties in the model, as described in the previous sections. Also for the other parts of the river, except for the part as described in the beginning of this section, the discharges are estimated to be almost the same for this study as the design discharges used in the study of the USACE. In the study of the USACE the design discharges for the part of the

river around the 90-degree corner are much lower than the design discharges before and after this reach. However, this phenomenon is not found in this current study.

For the comparison between both studies it can be summarized that the design discharges given in the study of the USACE are almost the same as the discharges found in this study, except for the part of the river between the confluence with the Burbank Western Channel and the confluence with the Verdugo Wash. However, the translation from the discharges to the return times are different in both studies and can be explained mainly by the use of daily averaged discharges to determine the extreme value distribution, instead of the use of maximum peak discharges. In this study a two-dimensional model is used, where the USACE used a one-dimensional model. We still believe that a two-dimensional model is better able to simulate the LA River. However, various aspects lead to large uncertainties. USACE also had to deal with some of these aspects, but this was not always clear how this was done.

7 CONCLUSIONS AND RECOMMENDATIONS

In this chapter the conclusions of this research are drawn and some recommendations are given in order to guide further research.

7.1 CONCLUSIONS

In this study a two-dimensional model is set up to simulate the river flow in the Los Angeles River. With help of this model it is tried to answer the main research question: *In what way will the flood risks of the Los Angeles River change after the revitalization of the river?* This main research question was split up in 3 sub questions. Those sub questions will be answered in order to draw the conclusions of this study.

1. ***What is the current relation between precipitation in the Los Angeles River catchment and the discharge in the Los Angeles River and what is the current frequency distribution of these discharges?***

The precipitation in the catchment of the LA River and the discharge in the LA River are recorded by different weather stations and stream gauging stations. Those data series are taken and investigated in order to determine a relation between the discharge and the precipitation. It turned out that the discharge in the LA River is depends much on the precipitation that falls in the city. Both data series show on average very dry summers and also relatively dry winters. By looking at individual events it is seen that the peaks of the discharges are very high, and that the events are very short. By executing cross-correlation between the data series it was visible that there is a relation between the precipitation in the catchment and the runoff in the river. Unfortunately, it was not possible to quantify this relation accurately. This depends very much on the locations where the precipitation falls and the intensity of the precipitation at these locations. The discharge series are used to determine extreme value distributions for the different stream gauging stations in order to determine return times of discharges. For these distributions the daily averaged extreme discharges are used, because this was the most available data type. Three different types of distributions are determined of which the Generalized Extreme Value distribution is chosen for further use. The differences between these distributions are quite big for each station, which results in a high uncertainty by applying this technique to determine return times.

2. ***How well can the current system of the Los Angeles River be described by the two dimensional model Delft3D?***

The FLOW module of the suite Delft3D was used to set up a two-dimensional model of the LA River. The generation of the grid for the model was one of the most important steps in setting up this model. It was hard to generate a grid for this river, because of the size of the river. We tried to cover the river by enough cells to be as accurate as possible, but also as less as possible cells to save computing time. At some locations along the river this balance was found more easily than at other places. This resulted in an inaccuracy in the model, as well as with the bathymetry, observed from a Digital Elevation Map and checked with cross sections of the river, by coupling it with the grid.
The lateral inflows of the models are estimated by determining a relation between the upper boundary condition, which is near the stream gauging station at the Sepulveda Dam, and the main tributaries. These relations are also determined for three defined residual flow points, which

represent the several storm drains along the river. The model has been calibrated and validated with the available hourly data set, which was split up into two parts, one part for the calibration and one part for the validation. The results of these calibration and validation were acceptable. However, due to many adaptations in the grid and bathymetry of the part of the model between stations A and B we decided for the last part of the study to look only at flooding in the part of the river after stream gauging station B. Therefore, the levees next to the river between stations A and B have been increased to prevent the river for flooding in this part. With help of the built model, it is investigated that the current return time of the river at which it just not floods is once in about 160 years. With an event bigger than this, the river is firstly flooding at a point in the river between station B and C, which lies just before the confluence with the Burbank Western Channel and the LA River.

3. How will the return times of the Los Angeles River change due to human and natural environmental changes?

To answer this last sub question, three scenarios with human interventions have been simulated and discussed and one scenario about the change is climate is only discussed. For the three scenarios with human interventions in the river it turned out that none of these three scenarios have a negative effect on the safety in the whole river. The scenario with an implemented retention basin at the Piggyback Yard and the scenario with implemented side channels have only very local positive effects at the area of implementation. At these locations the water level drops with 20 to 40 centimeters when implementing the side channels and very locally up to 160 centimeters when implementing a retention basin, depending on the height of the levee between the basin and the river. By extrapolating the return times of stream gauging station C to the river at location of the Piggyback Yard, it can be concluded that only the implementation of a retention basin without a levee have some local positive effects on the flood safety of the river, namely about 12 to 16% at maximum. The implementation of a retention basin is not recommended at the location of the Piggyback Yard, because there are no problems at the Piggyback Yard and just downstream of it in the current or reference situation, according to the flood safety of the city. Due to the steep slope and small friction of the river bottom the flow velocities are high, which results in short backwater curves and thus no upstream effects of the implementation of the Piggyback Yard.
By extrapolating the return times of the stations B and C to the locations at which the side channels will be implemented, the safety of the river increases locally by 40 to 50% at the first side channel and 30 to 40% at the second, more downstream side channel. However, also due to the steep slope and small friction of the river bottom the flow velocities at these points are high, so there are no upstream effects of implementing side channels at these locations. The implementation of side channels can be useful only for increasing the water safety in the area of the river where the side channel is located.
The best alternative of human interventions in the river catchment to improve the flood safety in the city is to store the water that falls during big precipitation events before it flows into the river. This can be done by implementing retention basins next to the tributaries of the river or implementing infiltration systems in the streets, but also by small private projects such as green roofs and collecting water in big rain barrels. With 5% less discharge in the whole LA River the water level in the river reduces by about 15 centimeters which results in a 20% safer city. With 15% less discharge in the whole LA River the city will become 60% safer due to on average 40 centimeters lower water levels.
The influence of a change in precipitation due to climate change on the discharge in the LA River is hard to investigate. First, an accurate and quantitative relation between the precipitation in the catchment and runoff in the river is hard to determine, as concluded above. And secondly, the scientists have different opinions about the change in precipitation. Some scientists think the precipitation will decrease where others expect an increase in precipitation. It is clear that an increase in precipitation will decrease the safety level of the river, although the quantity is not known.

Finally, it needs to be clear that this research was investigating the effects of the human environmental changes on the safety of the river. In the project of restoring the LA River, this is only one of the objectives, although a very important objective. There may be lots of other good reasons to implement a side channel or a retention basin, such as developing multi-use public open space, increasing the water quality or restoring a functional ecosystem, but these are out of the scope of this study.

7.2 RECOMMENDATIONS

In order to guide some further research on the topic of the water safety for the city of Los Angeles some recommendations are given.

It is highly recommended to determine extreme value distributions with maximum peak discharges instead of daily averaged peak discharges. This will provide a better insight in the return times of the LA River in the current situation, but also in the scenarios of human interventions. This will also provide a better possibility to compare this study with the Feasibility Study of the USACE (2013a).

To investigate other local measures or to investigate the implemented measures in more detail, a finer grid of the river for especially the upper part of the river is recommended. This will provide a more accurate model. However, a finer grid needs also more computing power and time. Therefore, it would be wise to split up the model in parts which are the most interesting to study. By implementing a finer grid, also a better method for determining the bathymetry should be used, because the resolution of the Digital Elevation Map, which is about 3 meter, is too coarse. For example, for investigating some local measures, it will be recommended to do some local measurements of the bathymetry as input for the model.

For increasing the flood safety of the LA River it is recommended to invest in studying the possibilities to store the water in the Los Angeles catchment before it flows into the Los Angeles River. As concluded in this study this measure is the best alternative in increasing the flood safety of the river. Storing the water in the Los Angeles catchment has also lots of other advantages in such a dry climate as there is in this region.

REFERENCES

Berg, N., Hall, A., Sun, F., Capps, S., Walton, D., Langenbrunner, B., & Neelin, D. (2015). 21st Century Precipitation Changes over the Los Angeles Region. *Journal of Climate*, *28*(2), 401–421. http://doi.org/http://dx.doi.org/10.1175/JCLI-D-14-00316.1

Booij, M. J. (2010). *Inleiding Waterbeheer Dictaat Faculteit Construerende Technische Wetenschappen*. Enschede: University of Twente.

Brink, H. W. van den, Können, G. P., & Opsteegh, J. D. (2005). Uncertainties in extreme surge level estimates from observational records. *Philosophical Transactions of the Royal Society of London A: Mathematical, Physical and Engineering Sciences*, *363*(1831), 1377–1386. http://doi.org/10.1098/rsta.2005.1573

Casey, K. (2015). Interview about the Los Angeles River. (T. Lassche, Ed.). Los Angeles: U.S. Army Corps of Engineers.

Chow, V. Te. (1959). The Table of Manning's Roughness Coefficient. In *Open-Channel Hydraulics*. New York: McGraw-Hill Book Company.

City of Los Angeles. (2014a). Los Angeles River Revitalization. Retrieved from http://www.lariver.org/index.htm

City of Los Angeles. (2014b). Los Angeles River Revitalization - LA River Facts. Retrieved from http://www.lariver.org/about/lariverfacts/index.htm

City of Los Angeles - Department of Public Works, United States Army Corps of Engineers, & Tetra Tech Inc. (2007). *Los Angeles River Revitalization Master Plan*. City of Los Angeles, Department of Public Works, Bureau of Engineering.

Davis, J. C. (2002). *Statistics and Data Analysis in Geology* (Third). New York: John Wiley & Sons, Inc.

Deltares. (2014a). *Delft3D-FLOW, User Manual, version 3.15.34158*. Delft.

Deltares. (2014b). *QUICKIN, User Manual, version 4.00.34158*. Delft: Deltares.

Deltares. (2014c). *RGFGRID, User Manual, version 4.00.34074*. Delft: Deltares.

Deltares. (2015a). About Delft3D. Retrieved from http://oss.deltares.nl/web/delft3d/about

Deltares. (2015b). Grid quality. Retrieved from http://publicwiki.deltares.nl/display/D3DGUIDE/Grid+quality

Evelyn, J. B. (1980). Operation and Performance of Corps of Engineers Flood Control Projects in Southern California and Arizona during 1978-80. *Storms, Floods, and Debris Flows in Southern California and Arizona 1978 and 1980*. Pasadena, California: National Academy Press.

Google Earth. (2015). Los Angeles. Google Inc. Retrieved from http://www.google.com/earth/

Gumprecht, B. (2001). *The Los Angeles River: Its life, death, and possible rebirth*. JHU Press.

Hosking, J. R. M., & Wallis, J. R. (1997). *Regional Frequency Analysis*. Cambridge, UK: Cambridge University Press.

Interagency Advisory Committee on Water Data (IACWD). (1982). *Guidelines for determining flood flow frequency, Bulletin 17B of the Hydrology Subcommittee*. Reston, VA: U.S. Geological Survey.

Killam, D., Bui, A., Patzert, W. C., Willis, J. K., LaDochy, S., & Ramirez, P. (2010). California rainfall is becoming greater, with heavier storms. In *22nd Conference on Climate Variability and Change* (p. 4 pp). American Meteorological Society. Retrieved from https://ams.confex.com/ams/90annual/techprogram/paper_163828.htm

Los Angeles County. (2011). 2006 10-foot Digital Elevation Model (DEM) - LAR-IAC - Public Domain. Retrieved from http://egis3.lacounty.gov/dataportal/2011/01/26/2006-10-foot-digital-elevation-model-dem-public-domain/

Los Angeles County - Department of Public Works (LACDPW). (1996). *LA River Master Plan*.

Los Angeles County - Department of Public Works (LACDPW). (2014). Los Angeles River Watershed. Retrieved from http://www.ladpw.org/wmd/watershed/la/

Los Angeles County - Department of Public Works (LACDPW). (2015a). Drainage Area station F319-R. Retrieved November 13, 2015, from http://www.dpw.lacounty.gov/wrd/Runoff/dispimg.cfm?showimg=graphics/d319.gif

Los Angeles County - Department of Public Works (LACDPW). (2015b). Index of Stream Gauging Stations. Retrieved from http://www.dpw.lacounty.gov/wrd/Runoff/index.cfm

Los Angeles County - Department of Public Works (LACDPW). (2015c). Mean Daily and Hourly flow data or stream gauging stations F34D-R, F57C-R, F300-R and F319-R. Water Resources | Records & System Support.

Los Angeles Regional Water Quality Control Board. (2013). *Recreational use reassessment of the engineered channels of the Los Angeles River Watershed*.

Mathwave Technologies. (2015). Easyfit Professional. Retrieved from http://www.mathwave.com/easyfit-distribution-fitting.html

Millington, N., Das, S., & Simonovic, S. P. (2011). *The Comparison of GEV, Log-Pearson Type 3 and Gumbel Distributions in the Upper Thames River Watershed under Global Climate Models*. London, Ontario, Canada: The University of Western Ontario, Department of Civil and Environmental Engineering.

National Oceanic and Atmospheric Administration (NOAA). (2015a). Climate Data Online. Retrieved from http://www.ncdc.noaa.gov/cdo-web/

National Oceanic and Atmospheric Administration (NOAA). (2015b). Harmonic Constituents for 9410680, LONG BEACH, TERMINAL ISLAND CA. Retrieved from http://tidesandcurrents.noaa.gov/harcon.html?id=9410680

National Oceanic and Atmospheric Administration (NOAA). (2015c). What is LIDAR? Retrieved from http://oceanservice.noaa.gov/facts/lidar.html

Oregon State University. (2007). Analysis Techniques: Flood Frequency Analysis. Retrieved from http://streamflow.engr.oregonstate.edu/analysis/floodfreq/Flood_Frequency2007.pdf

Shaw, E. M., Beven, K. J., Chappell, N. A., & Lamb, R. (2011). *Hydrology in practice* (fourth). Abingdon, Oxon, United Kingdom: Spon Press.

Starr, K. (1996). *Endangered Dreams: The Great Depression in California*. Oxford University Press.

U.S. Army Corps of Engineers (USACE). (2013a). *Los Angeles River Ecosystem Restoration, Integrated Feasibility Report*. Los Angeles County, California.

U.S. Army Corps of Engineers (USACE). (2013b). *Los Angeles River Ecosystem Restoration, Integrated Feasibility Report, Draft - Appendix E Hydrology and Hydraulics*. Los Angeles County, California.

U.S. Census Bureau. (2015). Annual Estimates of the Resident Population: April 1, 2010 to July 1, 2013. Retrieved from http://www.census.gov/popest/data/metro/totals/2013/index.html

U.S. Environmental Protection Agency. (2014). Urban Waters Federal Partnership Works to Restore an Increase Access to the Los Angeles River. Retrieved from http://www2.epa.gov/sites/production/files/2014-05/documents/uw-factsheet-losangeles2014.pdf

U.S. Geological Survey (USGS). (2015). National Water Information System. Retrieved from http://waterdata.usgs.gov/nwis/inventory?agency_code=USGS&site_no=11092450

Wikipedia. (2015). Los Angeles River. Retrieved from http://en.wikipedia.org/wiki/Los_Angeles_River

Williams-Villano, M. E. (2014). Revitalizing Our Concrete Rivers. *Soil Erosion and Hydroseeding*, *12*(5), 24–29.

Wit, M. J. M. de, & Buishand, T. A. (2007). *Generator of Rainfall And Discharge Extremes (GRADE) for the Rhine and Meuse basins*. Lelystad, The Netherlands.

APPENDIX A: FREQUENCY FACTORS FOR LOG-PEARSON TYPE III DISTRIBUTIONS

TABLE A 1: FREQUENCY FACTORS K FOR LOG-PEARSON TYPE III DISTRIBUTIONS (IACWD, 1982)

Skew coefficient C_s	Recurrence Interval in Years									
	1.0101	**2**	**5**	**10**	**25**	**50**	**100**	**200**	**500**	**1000**
1	-1.588	-0.164	0.758	1.340	2.043	2.542	3.022	3.489	4.088	4.531
0.9	-1.660	-0.148	0.769	1.339	2.018	2.498	2.957	3.401	3.969	4.388
0.8	-1.733	-0.132	0.780	1.336	1.993	2.453	2.891	3.312	3.850	4.244
0.7	-1.806	-0.116	0.790	1.333	1.967	2.407	2.824	3.223	3.730	4.100
0.6	-1.880	-0.099	0.800	1.328	1.939	2.359	2.755	3.132	3.609	3.956
0.5	-1.955	-0.083	0.808	1.323	1.910	2.311	2.686	3.041	3.487	3.811
0.4	-2.029	-0.066	0.816	1.317	1.880	2.261	2.615	2.949	3.366	3.666
0.3	-2.104	-0.050	0.824	1.309	1.849	2.211	2.544	2.856	3.244	3.521
0.2	-2.178	-0.033	0.830	1.301	1.818	2.159	2.472	2.763	3.122	3.377
0.1	-2.252	-0.017	0.836	1.292	1.785	2.107	2.400	2.670	3.000	3.233
0	-2.326	0.000	0.842	1.282	1.751	2.054	2.326	2.576	2.878	3.090
-0.1	-2.400	0.017	0.846	1.270	1.716	2.000	2.252	2.482	2.757	2.948
-0.2	-2.472	0.033	0.850	1.258	1.680	1.945	2.178	2.388	2.637	2.808
-0.3	-2.544	0.050	0.853	1.245	1.643	1.890	2.104	2.294	2.517	2.669
-0.4	-2.615	0.066	0.855	1.231	1.606	1.834	2.029	2.201	2.399	2.533
-0.5	-2.686	0.083	0.856	1.216	1.567	1.777	1.955	2.108	2.283	2.399
-0.6	-2.755	0.099	0.857	1.200	1.528	1.720	1.880	2.016	2.169	2.268
-0.7	-2.824	0.116	0.857	1.183	1.488	1.663	1.806	1.926	2.057	2.141
-0.8	-2.891	0.132	0.856	1.166	1.448	1.606	1.733	1.837	1.948	2.017
-0.9	-2.957	0.148	0.854	1.147	1.407	1.549	1.660	1.749	1.842	1.899
-1	-3.022	0.164	0.852	1.128	1.366	1.492	1.588	1.664	1.741	1.786

APPENDIX B: PARAMETERS CORRESPONDING WITH EXTREME VALUE DISTRIBUTIONS

TABLE B 1: PARAMETERS CORRESPONDING WITH EXTREME VALUE DISTRIBUTIONS WITH ANNUAL PEAK DISCHARGES

		Parameters			
Station	**Distribution type**	*a*	*b*	*k*	*K*
A	*Gumbel*	76.002	58.795		
	GEV	72.364	56.141	0.086	
	LPIII				-0.234
B	*Gumbel*	86.000	96.953		
	GEV	79.859	59.487	0.325	
	LPIII				0.275
C	*Gumbel*	141.783	142.578		
	GEV	130.000	106.270	0.240	
	LPIII				0.123
E	*Gumbel*	254.846	286.173		
	GEV	235.900	178.440	0.319	
	LPIII				0.322

TABLE B 2: PARAMETERS CORRESPONDING WITH EXTREME VALUE DISTRIBUTIONS WITH TOP EXTREME DISCHARGES

		Parameters			
Station	**Distribution type**	*a*	*b*	*k*	*K*
A	*Gumbel*	107.666	48.446		
	GEV	104.450	45.000	0.100	
	LPIII				0.266
B	*Gumbel*	135.262	87.908		
	GEV	129.160	51.322	0.354	
	LPIII				0.880
C	*Gumbel*	230.638	118.744		
	GEV	220.430	87.988	0.246	
	LPIII				0.623
E	*Gumbel*	447.268	256.451		
	GEV	425.310	160.100	0.333	
	LPIII				0.825

APPENDIX C: FREQUENCY DISCHARGES USED IN THE FEASIBILITY STUDY OF THE USACE

ARBOR Reach	RS	2-yr	5-yr	10-yr	25-yr	50-yr	100-yr	200-yr	500-yr	Design
Reach 1	692+94	16,200	27,200	31,800	42,000	54,300	71,400	81,200	96,800	55,000
Reach 1	691+24	17,500	30,200	35,600	47,500	59,700	76,800	87,600	103,000	57,000
Reach 1	639+73	18,400	32,700	38,600	51,800	63,900	81,000	92,700	109,000	40,000
Reach 2	546+45	20,300	37,200	44,200	59,900	71,800	88,900	102,000	118,000	40,000
Reach 3a	475+68	20,300	37,200	44,200	59,900	71,800	88,900	102,000	118,000	40,000
Reach 3b	474+07	21,600	40,500	48,200	65,800	77,500	94,600	109,000	125,000	78,000
Reach 4	432+16	21,600	40,500	48,200	65,800	77,500	94,600	109,000	125,000	78,000
Reach 5	358+63	21,600	40,500	48,200	65,800	77,500	94,600	109,000	125,000	78,000
Reach 6a	270+28	21,600	40,500	48,200	65,800	77,500	94,600	109,000	125,000	78,000
Reach 6b	257+85	21,400	41,000	49,400	69,600	82,000	93,800	106,000	118,000	83,700
Reach 7a	142+91	21,400	41,000	49,400	69,600	82,000	93,800	106,000	118,000	83,700
Reach 7b	128+71	22,900	44,200	53,600	79,800	94,400	109,000	124,000	141,000	104,000
Reach 8	86+07	22,900	44,200	53,600	79,800	94,400	109,000	124,000	141,000	104,000
Burbank Western	18+04	2,150	4,320	4,990	7,040	8,360	12,400	14,200	16,900	15,000
Verdugo Wash	12+62	3,790	7,550	8,720	12,700	15,100	23,200	26,500	30,300	42,900
Arroyo Seco	9+26	1,500	3,200	4,190	10,200	12,500	17,700	22,200	26,400	43,000

River, Reach, and River Station (RS) from HEC-RAS Models
There are 3 discharge locations for Reach 1 because the HEC-RAS models extended upstream from the ARBOR reach.
Discharges in ft³/s from 1992 LACDA Feasibility Study Hydrology Appendix

TABLE C 1: FREQUENCY DISCHARGES USED IN HEC-RAS MODELS (USACE, 2013B) (REACH 1, RS 692+94 CAN BE COMPARED WITH RIVER STATION B AND REACH 6B CAN BE COMPARED WITH RIVER STATION C)

APPENDIX D: DETERMINING RELATIONS BETWEEN STATION A AND LATERAL INFLOWS

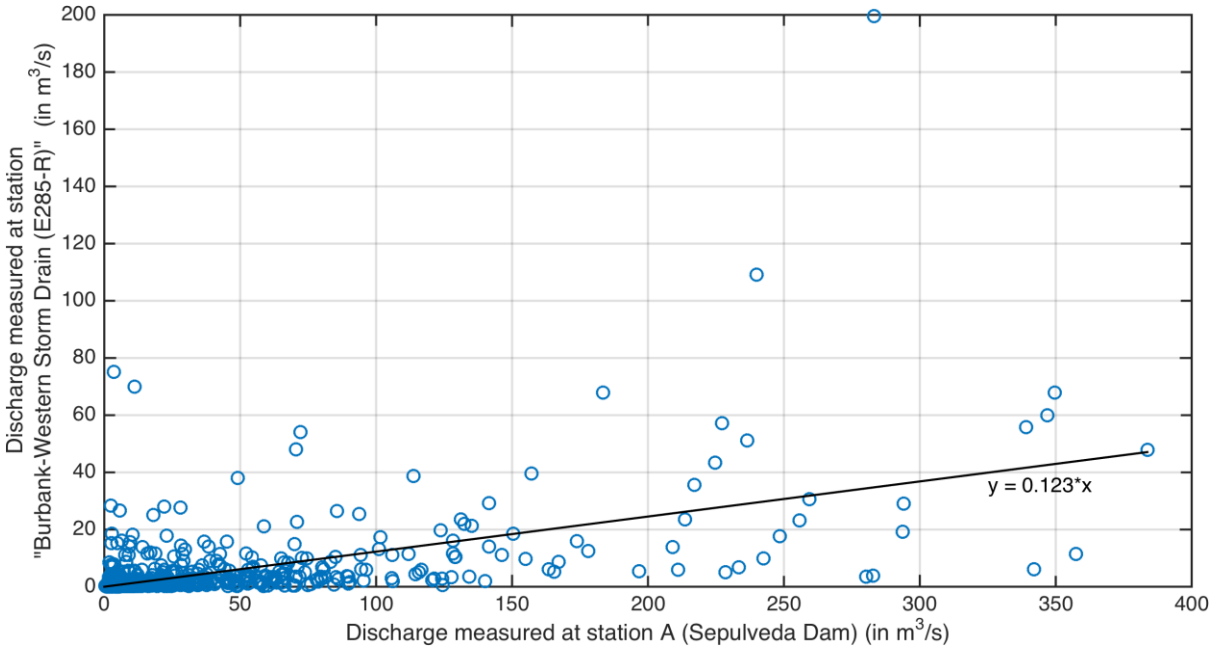

FIGURE D 1: FIGURE TO DETERMINE THE RELATION BETWEEN THE DISCHARGE MEASURED AT STATION A AND THE DISCHARGE MEASURED AT STATION 'BURBANK WESTERN STORM DRAIN'

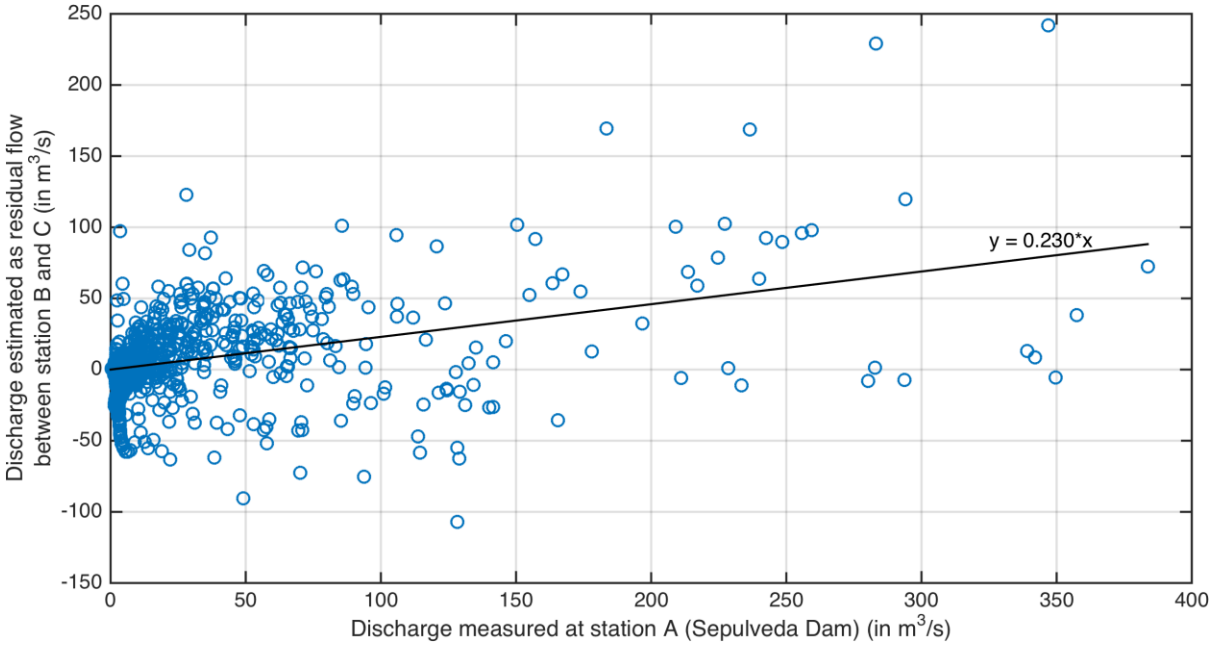

FIGURE D 2: FIGURE TO DETERMINE THE RELATION BETWEEN THE DISCHARGE MEASURED AT STATION A AND THE DISCHARGE ESTIMATED AS RESIDUAL FLOW BETWEEN STATIONS B AND C

APPENDIX E: EXTREME VALUE DISTRIBUTIONS FOR SCENARIO 1

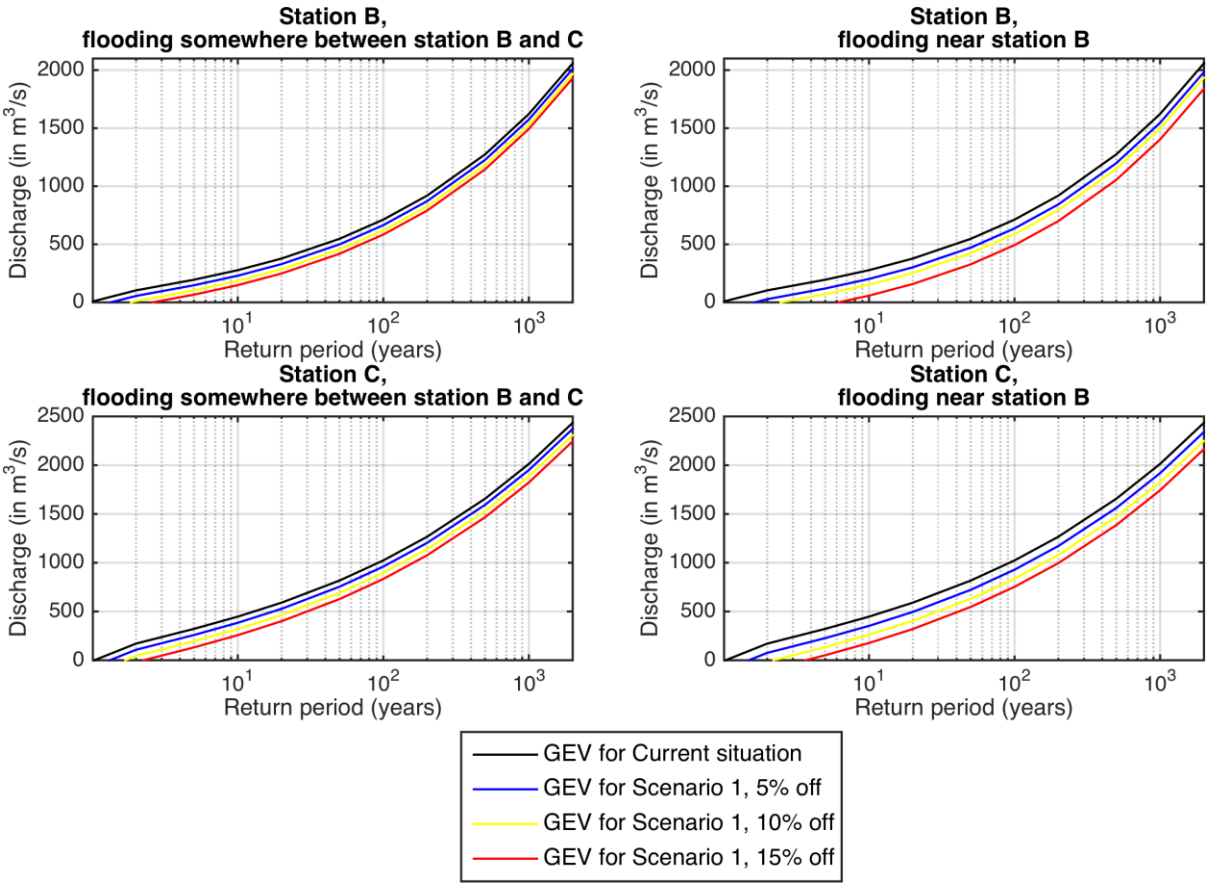

FIGURE E 1: EXTREME VALUE DISTRIBUTIONS TO DETERMINE THE RETURN TIMES FOR FLOODING IN SCENARIO 1, WITH LOGARITHMIC X-AXIS

APPENDIX F: BATHYMETRY OF RIVER AT LOCATION OF MEASURES FOR SCENARIO 2

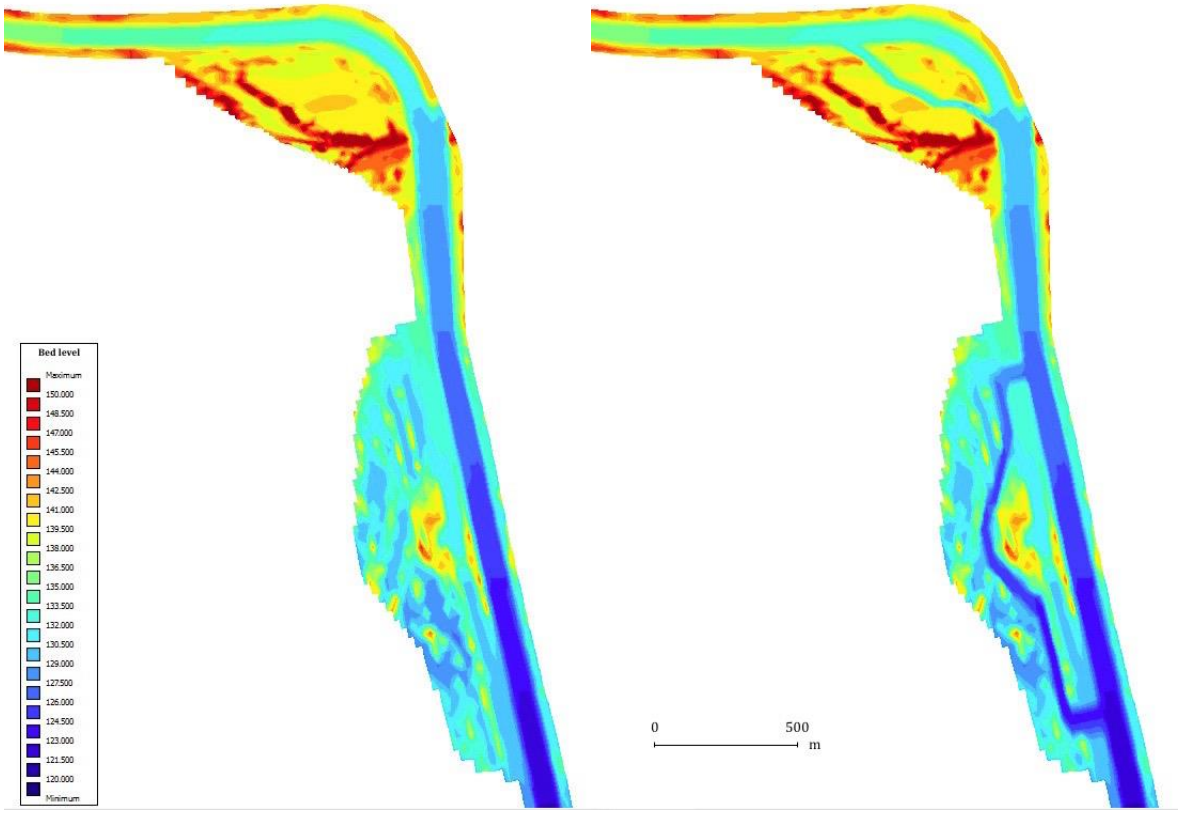

FIGURE F 1: (A) RIVER PROFILE IN REFERENCE SITUATION AT LOCATION OF MEASURES FOR SCENARIO 2, (B) RIVER PROFILE OF LOCATION OF MEASURES FOR SCENARIO 2

APPENDIX G: BATHYMETRY OF RIVER AT LOCATION OF MEASURES FOR SCENARIO 3

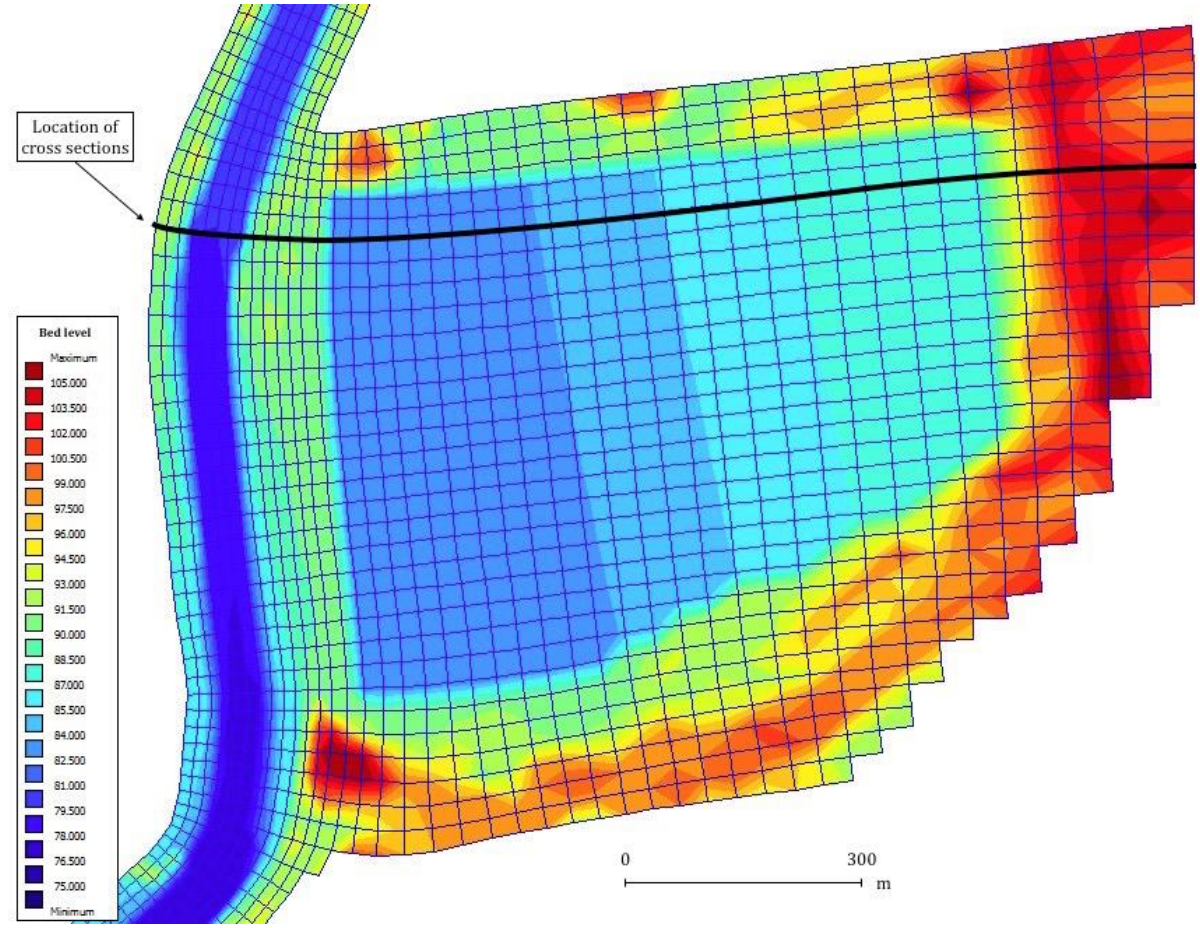

FIGURE G 1: BATHYMETRY OF THE EXCAVATED PIGGYBACK YARD FOR SCENARIO 3, WITH CURRENT LEVEE

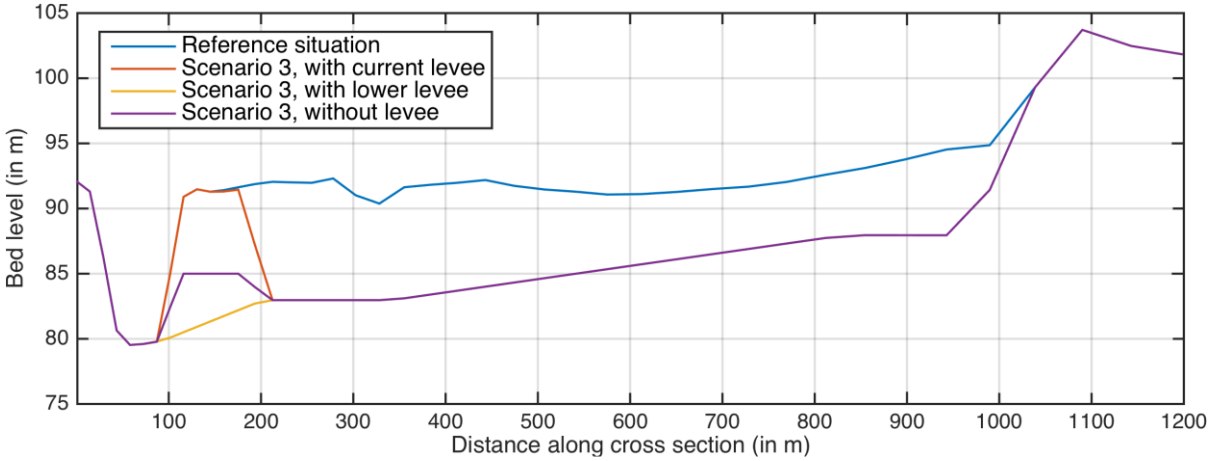

FIGURE G 2: CROSS SECTIONS OF THE PIGGYBACK YARD AT THE LOCATION OF THE BLACK LINE IN FIGURE F 1 FOR THE REFERENCE SITUATION AND FOR THE DIFFERENT ALTERNATIVES OF SCENARIO 3